CLAY-ORGANIC INTERACTIONS

A thesis submitted to

THE NATIONAL INSTITUTE FOR HIGHER EDUCATION

for the award of M.Sc. degree

by

JOHN JOSEPH FLYNN

Based on research carried out in the department of chemistry

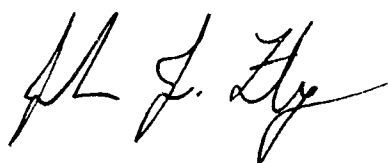N.I.H.E. Dublin, under the supervision of Dr. Christopher Breen.

DECLARATION

I declare that the work described within this thesis is all my
own work.

John Joseph Flynn.

School of Chemical Sciences

N.I.H.E. Dublin.

ABSTRACT

The aim of this present work was to study the interaction of various organic compounds with a range of cation exchanged montmorillonites. The first part of the study involved investigating the rate of sorption of methanol,Propan-2-ol (i-propanol), 2-methyl-propan-2-ol (t-butanol), tetrahydropyran (THP), tetrahydrofuran (THF), and 1,4-dioxan, onto a Wyoming montmorillonite saturated with Al^{3+}, Cr^{3+}, or Fe^{3+}-cations using isothermal gravimetry in the temperature range $18°-105°C$, using samples of differing weights and grain size distributions. The sorption rates for all the compounds increased with decreasing sample and grain size demonstrating that inter- rather than intraparticle mass transfer was the rate limiting process. The optimum sample paramaters (2mg sample of $<45\mu m$ grain size, pretreated at $120°C$ with a vapour flow of $>200cm^3 min^{-1}$) yielded integral diffusion coefficients at $18°C$ of $1.1 \times 10^{-14} m^2 s^{-1}$ for t-butanol for the Cr^{3+}-form, and $2.0 \times 10^{-14} m^2 s^{-1}$ for methanol and i-propanol for the Al^{3+}-form, $0.5 \times 10^{-14} m^2 s^{-1}$ for 1,4-dioxan for the Cr^{3+}-clay, and $3.5 \times 10^{-14} m^2 s^{-1}$ for THF and $2.4 \times 10^{-14} m^2 s^{-1}$ for THP both on Al^{3+}-clay. In general the sorption rate decreased as THF $\geqslant$ THP $>$ methanol $\geqslant$ i-propanol $>$ t-butanol $>$ 1,4-dioxan. For the alcohols sorption rate no temperature dependence was found, but the rate was found to be dependent on the cations present with $Fe^{3+} < Cr^{3+} < Al^{3+}$. In general the cyclic ether sorption rate of THF and THP was dependent on concentration or the 1,4-dioxan sorption rate was retarded by bidentate coordination to Al^{3+}-ions at the edges of the clay platlets.

The second part of the investigation involved the examination of the interactions of the alcohols and cyclic ethers with various cation exchanged montmorillonite. Variable temperature (20°, 50°, 100°, 150°, and 200°C) infra-red and temperature programmed desorption profiles (20°-800°C) were recorded for Na^+, Ca^{2+}, Al^{3+}, Fe^{3+}, and Cr^{3+}-exchanged montmorillonite, presaturated with methanol, propan-1-ol (n-propanol),

1-propanol, t-butanol, THP, THF, and 1,4-dioxan. The alcohol saturated trivalent cation-exchanged samples exhibit desorption maxima at 20° and 110°C(methanol), 30° and 160°C (n-propanol), 20° and 110°C (i-propanol), and 30°, 50°, and 70°C (t-butanol) The alcohol saturated Na^+ and Ca^{2+}-montmorillonite exhibit desorption maxima at higher temperatures than in the i-propanol (20° and 140°C) and t-butanol (30° 90° and 110°C) desorption profiles, but at the same temperature for methanol and n-propanol This behaviour is interpreted in terms of acid-catalysed dehydration of i-propanol and t-butanol to alkenes, and n-propanol to di-prop-1-yl ether over M^{3+}-exchanged montmorillonite. The cyclic ether saturated montmorillonite exhibit little uniformity in the positions of the desorption maxima from the different cation exchanged forms, (listed in Table 6.111.), but some trends are disernable and these results are interpreted as acid-catalysed ring opening of the THP and THF to form alkenes which would undergo oligomerisation in the M^{3+}-montmorillonites. 1,4-Dioxan was found to desorb without modification, indicating that in both a dynamic and an equilibrium sense, 1,4-dioxan is relatively stable towards acid attack in these systems.

CONTENTS

 1

CHAPTER 1

1 1 Clay Minerals an Introduction

In the following thesis some of the properties of Wyoming Montmorillonite clay will be investigated and later discussed The term 'clay' may be considered from two perspectives, firstly the mineralogical term clay

This refers to a group of mineral compounds, the products of weathering, formed by hydrothermal action and deposited as sediment. Grim[1] defines clay as a natural, earthy, fine-grained material, which develops 'plasticity' if mixed with a limited amount of water Plasticity means the ability of the clay to be deformed under applied pressure, with retention of the deformed shape upon removal of the applied pressure.

The second perspective is the particle size definition of a clay. The Wentworth[2] scale defines a clay as any material whose particle size is 4μm or less in any soil or naturally occuring earthy material This scale is primarily used to define a clay mineral in geological and mineralogical investigations

throughout this thesis a slightly different particle size definition of a clay mineral will be used The technique of slaking a clay in water is commonly used to separate clay minerals from non-clay mineral components in a soil or naturally occuring earthy material When the soil is slaked the larger particles sink to the bottom, leaving the fine-grained clay minerals in suspension, and the larger clay mineral particles break down to a particle size of 2μm or less. The suspended clay particles may be collected and sedimented to give a reasonably pure clay mineral fraction, (this process of separating clay from non-clay minerals is covered in greater detail in section 2),

of a particle size not greater than 2μm.

The investigation of the structure and properties
of clay minerals has become a precise science. However the use of,
and experimentation with clays, dates from antiquity, when the
earliest earthenware vessels and ceramics were made. The first
serious scientific investigations of montmorillonite clay began
much more recently, when in 1847 Damour and Salvett[42] gave the
name montmorillonite to a clay from the Montmorillon region of
France At this time some of the properties of clays were being
studied and the results documented, (eg. in 1852 Way[3] investigated
the ability of clays to adsorb organic compounds (manures))

The chemical analysis of the clays, whose physical
properties were being examined, yielded little information. It was
found that all clay minerals had very similar chemical compositions,
consisting of mainly silica, alumina, magnesia and water in
varing amounts. However these clays of similar chemical composition
exhibited very different physical properties The difficulty
in obtaining a reasonably pure clay mineral, and the fine-
grained nature of the clay, caused this situation to persist
until the middle of this century, The development of separation
and preparation techniques for purifying clays, combined with
the electron microscope, infa-red, X-ray and differential
thermal analysis techniques have led to a rapid increase in the
knowledge and understanding of the relationship between the
chemical composition or structure of the clay and the physical
properties of that clay mineral

Clay minerals are today described as hydrous
aluminium (or magnesium) silicates. All clays have these fundamental
components with appreciable amounts of iron, alkalies, alkaline

earths and water. The great diversity of properties and similarity
of composition is explained by the differences in the structural
arrangments of these chemical components, which gives rise to
the diverse physical properties.

Simply clays may be described as layer silicates,
that is, comprised of layers or sheets where each sheet is
a two dimensional polymer of one of two basic unit cells. A very
brief mention of the structure of the 2:1 type layer silicate,
montmorillonite will serve to illustrate the basic structure of a
clay, (see Fig 1.1.)

The silicate layers are made up of three sheets,
formed from two basic structural units. The basic structural unit
of the tetrahedral sheet is a silicon cation with four oxygen
ions or hydroxyl groups, tetrahedially coordinated about the
cation. In a 2 1 type clay, two of these sheets are separated by
an octahedral sheet, which is a two dimensional polymer of an
aluminium cation octahedrally coordinated by six oxygen ions
or hydroxyl groups. (this structure is outlined in much greater
detail in the following chapter).

These layers of silica and alumina sheets carry
a net negative charge, (when isomorphous substitution has occurred)
It is this charge on the layers that gives rise to many of the
properties of a montmorillonite clay. Substitution of cations of
a different charge, than aluminium or silicon into the sheet
structure causes this accumulation of negative charge on the
clay layers This excess charge on the clay layers is balanced
by the sorption of additional exchangable cations between
the layers, (ie interlayer cations)

The charge on the layers also helps to maintain
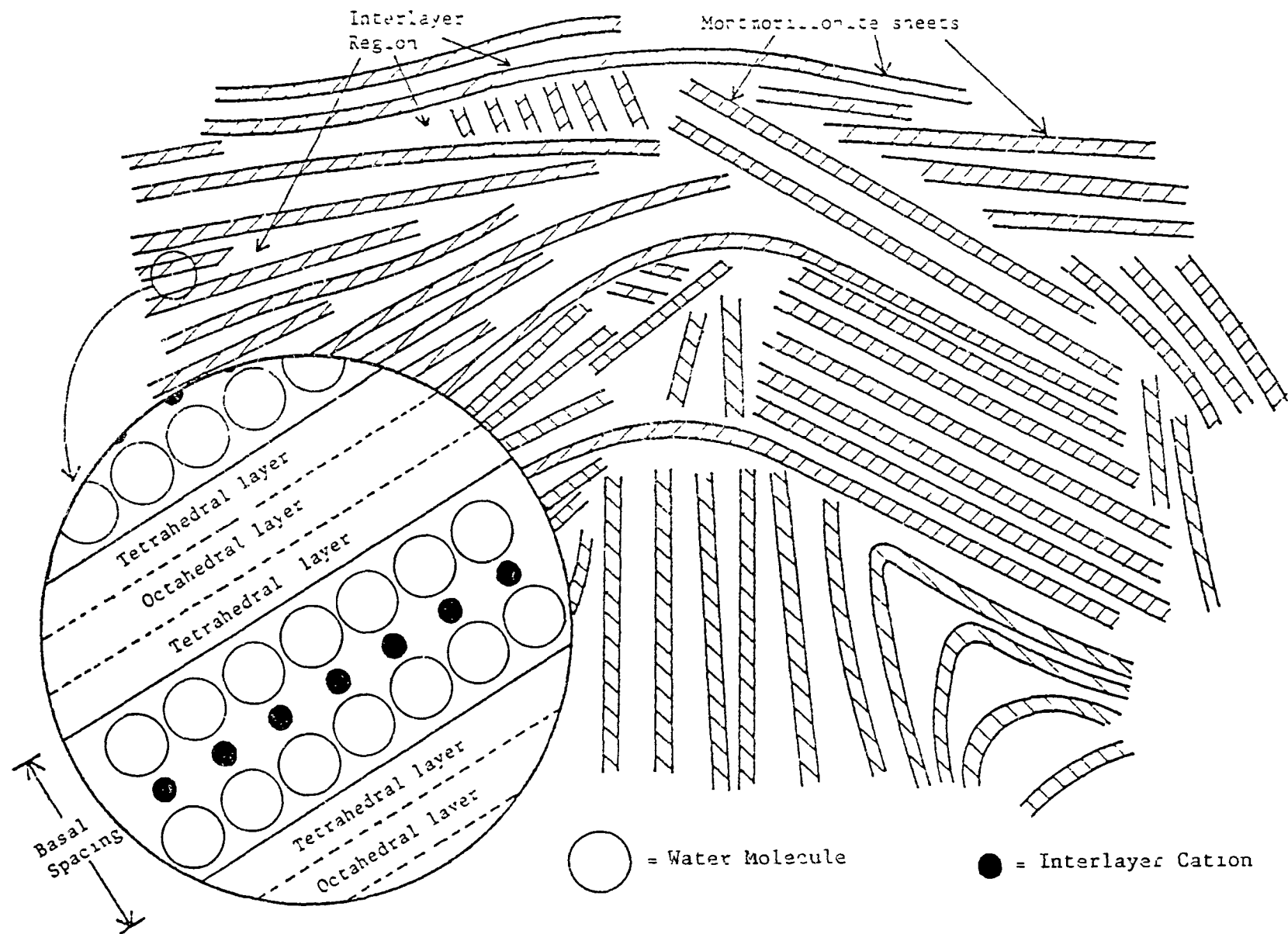
Fig 1.1. Schematic diagram of a clay grain, showing interlayer region in the insert. (adapted from Cebula et al[86])

the clay in a stable structural state. The electrostatic interactions between the negatively charged layers and the interlayer cations, combined with Van Der Waals forces and hydrogen bonding between the water molecules of the hydration sphere of the interlayer cations and the oxygen molecules and the hydroxyl groups of the tetrahedral sheets, bind the layers together.

The diversity of physical properties in clays with a similar structure is due to the possible substitution of cations in any of the three types of sites, ie. tetrahedral, octahedral or interlayer. An example of this is the swelling property of montmorillonite, that is the ability of the clay to absorb water into the interlayer space and so expand or swell. Although common in many clay types, it is the feature of montmorillonite that gives rise to one of its newer applications as a solid acid catalyst.

Ion exchanged montmorillonites may be used to successfully catalyse a great variety of chemical reactions. Table 1.i. gives a brief outline of the types of reactions for which this type of solid acid catalysts have been used. This is a short synopsis from a long list of reactions for which cation-exchanged montmorillonites may be used. If the formation of ethers is examined more closely, using reaction type 2 (from table 1.i.), the formation of Methyl-t-Butyl Ether (MTBE) from Methanol and Isobutene occurs, as an example. Then under certain conditions the acid catalyst will give a high yield of MTBE with very little production of impurities due to side reactions as shown by Adams et al[6]. The interest in the production of MTBE is due to its application as an alternative, non-lead based compound added to gasoline (or petrol), to increase

TABLE 1.i.

No.	Reaction Type.	Reference.
1.	Alkene + Water = Alcohol eg. $CH_2=CH_2 + H_2O = C_2H_5OH$	5,6
2.	Alkene + Alcohol = Ether. eg. $CH_3OH + CH_2=C(CH_3)_2 = CH_3-O-C(CH_3)_3$	7,8
3.	Alkene + Carboxylic Acid = Ester. eg. $CH_2=CH_2 + CH_3COOH = CH_3COOC_2H_5$	9,10
4.	Diels Alder Cycloaddition Reaction. eg. $CH_2=CH-CH=CH_2 + CH_2=CHR = C_6H_9R$	11
5.	Dehydration of Alcohols to Ethers. eg. $RCH_2CH_2-OH + R-OH = RCH_2CH_2-O-R + H_2$	12
6.	Elimination of Ammonia from Primary Amines. eg. $RCH_2-NH_2 + RCH_2-NH_2 = RCH_2-NH-CH_2R + NH_3$	13,14
7.	Elimination of Hydrogen Sulphide from Thiols. eg. $RCH_2-SH + RCH_2-SH = RCH_2-S-CH_2R + H_2S$	15

its octane rating. With increasing awarness of the environmental

damage caused by alkyl lead compounds, there is a parallel

interest in any process that provides cheap, alternative compounds,

such as the use of clay catalysts to synthesise MTBE.

The ability of smectite clays to catalyse such

reactions, to intercalate inorganic cations, and to absorb

water and organic molecules into the interlayer are all properties

of clays that have been exploited. In this thesis, the rate

of uptake and the relationship between the rate of uptake and

the structure and polarity of the molecules being absorbed,

will be investigated. Also the type of site on the clay to

which these adsorbed molecules bond, and the strength of that

interaction will be investigated for a variety of compounds,

in an attempt to understand the interlayer processes of a

cation-exchanged montmorillonite clay in greater detail.

CHAPTER 2

The Structure of Clay Minerals, Their Cation-Exchange
Capacity and Swelling Properties.

2.1. The Basic Sheet Silicates

All clay minerals are formed from two basic sheet-
forming units, the silicon tetrahedral unit and the aluminum
or magnesium octahedral unit These units combine to form
two-dimensional sheet structures, which are stacked one on top
of the other to form the clay layers in a clay particle.

2 1 i The Tetrahedral Sheet

The silicon tetrahedral unit (Fig 2 i a) is polymerised into
a two-dimensional array or sheet, by linkage of three oxygen
atoms at the base of each tetrahedron, with three adjacent
tetrahedra, to form a flat tetrahedral sheet The bases of the
tetrahedra all lie in the same plane and the apices all point
in the same direction (Fig 2 i b) The chemical composition
of the single tetrahedron is SiO_4 , and the chemical compositon
of the tetrahedral sheet is expressed as $Si_4O_6(OH)_4$, with open
hexagonal rings of oxygen atoms infinitely repeated in two
dimensions. (Fig 2 ii)

2 1 ii The octahedral Sheet.

The octahedral sheet is based on either an aluminum-
oxygen octagon (Gibbsite) or a magnesium-oxygen octagon (Brucite).
The aluminum or magnesium is coordinated with six oxygen atoms
or hydroxyl groups. The octahedral units (Fig 2 iii.a) are
polymerised into a two-dimensional array or sheet, known as
the octahedral sheet. Here the oxygen atoms and hydroxyl groups
combine to form two parallel planes with the cation lying
between these planes (Fig 2 iii.b.) The hydroxyl species is

$\bigcirc$ and $\bigcirc$ = Oxygens $\bigcirc$ and $\bullet$ = Silicons
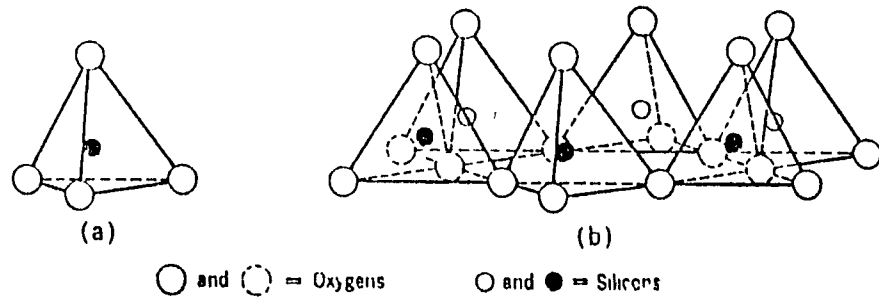
Fig. 2.1: Diagrammatic sketch showing.

(a) A single silica tetrahedron.

(b) The sheet structure of silica tetrahedrons.
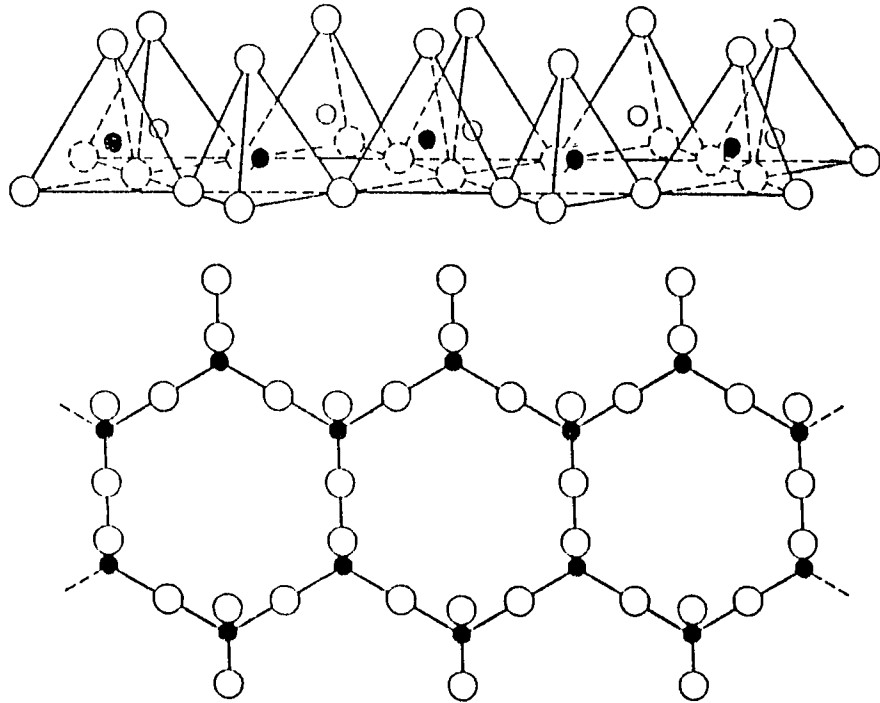
Fig. 2.11: A view of the silica tetrahedral sheet projected on

the plane of the base of the tetrahedrons, showing

the hexagonal network.

formed in the sheet when the oxygen atoms gain a negative charge, due to the bonding between the octahedrons in the sheet, and bind a proton (H^+) to satisfy their valancy requirments.

2.2 The Layer Silicates

The differences between the various types of clays is the way in which the tetrahedral and octahedral sheets combine to form the clay layer In fact the ratio of tetrahedral to octahedral sheets and the type of cation in the sheets, is the basis for a classification system used to assign clays to various groups (eg Table 2 1)

The symmetry and almost identical dimensions of the tetrahedral and octahedral sheets, allows for sharing of the oxygen atoms between the two sheets (Fig 2 iv.). When one tetrahedral and one octahedral sheet combine to form a layer, this is said to be a 1 1 type clay such as a kaolinite. If two tetrahedral sheets sandwich one octahedral sheet between them, this is known as a 2:1 type clay, of which smectite clays are an example This combining of the tetrahedral and octahedral sheets occurs when the oxygen atoms at the apices of the tetrahedral sheets are shared with the plane of oxygen atoms in the octahedral sheet (as shown in Fig 2 iv.)

2 3 The Structural Classification of Clays

Most clays fall into either the 1 1 or 2·1 type clay groups, and clays that are not members of these groups are usually structurally modified 1 1 or 2 1 clay types. Table 2.1. lists the major groups of clays and arranges them according to their structural classification It also gives some examples of the clay minerals belonging to these groups The differences between clays are often expressed in terms of the following three

○ and ◌ = Hydroxyls   ● Aluminums, magnesiums, etc
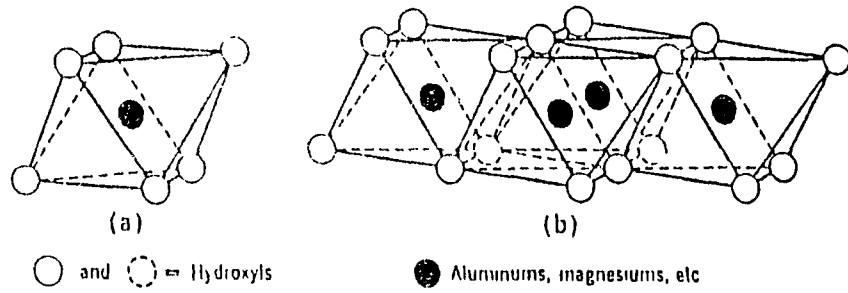
Fig. 2.iii· Diagrammatic sketch showing.

(a) A single octahedral unit.

(b) The sheet structure of the octahedral units.

Exchangeable cations
nH₂O

○ Oxygens   ⊚ Hydroxyls   ● Aluminum, iron, magnesium
○ and ● Silicon, occasionally aluminum
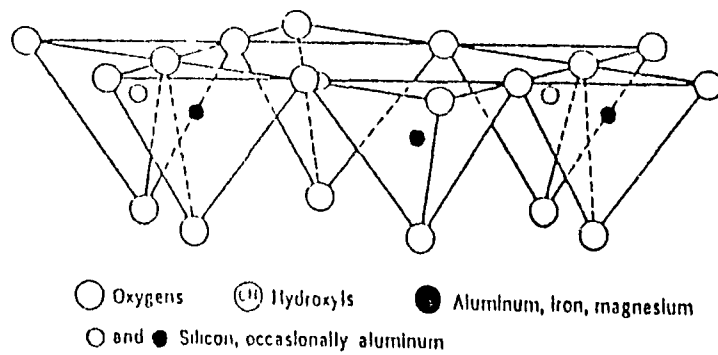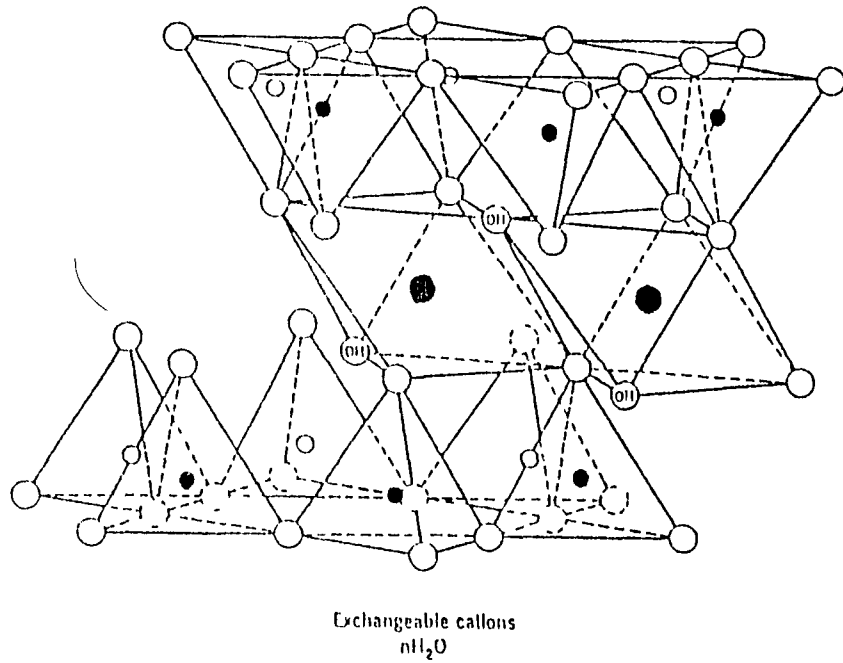
Fig 2.iv: Diagrammatic sketch of the combined tetrahedral and
octahedral sheets in a smectite clay.

parameters,

(i)   The layer charge.

(ii) Isomorphous substitution of interlayer cations.

(iii) Ability to intercalate water, organic molecules or cations.

This basis will now be used to examine some of the clay types

shown in Table 2 1.

(a) The Kaolinite-Serpentine Group

examples· kaolinite $[Al_4Si_4O_{10}(OH)_8]$

Chrysolite $[Mg_6Si_4O_{10}(OH)_8]$

(i)   Overall the layers are amphoteric carrying a negative

charge on one side of the layer and a positive charge

on the opposite side

(ii) Interlayer cations do not occur as hydrogen bonding

and strong electrostatic forces hold the layers tightly

together

(iii) Intercalation is limited, but is possible with polar molecules.

(b) The Pyrophyllite-Talc Group.

examples· Pyrophyllite $[Al_4Si_8O_{20}(OH)_4]$

Talc $[Mg_6Si_8O_{20}(OH)_4]$

(i)   Carry no layer charge

(ii) Isomorphous substitution does not occur

(iii) Intercalation is rare, although there have been some

reports that water molecules and organic molecules have

been detected between the layers.

(c) The Smectite Group.

examples: Montmorillonite $[(Na_{0.6})(Al_{3.4}Mg_{0.6})Si_8O_{20}(OH)_4]$

$[(Na_{0.6})(Mg_6)(Si_{7.4}Al_{0.6})O_{20}(OH)_4]$

(i)   Carries a layer charge of 0 5-1 0 units per unit cell.

(ii) Isomorphous substitution readily occurs, with the cations

absorbed to balance the layer charge.

TABLE 2.1.

Type	Clay Group.	Sub Group	Mineral.
1:1 1·0	Kaolinite-Serpentine	Di-octahedral Kaolinites Tri-octahedral Kaolinites	Kaolinite Halloysite Chrysotile
2:1 1·0·1	Pyrophyllite- Talc	Di-octahedral Pyrophyllite Tri-octahedral Talc	Pyrophyllite Talc
	Smectite	Di-octahedral Montmorillonite Tri-octahedral Saponites	Montmorillonite Nontronite Saponite Hectorite Glauconite
	Vermiculite	Di-octahedral Vermiculite Tri-octahedral Vermiculite	Vermiculite
	Illite	Di-octahedral Illite Tri-octahedral Illite	Illite
	True Mica	Di-octahedral Mica Tri-octahedral Mica	Muscovite Paragonite Phlogopite Biotite
	Brittle Mica	Di-octahedral Brittle Mica Tri-octahedral Brittle mica	Margarite Clintonite
2 1:1 (T·O 1 modified)	Chlorite	Di-octahedral Chlorite Tri-octahedral Chlorite	Pennine Donbassite Clinochlore Prochlorite

(iii)   Intercalation of a wide range of compounds is well
        documented[5 - 15]

(d) The Vermiculite Group

examples: Vermiculite $[(Mg_{0.6})(Al_4)(Si_{6.8}Al_{1.2})O_{20}(OH)_4]$

(i)   Carry a high layer charge of 1-2 units per unit cell.

(ii)   Isomorphous substitution occurs only in the tetrahedral sheet.

(iii)   Intercalation of water and organic molecules also occurs.

(e) The Illite Group

examples·   Illite $[(K_{1.6})(Mg_6)(Si_{6.4}Al_{1.6})O_{20}(OH)_4]$

(i)   Carry a layer charge of about 1 6 units per unit cell.

(ii)   Isomorphous substitution occurs, but exchange of the
        interlayer cations is difficult.

(iii)   Strong interlayer bonding makes intercalation very rare.

(f) The True Mica Group

examples   Muscovite $[(K_2)(Al_4)(Si_6Al_2)O_{20}(OH)_4]$

(i)   Carry a layer charge of 2 units per unit cell, causing
        strong interlayer bonding

(ii)   Interlayer substitution of cations is rare.

(iii)   Intercalation is also very rare.

(g) The Brittle Mica Group

examples   Margarite $[(Ca_2)(Al_4)(Si_4Al_4)O_{20}(OH)_4]$

(i)   Carry a layer charge of 4 units per unit cell, causing
        very strong interlayer bonding.

(ii)   Isomorphous substitution in tetrahedral sites only.

(iii)   Intercalation is consequently very rare.

(h) The Chlorite Group

examples   Donbassite $[Al_8Si_5O_{22}(H_2O)_7]$

           Clinochlore $[Mg_{12}Si_8O_{20}(OH)_6]$

(i)   No layer charge occurs in this group.

(ii)   Interlayer cations are not replaceable.

(iii)   Intercalation of water occurs only when the hydrogen

        bonding between the layers is disrupted.

Following this brief overview of the different clay types,

the mineral montmorillonite from the smectite group of 2:1 type

clays will be considered in greater detail

2 4 The Structure and Properties of Montmorillonite

A two-dimensional representation of the three-

dimensional structure of montmorillonite is shown (Fig 2 v.).

This is the Hofmann-Endel-Wilm[16] model of the structure of

montmorillonite, as modified by Marshal[24], Madgefrau and Hofmann[60], and

Hendricks[18] This is generally accepted as the structure of montmorillonite

and is the model that will be used throughout this thesis.

Montmorillonite layers differ from the other pyrophyllite

clay layers, in that the montmorillonite is an aluminous smectite,

ie Al^{3+} cations are isomorphously substituted by Mg^{2+} or Fe^{2+}

cations in the octahedral sheet This results in the accumulation

of a negative charge on the layers. Isomorphous substitution

of Si^{4+} cations by Al^{3+} cations in the tetrahedral sheet also

occurs, but to a much lesser extent.

The modifications of the Hofmann-Endel-Wilm model

suggested by Marshall and Hendricks, were to account for the

large cation exchange capacity of montmorillonites. They postulated

that the isomorphous substitution in the tetrahedral and octahedral

sheets, results in a negative charge on the layers. This charge

is balanced by the uptake of cations into the interlayer, the

electrostatic or Van der Waals forces between these cations and

the layers, not only maintains the clay in a stable structure,

but also accounts for many of the properties of a montmorillonite,
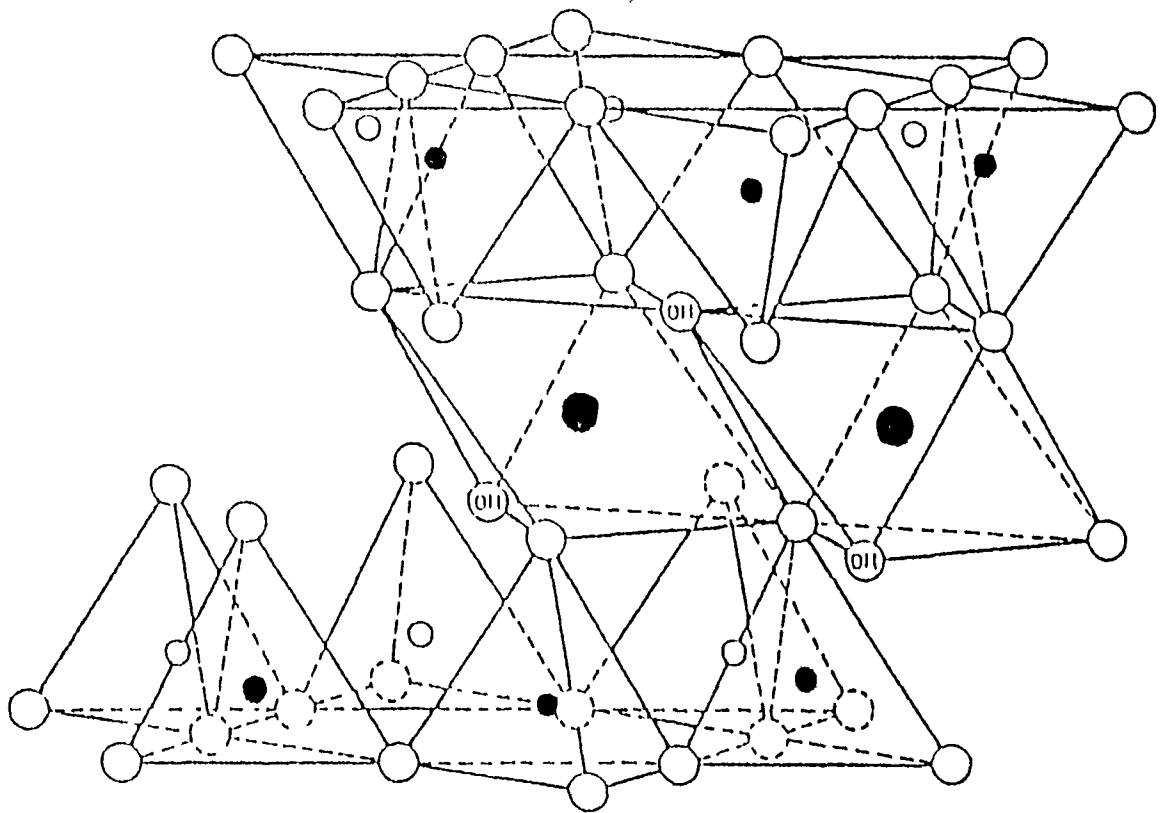
Lxchangeable cations

nH₂O
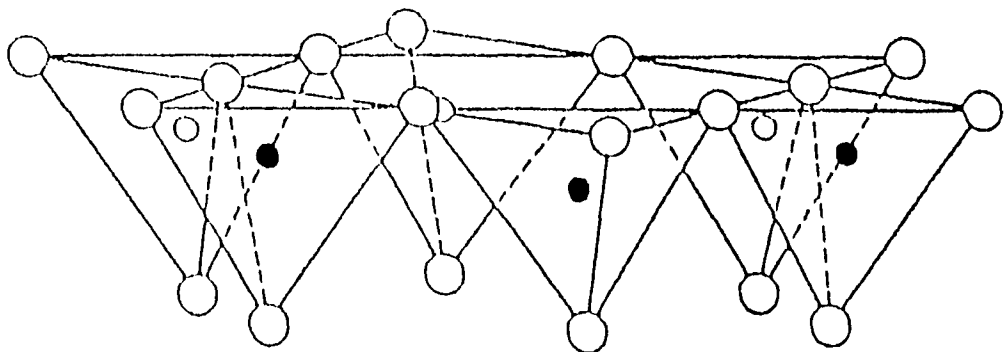
Oᵧygens   Hydioxyls   Aluminum, Iron, magnesium

and Silicon, occasionally aluminum

Fig. 2.v: Diagrammatic sketch of the Hofmann-Endel-Wilm and

Marshall-Hendricks model of a smectite clay.

especially intercalation of organic molecules and water.

It should be noted that Edelmann and Favajee[17] suggested an alternative structure for montmorillonite in the 1940's, as shown in Fig 2 vi This shows every alternate silicon tetrahedron in the tetrahedral sheet is inverted, so that all the apical oxygen atoms in the tetrahedral sheet do not lie in the same plane This was later modified from every alternate tetrahedron to 20% of the tetrahedrons in the tetrahedral sheet being inverted. This was to account for the observed cation exchange capacities of montmorillonite, which could not be explained by the previous suggestion Any gaps that occur in the structure as a result of inverting the tetrahedrons, are filled by hydroxyl groups, which also replace apical oxygen atoms on the outer side of the tetrahedral sheet

With this structure they suggest, no isomorphous substitution occurs in either the tetrahedral or octahedral sheets Dissociation of the hydroxyl groups on the layer surface is said to account for the cation exchange capacity of montmorillonite. This structure is not widely accepted today, although it has been suggested that the Edelmann-Favajee model is representative of a Cheto montmorillonite clay, and the modified Hofmann et al model represents the Wyoming montmorillonite clay In this thesis only the modified Hofmann et al model will be considered

2 5   The Cation Exchange Capacity of Montmorillonite.

Naturally occuring clay minerals have the ability to absorb certain cations, (naturally occuring montmorillonite is usually a sodium cation exchanged clay, although some calcium cations are often present). If this clay is exposed to a solution of a different cation, it is possible to replace the previously
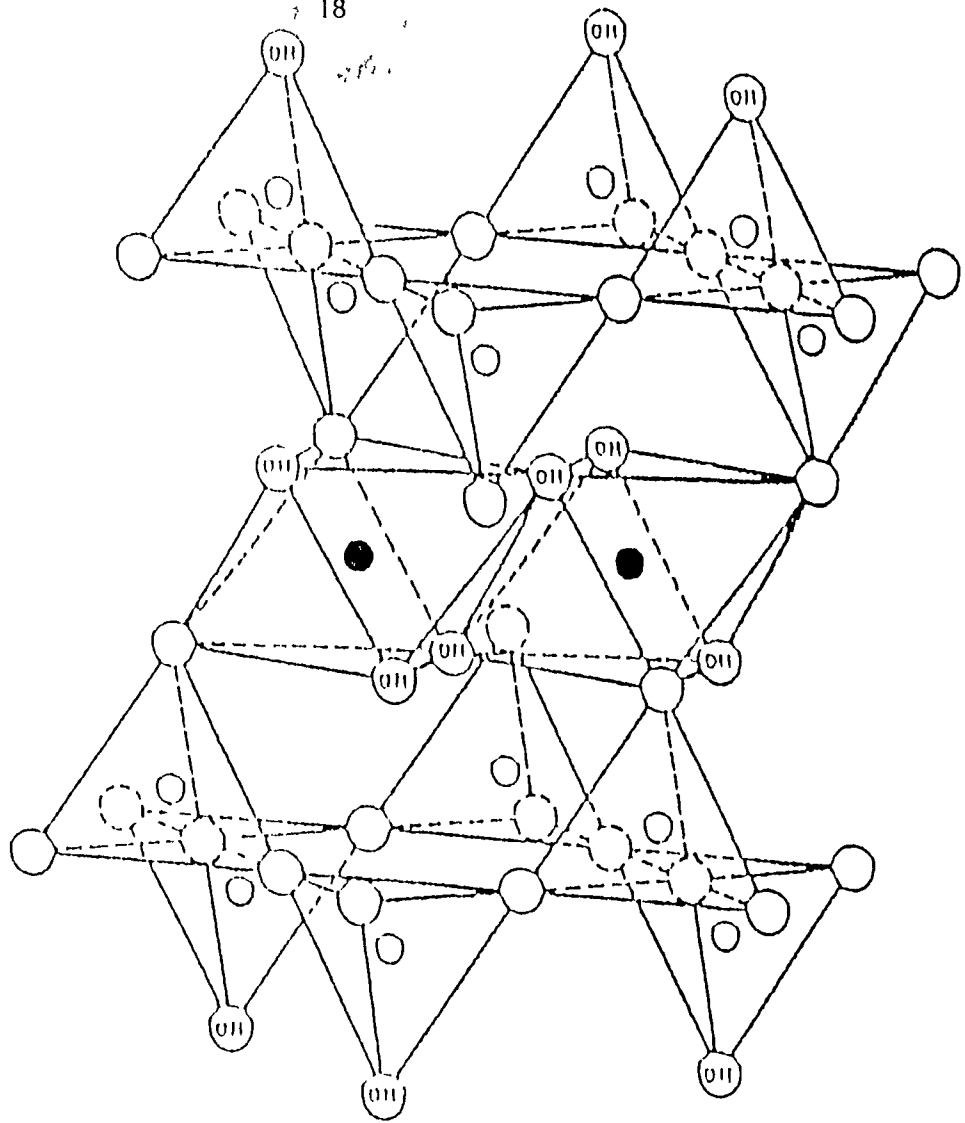
Exchangeable Cations

nH₂O
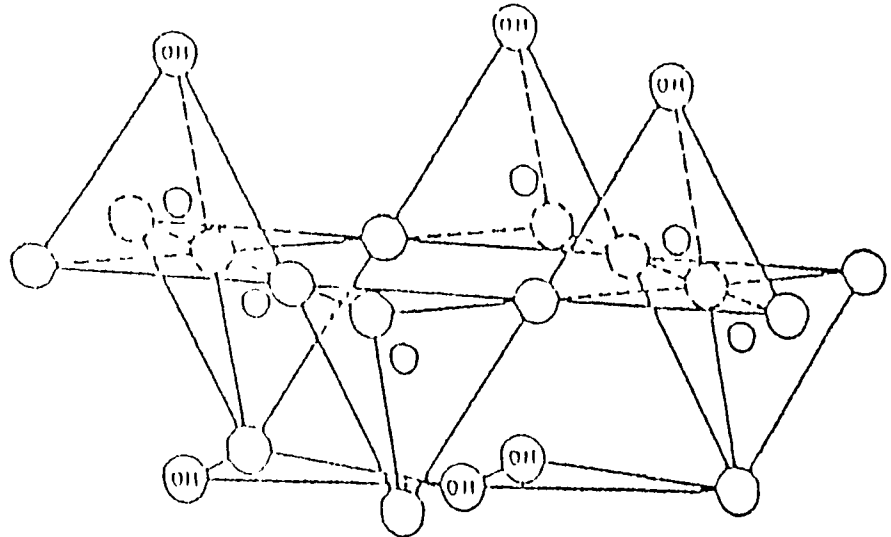
Fig. 2.vi: Diagrammatic sketch of the Edelman and Favejee model
of a smectite clay.

sorbed cations with those in the solution Attempts to determine the cation exchange capacity (cec) of a clay were among the earliest clay properties discussed in the scientific literature ie. Way's[4] paper in 1847 The cec of a clay is usually expressed in milliequivalents of exchangible cations per 100 grams of clay, (meq/100g), for montmorillonite this is usually 80-150 meq/100g The cec of a clay is influenced by several factors, and to a large extent depends on the structure of the clay.

(1) Broken Bonds at the Edges of the Silicate Layers

This is a significant factor in 1 1 type clays, such as halloysite as no isomorphous substitution occurs, so broken bonds become the major contributing factor to the cec of a 1 1 type clay In the case of 2 1 type clays, such as the smectite minerals isomorphous substitution is extensive, hence broken bonds account for only 15-20% (or less) of the total cec of these clays.

(2) Isomorphous Substitution

For montmorillonite clays this is usually Mg^{2+} or Fe^{2+} cations for Al^{3+} cations in the octahedral sheet, and less commonly Al^{3+} for Si^{4+} in the tetrahedral sheet. The negative charge on the clay layers caused by isomorphous substitution, is balanced by the uptake of cations into the interlayer or interlamellar space. This process accounts for about 80% of the total cec of a montmorillonite clay

(3) Replacement of the Hydrogen Atoms of Exposed Hydroxyl Groups

This is thought to account for any remaining cec of a montmorillonite, not already accounted for by the previous two processes. Consequently this represents a small amount of the total cec of montmorillonite clays Kaolinite or 1·1 type clays have an exposed plane of hydroxyl groups on one side of the silicate layer, so replacement

of the hydrogen atoms of these groups, would make a significant contribution to the total cec of kaolinite clays. However, this is not thought to be the case as the hydrogen ions or protons are very tightly bound to the oxygen atoms, making it difficult to displace them with a sterically large di- or tri-valent cation. Indeed this is one of the arguments against the Edelmann-Favajee model for the structure of montmorillonite, since the inversion of 20% of the silicon tetrahedron's in the tetrahedral sheet exposes a hydroxyl surface to the interlayer space, and displacement of the protons from these groups would have to account for about 80% of the cec of montmorillonite clays, and this is thought to be unlikely. Table 2 11 gives an indication of the magnitude of the cec's of different clay types

TABLE 2.11

Mineral	Cation Exchange Capacity.	
Kaolinite	3-15	meq/100g.
Halloysite $4H_2O$	40-50	meq/100g.
Montmorillonite	80-150	meq/100g.
Vermiculite	100-150	meq/100g.
Illite	10-40	meq/100g.
Chlorite	10-40	meq/100g.

2 6. The Exchangable Cations

The position of the exchangable cation in the clay structure is determined largely by the size and charge of the cation. Of the total cec of montmorillonite approximately 20% of the exchangable cations are assocated with broken bonds at the edges of the silicate layers. Here the cation is held beside

2 1

the negatively charged site, or it may be bonded to an oxygen atom

of a dissocated hydroxyl group. The remaining 80% of the cec is

due to the exchangable cations being held on or between the

basal surfaces of the silicate layers. This occurs when a

negative charge accumulates on the clay layers due to isomorphous

substitution within the layer structure.

The positions of sites within the interlayer occupied

by the cations depends greatly on the hydration state of the clay.

For example, in an anhydrous montmorillonite the cation may

occupy the hexagonal cavity in the tetrahedral sheet,(see Fig 2.iii.).

if the cation is small enough If the clay becomes partly hydrated

and adsorbs one layer of water into the interlayer the cation will

remain in the hexagonal cavity. However, when two or more layers

of water are adsorbed by the clay, the cation is displaced and lies between

the two layers of water, ie separated from the basal planes

of the montmorillonite by a layer of water (Fig 2.vii.) on each

side The precise position of the cation in the interlayer

not only depends on the hydration state of the clay, but also

on the charge and size of the cation in question. However, the

20% of the cations bound at the clay layer edges are unaffected

by the hydration state of the clay.

The term ion-exchanged clay refers to a clay whose

available cation sites are saturated, usually with the naturally

occurring cation, mostly sodium in the case of montmorillonite

These cations are then exchanged or replaced with a different

cationic species using a cation exchange process. However not every

cationic species is exchangable, and the following rules govern

weather a cation is exchangable or not.

(i)   Ions of higher valency replace those of lower valency, and

are bound more tightly to the interlayer exchange sites.

(ii)   If the ions have the same valancy. The larger the ion,
the better it will be at displacing a smaller ion of the same
valency This rule holds until the exchanging ion's size and
coordination properties do not allow it to fit the hexagonal
cavity of the tetrahedral sheet optimally It should be noted
that hydrogen is an exception to these rules as it can behave
as a di- or tri-valent cation

2.7. Sorption by Clays.

2.7. i.   Adsorption of Water by Layer Silicates.

          Swelling or the adsorption or intercalation of
water into the interlayer space causes the basal spacing of the
clay (Fig 2.viii) to increase, or the clay to increase in
volume, ie swell. This processes is greatly influenced by
the nature of the interlayer cations . The water in the interlayer
is an integral number of water molecules thick. The number of
layers of water formed was shown to depend upon the exchangable
cation and the partial pressure of the water Norrish[20] showed
that the layers of a sodium montmorillonite could be expanded,
stepwise, (ie water layer on top of water layer), to a basal
spacing of 40Å (anhydrous sodium montmorillonite has a basal
spacing of about 9 6Å) When the basal spacing increases above
40Å the layers are taken to be completely dissociated. However
it was also shown that calcium montmorillonite clay could not
be significantly expanded beyond 15.4Å, and this basal spacing
corresponds to two layers of water in the interlayer. This
type of limited expansion was also found for potassium and
magnesium cation-exchanged montmorillonite clays This agrees
with Ballantine et al's[43] findings that the physical characteristics of

23

Silicate layers

Cation held between
the water layers

Cation in the hexagonal cavity of the
tetrahedral sheet of the silicate layer

◯ = Water Molecule.
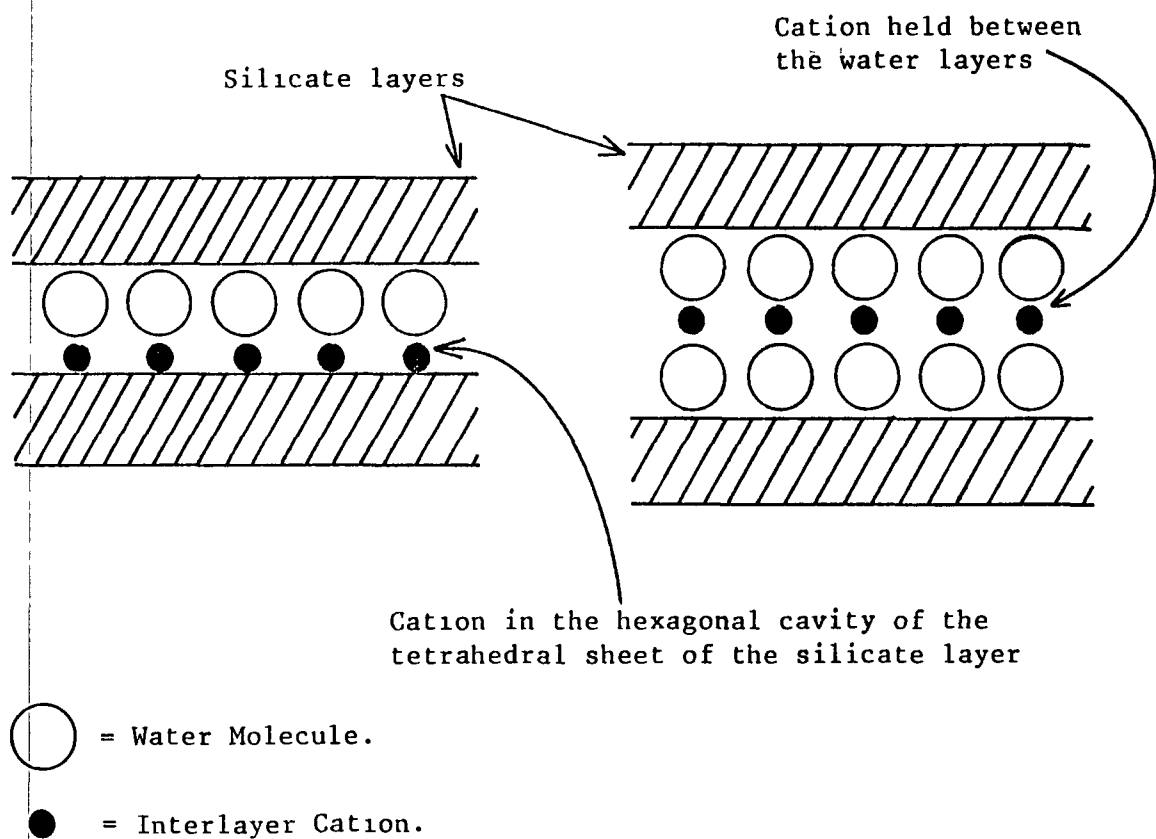
⬤ = Interlayer Cation.

Fig 2.vii. The location of the cation in hydrated montmorillonite.

(note, this depends on the water content of the clay)

$(H_2O)_{in}$ →

Increased
basal
spacing
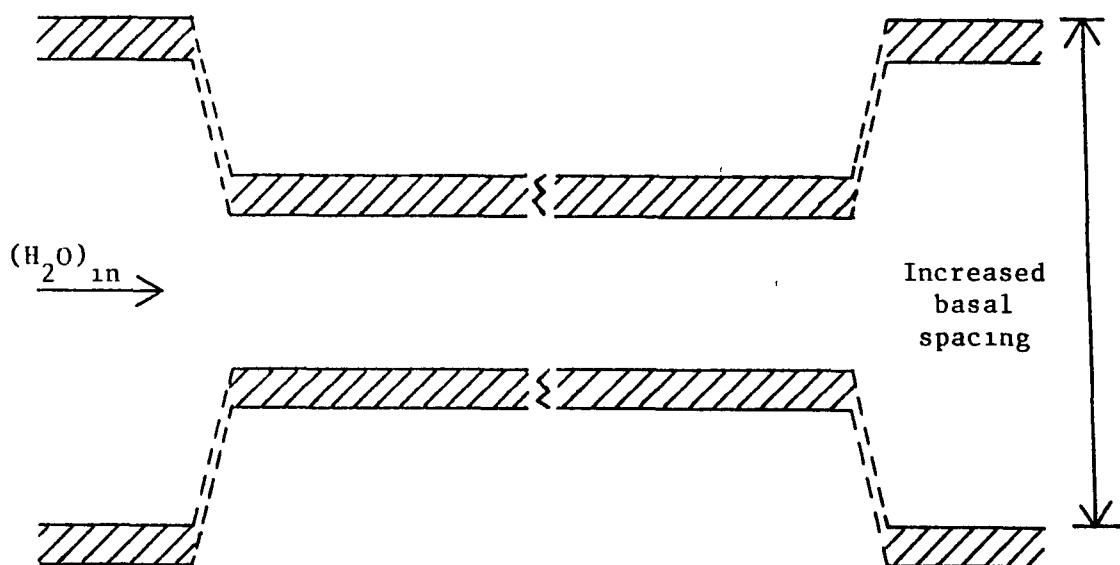
Fig 2.viii. The expansion of the clay layers upon intercalation.

(note, the clay layers expand from the edges inwards)

smectites are related to the interlayer sheets of water. Also
the layer charge which is low for montmorillonites (see
section 2.3.C), influences the tendency of the clay to
intercalate water layers, and other organic molecules
The clay minerals with a high layer charge have a lower tendency
to intercalate water or organic species by swelling, as the
electrostatic interactions between the layers and the cations,
make it more difficult, (ie more energy is required), for
the intercalating molecules to force the layers apart.

Interlayer water molecules have been found to
be very stable, and this is thought to be due to the fact
that six water molecules fill the coordination or hydration
sphere of the interlayer cations, forming hydrogen bonds
with the oxygen atoms and hydroxyl groups of the silicate
layers Futher uptake of water is thought to form hydrogen
bonds with the existing oxygen atoms of the water in the cation
hydration sphere, and the oxygen atoms and hydroxyl groups
of the silicate layers This continues with certain cations
such as sodium until the interactions between the silicate
layers and the cations in a water suspension are so remote
that the layers may be considered to be competely dissocated.

2 7 (ii).   Adsorption of Polar Organic Molecules on Inorganic

Cation Exchanged Clays.

Polar organic molecules are readily intercalated
by many clay minerals and especially by ion-exchanged
montmorillonite clays Fig 2.ix. represents Mac Ewans [22] findings
that a halloysite or 1·1 type clay intercalates a single layer
of polar organic molecules, due to the ampholetic nature of the
halloysite layers Montmorillonite on the other hand can form

multilayers of interlayer polar molecules, due to the overall

negative charge on the montmorillonite layers. Recent infa-red

studies[23] have shown that polar organic molecules in the interlayer

do not follow the pattern shown by the simple model in Fig 2.1x.

But they actually compete with water molecules in the hydration

sphere of the interlayer cation, occupying sites in the outer

coordination sphere of the cations In some cases such as a

strongly polarising cation, the polar organic molecules can

occupy sites in the inner coordination sphere of the cations, and

Al^{3+} cation-exchanged montmorillonite clay gives an example

of this effect.

2 8.   Sedimentation of Montmorillonite as a Separation Technique.

This is based on Stokes'Law for particles of a

radius, a, falling with terminal velocity, v, through a liquid

medium viscosity, §

$$F = 6\text{¶}a\text{§}v$$

F = the force on the particle

The international standard maximium limit is ~2μm for the

particle diameter of a montmorillonite clay. The solution

of clay and water is mechanically stirred for one hour to ensure

an even distribution of clay particles throughout the water. This

solution is allowed to stand for a calculated time, and the top

10cm fraction of the solution is siphoned off This is then

centrifuged to sediment the clay particles. A reasonably pure

clay is obtained, as most of the impurities such as micas, quartz,

and ioin-oxide bonded platelets have a greater density

than the clay fraction, so they will sink further than 10cm

during the sedimentation period

So assuming spherical particles Stokes' Law becomes,
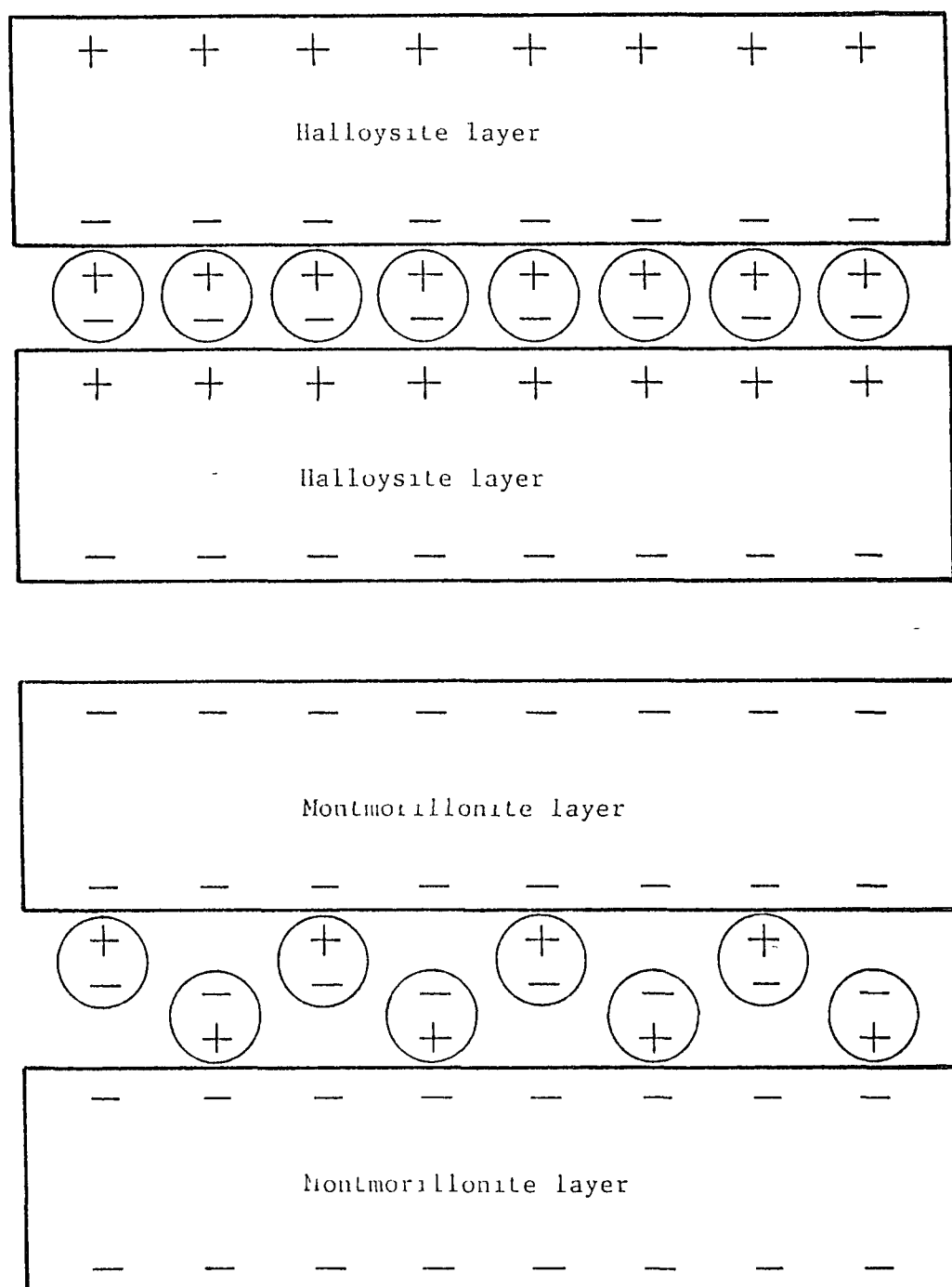
Fig 2.1x.   Schematic diagram of the positions of polar molecules
in the interlayer of a 1 1 type clay and a 2.1 type
clay (note, the amphoteric nature of the 1 1 type clay)

$$F = mg = (4/3)\P a^3 Yg$$

where Y = the particle density = 2.65×10^3 Kgm^{-3}

$a = 10^{-6}$ m

$\S = 10^{-3}$ Kgm^{-1}s^{-2} (at 20°c)

v = distance/time = d/t

$g = 9.81$ ms^{-2}

therefore, the sedimentation period is :-

$$t = (9/2)\S(d/Ya^2 g)$$

So if the clay solution is left to stand overnight (> 16 hours)

the particle size obtained will be <1.4µm, hence conforming

to the international standard particle size definition.

CHAPTER 3

Experimental Procedures.

3.1   Preparation of the Basic Montmorillonite Clay

A raw or unprocessed Wyoming montmorillonite clay was used, (supplied by Volclay Ltd., Wallasey, Cheshire). The raw clay is processed using a sedimentation technique to remove impurities such as flakes of mica, quartz and other non-clay minerals, leaving a sodium exchanged montmorillonite clay (this may be 80% sodium and 20% calcium depending on its origin).

Firstly a suspension of approximately 10g clay/1000 cm^3 of distilled water is mechanically stirred for 1 hour. The container is then covered and left to stand overnight (ie >16 hours), the upper 10cm fraction of the suspension is then siphoned off and stored, (the explanation for these times and volumes is given in chapter 2 section 8) the volume of suspension removed from the container, is replaced with an equal volume of distilled water, stirred for 1 hour, and the whole process is repeated 3 or 4 times with the siphoned off fraction (this contains the clay of intrest) being stored each time. The initial stock suspension may then be disgarded as it contains mainly the impurities from the raw clay.

The stored fractions contain the sodium exchanged montmorillonite clay of a particle size <2μm. This clay is extracted from the suspension by centrifugation, with the water being disgarded and the clay sludge being left to air dry on a clock glass for 1 or 2 days, in an atmosphere that is free from solvent vapours. When dry the clay is ground to a fine powder using an electric coffee mill or a pestle and mortar, and is stored for use at a later date.

3 2. Preparation of Cation Exchanged Montmorillonite Clays.

The sodium exchanged montmorillonite clay is the usual naturally occurring form of the clay, and as described in chapter 2, it is possible to prepare other cation-exchanged forms of montmorillonite For these studies three ion-exchanged forms that are commonly used clay catalysts were chosen, ie.aluminium-exchanged montmorillonite (Al^{3+}-M), chromium-exchanged montmorillonite (Cr^{3+}-M), and iron-exchanged montmorillonite (Fe^{3+}-M) The technique used to prepare these clays is identical in each case, except,that the appropiate salt is used to give the cation required, eg. aluminium sulphate for a Al^{3+}-M clay.

A 0 3M solution of the sulphate salt of the appropiate cation is prepared. The air dry, previously prepared sodium-exchanged clay is added to this solution while continually stirring with a magnetic stirrer, in a ratio of 5mg clay/40cm³ of sulphate solution. The resulting suspension is stirred vigorously for 30 mins. and then centrifuged at 3000rpm for a further 30 mins The supernatant is disgarded and the clay resuspended in an equal volume of distilled water. This suspension is again stirred for 30 mins., and centrifuged for 30 mins. at 3000rpm and the supernatant disgarded This is regarded as one wash, and is repeated until the clay has been washed at least 6 times This washing is to remove any of the unadsorbed cations that may get trapped between the clay particles during centrifugation. To check that the clay has been throughly washed the supernatant from the sixth or final wash may be given a U.V scan to detect the presence of any remaining sulphate salts. Also if the appropiate sulphate salt is not available, a good second preference is the nitrate salt of the cation

When the washing is complete the clay sludge is spread

on a clock glass, dried and ground to a fine powder as before.

The efficiency of the exchange process may then be tested using a

back exchange technique

A final important note about the exchange procedure

is that the PH of the sulphate solution, the clay suspension and

each successive suspension after washing is monitored. It is best

to maintain the PH below PH 3 as a neutral or alkaline PH could

lead to the formation of hydroxy-metal species on the clay surface.

The coatings of hydroxyl groups on the surface can cause erroneous

results in the interpretation of the results of diffusion and

adsorption studies involving that clay. Should the PH rise above

PH 3 it may be reduced using a few drops of $Conc.H_2SO_4$, if a

sulphate salt is being used, or $Conc.HNO_3$, if the nitrate salt

is in use.

3.3 Preparation of Infra-Red Films and X - Ray Diffraction Slides.

X-Ray diffraction slides are prepared using standard

glass microscope slides cut in half to form two glass squares

approximately $2x2cm^2$ These are then coated with a layer of the

clay slurry (before the prepared clay has been allowed to dry)

The thickness of the clay layer is not critical in XRD slides,

however a film of 0 5-1.0mm thick is adequate. These slides are

then labelled and air dried in an atmosphere free from solvent vapours,

when dry they may be stored in a dessicator until required.

Infra-red films are also prepared from the clay slurry

before it is dried, using a polyethylene sheet to prepare the clay

films. A sheet of polyethylene approximately 2cm wide is taped

across a glass plate (Fig 3.1.), a few drops of the clay slurry

are placed on the end of the sheet, and are spread along the sheet

using the glass rod shown in Fig 3 11. This rod acts like a rolling

pin to spread the clay along the polyethylene sheet. However the rod
is raised from the surface of the sheet by 3 layers of 'Sellotape'
which effectively governs the thickness of the clay film on the
polyethylene sheet The clay is then left to air dry as before,
after which the clay film is removed from the polyethylene sheet
by stretching it across a blade, causing the film and sheet to
separate (Fig 3 iii). The clay is then cut into flakes approximately
2x2cm^2, as this size is adequate to fill the sample holder in the
I.R cell.

Some important points to note about this technique,
are that the thickness of the clay film is critical, ie. if the
clay film is too thick it will not transmit the I.R. radiation
and is useless, yet if the film is too thin, it will fall to
pieces when it is removed from the polyethylene sheet . Consequently
the clay film must be thick enough to be self-supporting and thin
enough to transmit the I R radiation. The viscosity or density
of the clay slurry used to make the films influences these factors
greatly If the slurry is too thick or has a high clay water
ratio the film will be too dense to transmit the IR radiation,
and will be of little use Conversely if the clay water
ratio is low the film will be too weak to support itself when
removed from the polyethylene backing and so will crumble
to pieces As a general rule, equal volumes of distilled water
and clay slurry from the end of the centrifuge tube will give a
suitable clay water ratio, to make a good I.R. film.

The optimal thickness of the film was found to be
3 layers of 'Sellotape', any less and the films crumbled, any
more than 3 layers and the films were to dense to transmitt I.R.
radiation. Once prepared the I.R. films were placed in holders
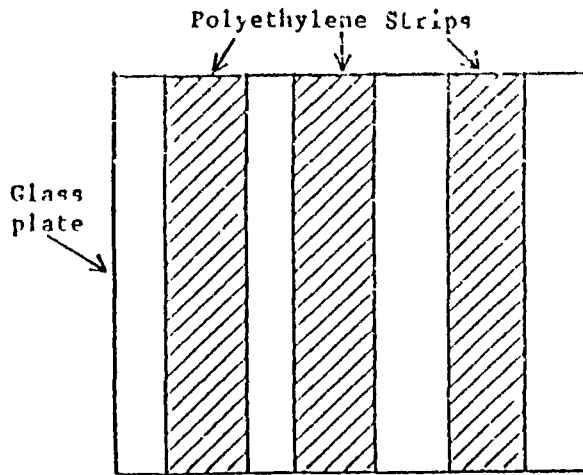
Fig 3.i. Schematic diagram of the glass
plate used to make clay films.
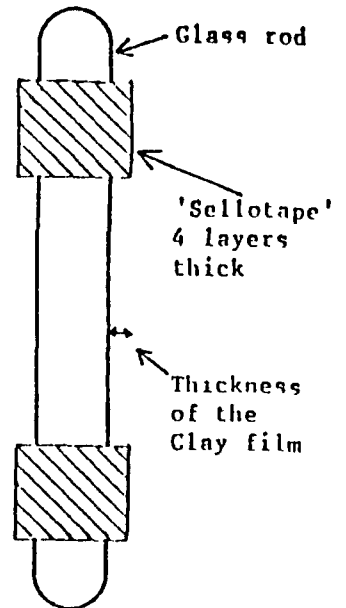
Fig 3.ii. Schematic diagram
the roller used to
make the clay films
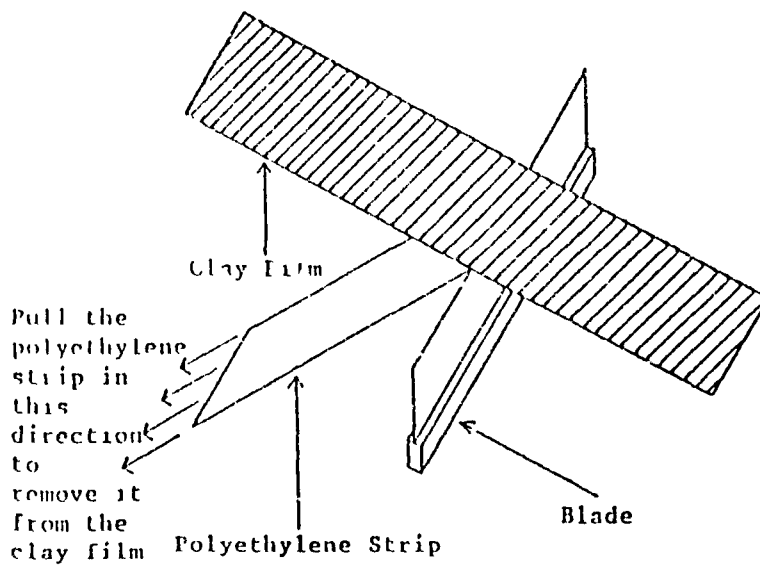
Fig 3.iii Schematic diagram of the method used to remove the clay
film from the polyethylene strips
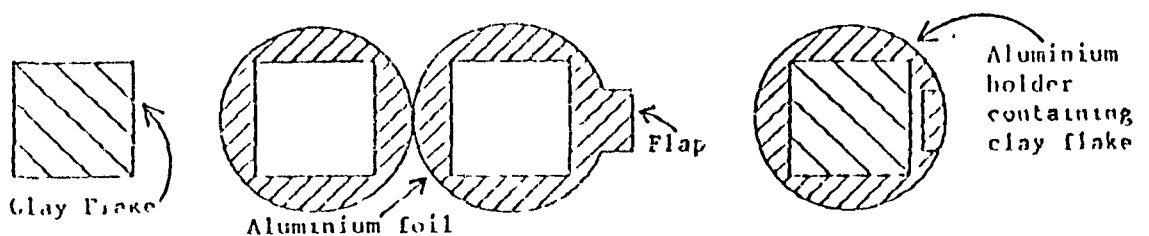
Fig 3 iv. Schematic diagram of the clay flake holder for the IR cell.
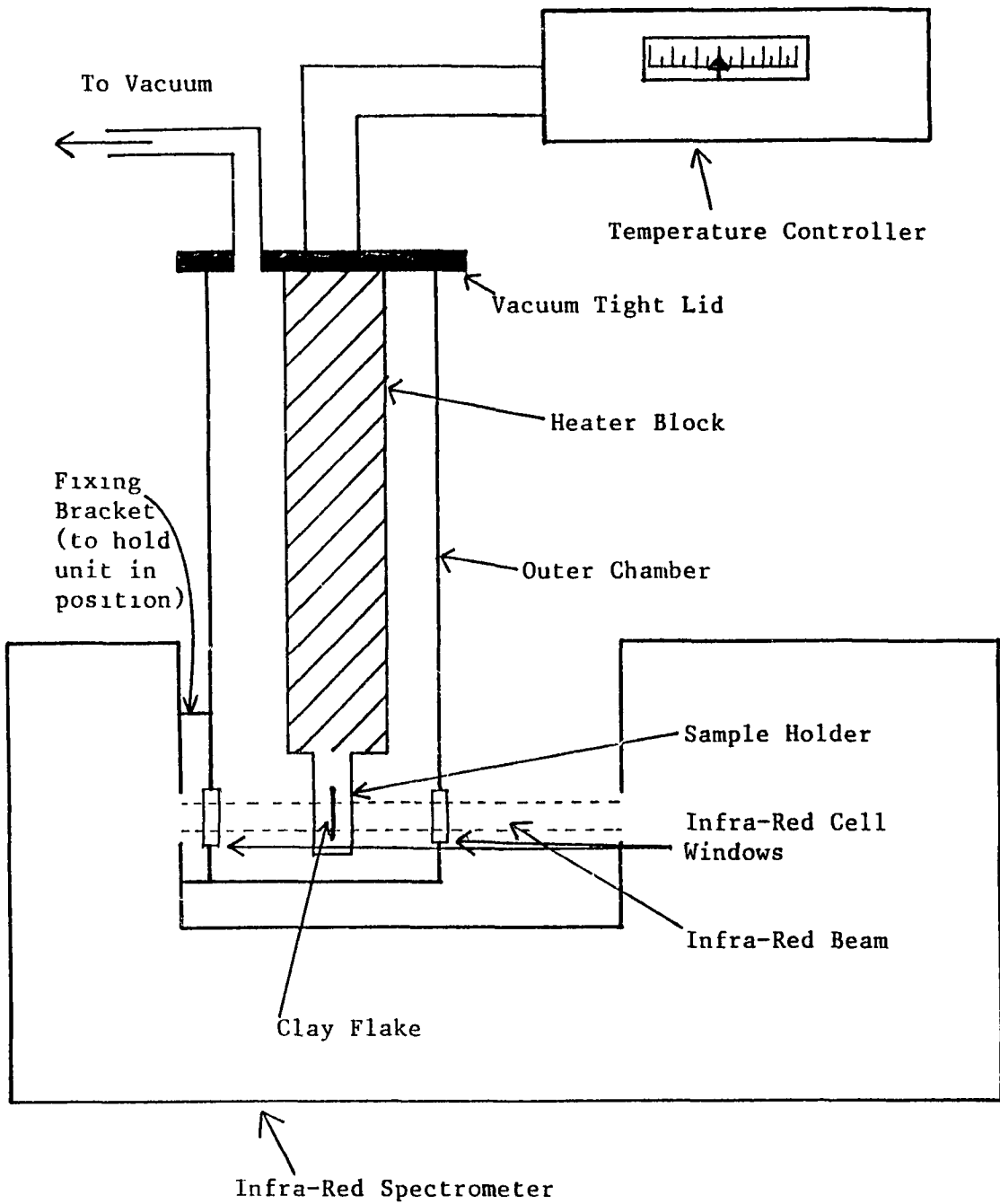
Fig 3.v. Schematic diagram of the infra-red variable temperature cell used to record the infra-red spectrum of the clay flakes at various temperatures under vacuum.

cut from heavy duty aluminum foil (Fig 3.iv.) labelled and stored

in a dessicator with the XRD slides. This holder serves two

purposes, firstly it provides protection for the fragile clay film

while moving it about, and secondly it fits tightly into the

circular sample holder of the variable temperature cell of the

I R instrument, (Fig 3 v).

3.4. Grain-Size Preparation

The clay powder perpared and ground as described in

3.1. and 3 2. was graded according to its grain size for use

throughout these investigations The clay was ground to a fine

powder in one of two ways, for clay samples of >1g an electric

coffee mill was used to circumvent laborious hand grinding For

clay samples <1g a pestle and mortar was used, because the coffee

mill did not work efficiently with small quantities of clay.

Once ground to a powder the clay was separated into

the following grain size groups.

(i)   >250μm

(ii)   250-125μm

(iii)   125-65μm

(iv)   65-45μm

(v)   <45μm

This was done using sieves with the appropiate mesh size supplied

and certified by Retsch, Haan, West Germany. After sieving, the

different clay fractions were stored in glass vials in dry

conditions where no solvent vapours were present.

3.5.   Thermal Gravimetric Analysis   (TGA)

The diffusion or uptake experiments were carried

out using a Stanton Redcroft TG-750 Thermobalance in conjunction

with a purpose built gas delivery system and a dual pen Linseis

Nitrogen gas from cyclinder

Dry nitrogen or vapour saturated nitrogen

'3-way' Taps

Counterweight

Drying column

Sample

Furnace

Pressure release tube

Temperature

Mass

Bubble chamber

Liquid of intrest

Blowback chamber

35
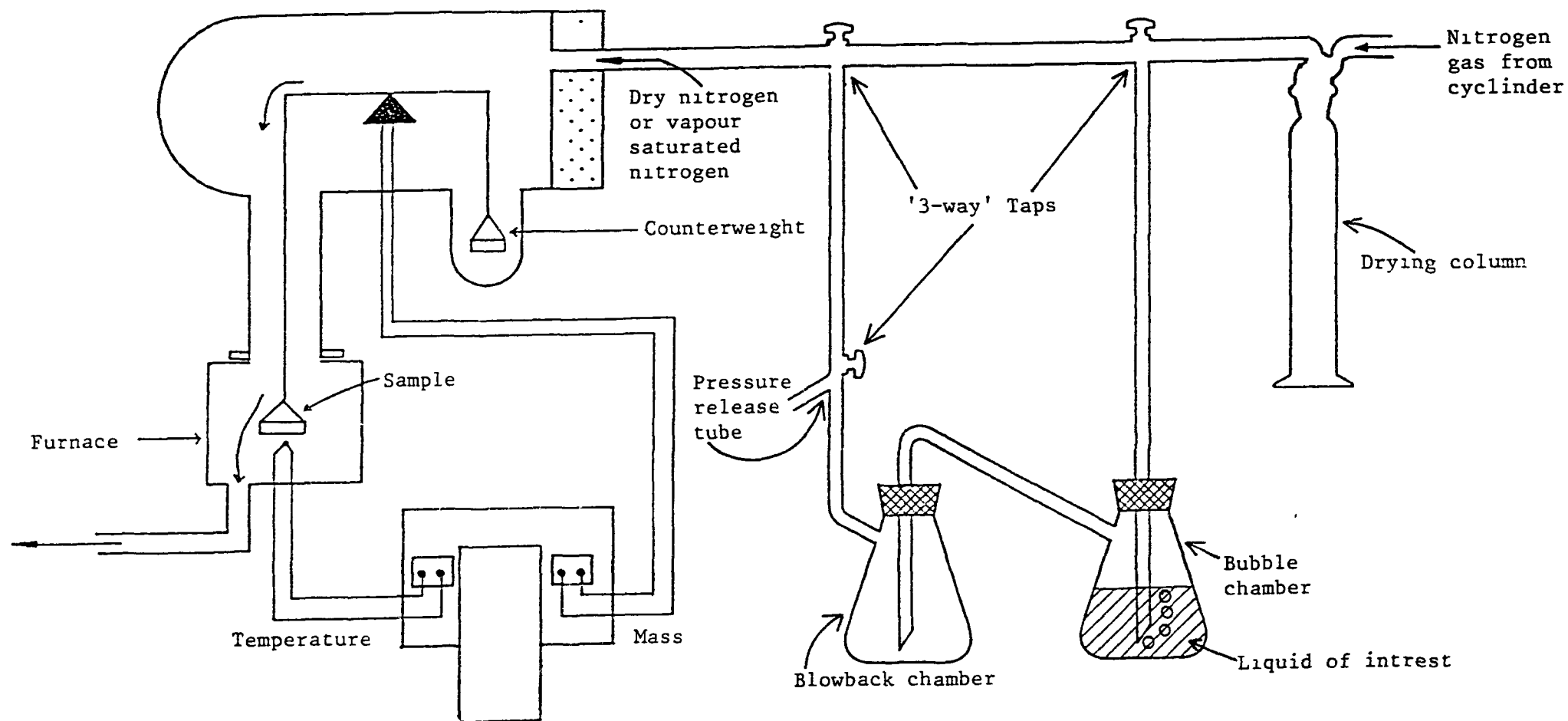
Fig 3.vi. Schematic diagram the thermobalance and the gas delivery system used throughout the experiments

chart recorder (Fig 3 vi) The same experimental set up with the

addition of a derivitising unit on the balance output was used

for the temperature programed desorption studies, using different

operating conditions as detailed in section 3.6.

The furnace was calibrated in the range 18-305°C using

the known melting points of the compounds listed in table 3.1.

Table 3 1

Melting Point Temperature (°C)	Compound.
42-44	Diphenyltindichloride
70-73	2,2'-Bipyridyl
104-105	Triphenyltinchloride
187-189	4-Aminobenzoic Acid
205-207	3,5-Dinitrobenzoic Acid
237-241	Dimethylglyxoime
302-305	2-Mercaptobenzimidazole

The dry nitrogen gas was passed through a drying

column, consisting of a 4Å synthetic zeolite, followed by P_2O_5

with a visible moisture indicator (ie. it turned green on contact

with water). The nitrogen flow was measured at the output from the

thermobalance, using a bubble flow meter and a stopwatch. For the

diffusion studies a flow of >250cm^3min^{-1} was found to be optimal

(Fig 3.vii)

A sample weight of 5mg was used for most of the studies

and if the weight was different from 5mg it is written on the

appropiate graphs or tables. Generally a heating rate of 20°Cmin^{-1}

was used to heat the furnace in conjunction with a chart speed of

20cm hour^{-1}

The typical experimental run procedure was as follows:

a sample of clay was placed in the sample bucket and preheated
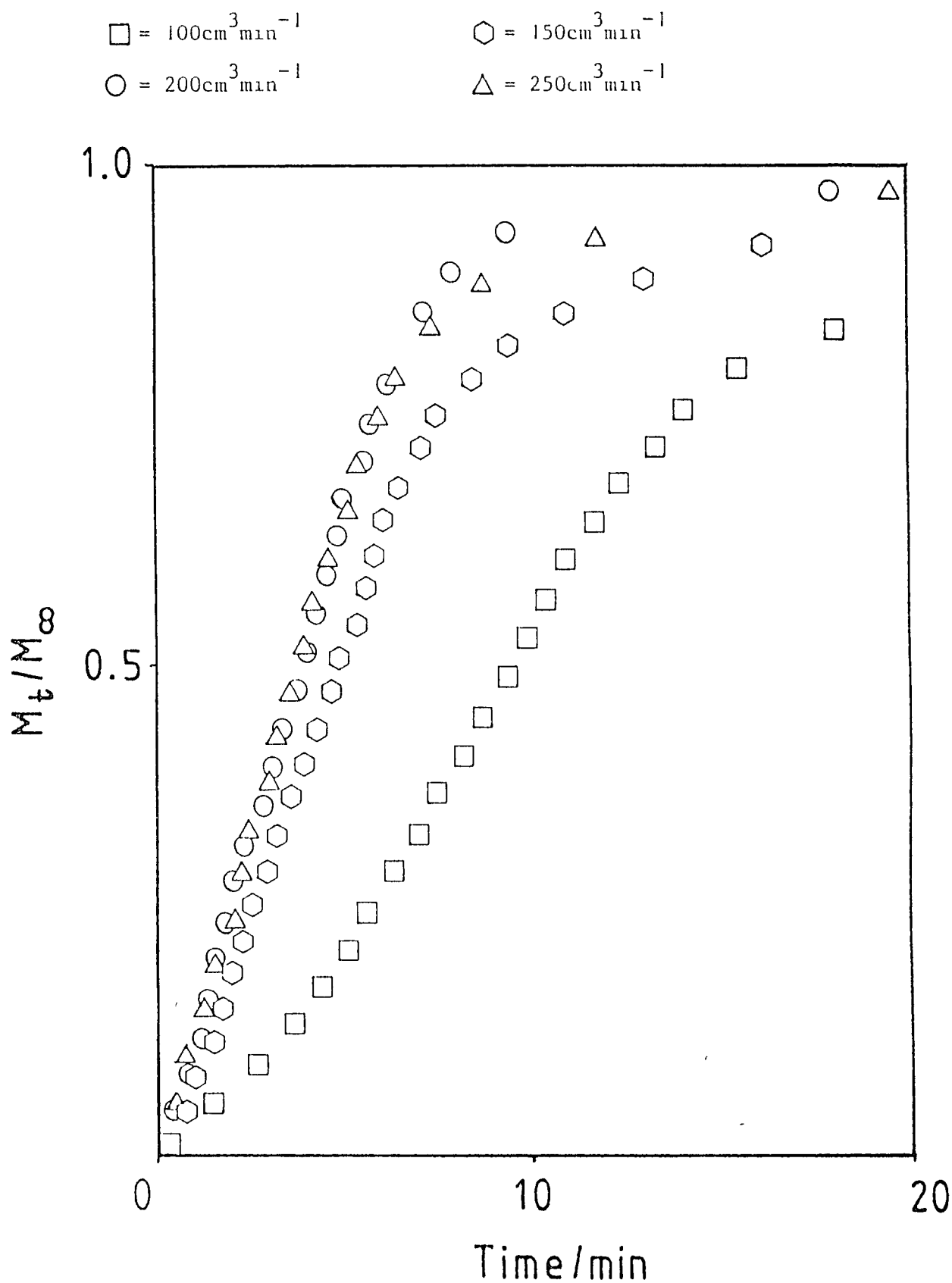
Fig 3.vii   Optimization of the flow rate for the uptake of

1-propanol upon Cr^{3+}-montmorillonite at $18°C$.

to 120°C at 5°Cmin^{-1} in a flow of dry nitrogen of >250cm^3 min^{-1}. The

temperature of the sample was maintained at 120°C for 15min or until

no further weight change occured The sample was then allowed to

cool to a known temperature (18°, 43°, 72° or 105°C), and by the turn

of a tap the dry nitrogen was directed through the alcohol reservoir.

This time was taken as zero for the mass uptake experiment.

Between runs (particularly when a change of alcohol was

necessary) the thermobalance was purged with dry nitrogen at a flow

rate in excess of 1000cm^{3}min^{-1}, whilst heating the furnace to 500°C

over a 30min period and then allowing it to cool. After cooling the

furnace, a clay sample was added to the sample pan and, if no

deviation from the baseline occurred within 15min, further purging

was considered unnecessary. (eg. typical trace from an experimental

run as described above is shown in Fig 3.viii.).

3 6. Temperature Programed Desorption   (TPD)

The studies were carried out on essentially the same

experimental setup as the TGA studies The output from the thermo-

balance was relayed to the chart recorder using a derivitising unit

(this gives the derivitised weight loss signal (Fig 3.ix.)). Also the

dry nitrogen flow is not run through the bubble chamber, so it is

never saturated with solvent vapour The nitrogen flow was 50cm^{3}min^{-1}

for the TPD experiments The furnace was heated to 800°C at 20°Cmin^{-1}

and the chart recorder was run at 20cm hour^{-1}. A sample weight of

7-8mg was used for all of the TPD experiments.

Sample preparation for a TPD investigation was as follows.

Approximately 0 1g of a <45µm fraction of a previously prepared clay

was used. This was labelled and placed in a small vial, this was then

placed in a gas-jar (the atmosphere of which was saturated with the

solvent vapour required), for 48 hours (Fig 3.x.).After this time
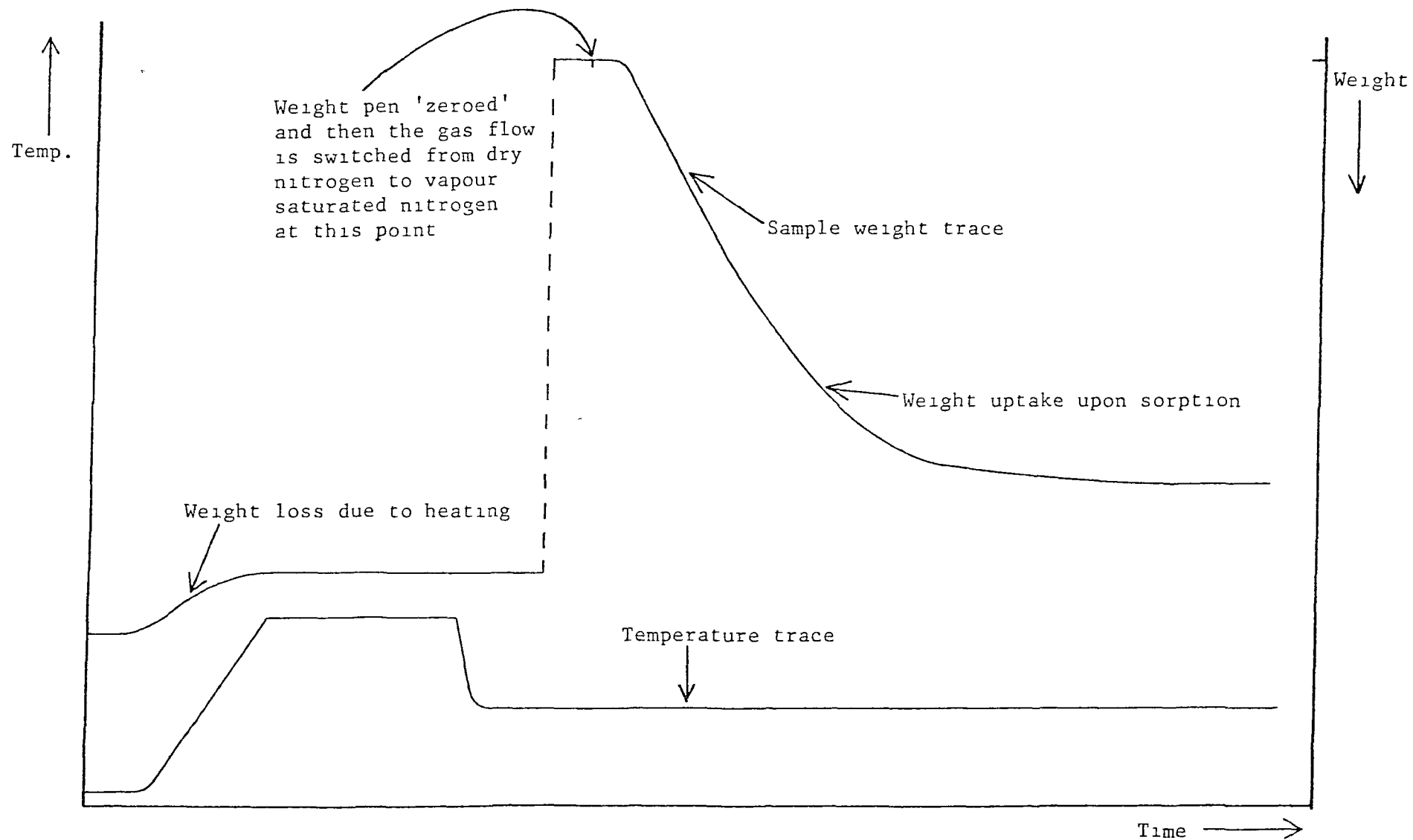
Fig 3 viii. Example of an experimental trace from a typical sorption uptake experiment.

39

a 7-8mg clay sample is quickly placed in the thermobalance, and its TPD profile obtained under the conditions outlined above. It should be noted that a small portion of physisorbed solvent is lost during the transfer of the sample from the gas-jar to the thermo-balance. This was not a problem since the more tightly bound, chemisorbed species were of more intrest.

3.7 Infa-Red Investigations.

These studies were used primarily to corroborate and aid the interpreation of the lower portion, (up to 200°C) of the TPD profiles Consequently, the samples were prepared in the gas-jars in the same way as the TPD samples, the difference being that a previously prepared I R film (section 3 3) replaced a clay powder sample

The infa-red spectrometer used was a Perkin Elmer 983.IR. equipped with presample chopping and with quoted accuracies at $1600cm^{-1}$ of 2% (ordinate) and $\pm 3cm^{-1}$ (abscissa). The I.R. spectra were recorded using an evacuuable variable temperature cell, at room temperature initially, and then after evacuuation for 1 hour at 50°C, 100°C, 150°C and finally 200°C (200°C was the maximium operating temperature of the variable temperature cell) The I.R. range scanned was $4000cm^{-1}$ to $600cm^{-1}$, however certain ranges were expanded as required, eg, the range $1800cm^{-1}$ to $1300cm^{-1}$ for the alcohol investigations

3 8. X-Ray Diffraction Studies (XRD).

The XRD slides were prepared in the same way as the I R films, and the TPD samples, using a gas-jar saturated with the required solvent vapour The XRD traces were recorded using a Jeol JDS-8X. Diffractometer operating at 40kV and 20mA.

Weight loss signal

Peak Area

Derivitised weight loss signal where the area under the peak is a measure of the magnitude of the weight loss.

Fig 3.ix.   Example of a TPD wgight loss profile.

Ground glass lid sealed with vacuum grease.

Open vials containing clay samples.

Gas-jar.

Top of support column (this is porous to allow adequate vapour flow in the gas-jar)

Gas-jar atmosphere saturated with vapour.

Open container of liquid under examination.

Tubular column with top to support sample vials.

Fig 3.x.   Schematic diagram of the gas-jar used to saturate clay samples

3.9. Quantification of the exchangable cations

To measure quantitatively the concentration of interlayer cations in a cation exchanged montmorillonite, a back-exchange technique is used. A 1g sample of dry, finely ground clay is added to $25cm^3$ of a 0.5M Ca^{2+} solution, (Calcium chloride is suitable as neither Ca^{2+} or Cl^- ions will interfere with the atomic absorption spectroscopy (AAS) spectra of the cations of interest in this work, (Al^{3+}, Fe^{3+}, and Cr^{3+}). This mixture is shaken vigorously to ensure thorough mixing, covered and left to equilibrate for at least 48 hours. The very high concentration of Ca^{2+} ions will replace the exchangable interlayer cations, forcing them into solution. After 48 hours the mixture is centrifuged, the supernatant collected, and the clay slurry is re-suspended, re-centrifuged, and the supernatant is again collected. The volume of combined supernatant is carefully noted and the solution is then analysed using AAS, for the concentration of the exchangable cations of interest. This will give the result in millimoles of cation per gram of clay.

In order to quantify the cation content of the silicate sheets a similar method is used. Firstly take a 3g sample of a dry finely ground clay and divide it into two portions of 1g and 2g respectively. The 1g sample is then assayed using the back exchange method described above to quantify the interlayer cation content. The 2g sample is assayed using a sodium fussion method[44]. The results are combined, and the total cation content minus the interlayer cation content, gives the concentration of cations in the sheet structure, again in $mmolg^{-1}$. These techniques are useful when assesing a newly made clay, to see if the exchange process has worked and the exchange cations have actually filled the interlayer sites, or to check for batch to batch variations in a cation exchanged montmorillonite.

3.10. Theoretical Background

A model is presented below for a gas diffusing isothermally at constant pressure into a cylindrical clay pellet through its curved lateral surface, in the absence of chemical reactions. The flat circular faces of the cylinder are assumed to be impermeable and the gas is assumed to be initially absent from the pellet Subsequently the cylinder is exposed to an atmosphere with a uniform concentration of the gas, the surface concentration approaching the value of this ambient concentration

In this analysis, $c(r,\theta,z,t)$ denotes the concentration of the gas at time t at the point with the cylindrical co-ordinates (r,θ,z). The pellet occupies the fixed right- circular cylinder $0 \leqslant r \leqslant a$, $0 \leqslant \theta \leqslant 2\pi$, $-\ell \leqslant z \leqslant \ell$. The diffusion of the gas is assumed to be Fickian, and the diffusivity D of the gas is assumed to be independent of concentration The concentration then satisfies the diffusion equation,

$$\frac{\partial c}{\partial t} = D\left[\frac{\partial^2 c}{\partial r^2} + \frac{1}{r}\frac{\partial c}{\partial r} + \frac{1}{r^2}\frac{\partial^2 c}{\partial \theta^2} + \frac{\partial^2 c}{\partial z^2}\right] \tag{1}$$

Initially the concentration satisfies,

$$c(r,\theta,z,0) = 0 \tag{2}$$

On the flat impermeable surfaces,

$$\frac{\partial c}{\partial z}(r,\theta,\pm\ell, t) = 0 \tag{3}$$

The concentration on the lateral surface is given by

$$c(a,\theta,z,t) = C_\infty (1 - e^{-\beta t}). \tag{4}$$

Here, $\beta > 0$ is expected to be large, so that the concentration on the curved surface rapidly approaches c .

The solution of the equations (1) – (4) is given in §5.3 of Crank[55]. Note that there is a misprint in Crank's equation (5.28).

It is fairly straightforward to show that,

$$c(r,\theta,z,t) = c_\infty \left[1 - e^{-\beta t} \frac{J_0(rd)}{J_0(ad)} \right]$$

$$- \frac{2\beta c_\infty}{a} \sum_{n=1}^{\infty} \frac{1}{n(\beta - D\alpha_n^2)} \frac{J_0(\alpha_n r)}{J_1(\alpha_n a)} e^{-\alpha_n^2 Dt} \tag{5}$$

Where $d = (\sqrt{\beta}/D)$, and (α_n) is the increasing sequence of positive

roots to the equation $J_0(a\alpha) = 0$ In equation (5), β cannot take the

values $D\alpha_1^2$, $D\alpha_2^2$, ... , and J_0 and J_1 are the Bessel functions of the

first kind of order zero and one respectively

Due to equation (2), the mass M_t of the gas adsorbed by the

clay during the time interval $(0,t)$ is given by

$$M_t = \int_{-\ell}^{\ell} \int_{0}^{2\pi} \int_{0}^{a} c(r,\theta,z,t) r \, dr \, d\theta \, dz$$

Equation (5) can be substituted into this expression to obtain

$$\frac{M_t}{M} = 1 - 2e^{-\beta t} \frac{J_1(ad)}{ad J_0(ad)} - \frac{4\beta}{a^2} \sum_{n=1}^{\infty} \frac{e^{-\alpha_n^2 Dt}}{\alpha_n^2(b - D\alpha_n^2)} \tag{6}$$

Where $M_\infty = 2\ell\pi a^2 c_\infty$ is the limiting value of the mass of gas adsorbed

by the clay particle As in equation (5), it is required in equation

(6) that $\beta \neq D\alpha_1^2$, $D\alpha_2^2$,   From kinetic absorption data for M_t/M_∞,

which was obtained using a gravimetric method, the constants D and B

can be determined using equation (6) Note that $M_0 = 0$.

In practice, the series in equation (6) must be truncated

in order to be evaluated numerically, and this truncated solution

will be inaccurate for small times. Because data for M_t/M_∞ were not

obtained at such times, the truncated solution was satisfactory. An

approximation that is accurate for small times can be found using the

techniques reported by Carslaw and Jaeger[56]

If the diffusion coefficient D(c) varies with concentration,

the value $\tilde{D}$ found using equation (6) represents a mean value, termed

the integral diffusion coefficient Crank[55] gave in §11.6 the relation

$$\widetilde{D} = \frac{1}{c_\infty} \int_0^{c_\infty} D(c) \, dc$$

The ambient temperature, T, is a parameter in the isothermal experiments that has thus far been suppressed Diffusion in porous crystals is normally assumed to obey the Arrhenius equation $\widetilde{D} = \widetilde{D}_0 \exp(-\Delta E/RT)$ Consequently, if D is determined over a range of temperatures, the activation energy ΔE and $\widetilde{D}$ can be calculated.

CHAPTER 4

Literature survey

4.1   General Introduction

For many centuries now, clays have been used to make products varing from earthenware vessels and ceramics to bricks and building materials Today the use and applications of clay minerals are much more extensive and technically demanding Clays are no longer taken straight from the earth for use, instead they undergo extensive processing to yield a range of structurally similar clays with a variety of properties.

These processed clays have been used in a number of applications including molecular sieves where the clay is used to seperate compounds on the basis of molecular size. Another application of clay that has expanded in recent years is its use in electrochemistry. This is demonstrated by Oyama and Anson[25], where sodium-montmorillonite was used to coat a graphite electrode, and the clay plays a primary role in catalysing the reduction of hydrogen peroxide at the electrode surface The reason suggested for this, is that iron cations (Fe^{3+}) which isomorphously substitute some of the Si^{4+} and Al^{3+} cations in the montmorillonite structure, (specifically the octahedral sites) may greatly enhance the activity of the electrode towards the reduction of hydrogen peroxide in solution Rudzinski and Bard[26] , examined the ability of montmorillonite to transport electrons within its structure. They concluded that for clays with large metal complexes in their interlayer space, (ie metal trisbipyridyl complex ions) the electron charge transport mechanism is primarily due to diffusion of externally adsorbed species For smaller metal complexes (ie $Ru(NH_3)_6^{3+}$) the transport mechanism is via diffusion through and around the clay sheets. This gives cation exchanged montmorillonite the potential for a wide

range of electrochemical applications.

In recent years pillared clays have been developed,
these are clays which have been modified so that the interlayer
cation is replaced by a large robust cation. The most commonly
used pillaring agents are aluminium based, such as $[Al_{13}O_4(OH)_{24}(H_2O)_{12}]^{7+}$
which is thought to be uniformly distributed on the interlayer
surfaces. The large cations give large basal spacings in the clays,
and reactant molecules can diffuse more quickly to the active
interlamellar sites, so where the reaction rate is diffusion
controlled reaction can occur more quickly Also Diddams et al[27] has
has shown that pillared clays can change the selectivity for certain
reactions, ether synthesis from pentanol among others, with the
selectivity differing significantly from those for non-pillared
clays Other examples of pillaring agents would be niobium and tantalum
$M_6Cl_{12}^{n+}$ cluster cations, ($Nb_6Cl_{12}^{2+,3+}$ and $Ta_6Cl_{12}^{2+}$) however such
examples are rare and aluminium based pillaring cations are more
commonly used

Cation exchanged clays and especially montmorillonites
have proven useful as selective catalysts for organic synthesis[28]
(section 4 2). The acidic nature of cation exchanged montmorillonite
is what gives it a wide potential degree of utility in acid
catalysed and other reactions, with shape selectivity and product
distribution ratio engineering also possible[28] Cation exchanged
montmorillonites provide a source of protons to catalyse reactions,
and choosing the optimum clay-solvent system is important. This
will allow the maximum product yield and the shape selective nature,
reduces the amount of side reactions occurring, (Table 1.1. list
some of these reactions). An example is a study by Adams et al[7,29]
where the reaction of methanol and isobutene over Al^{3+}, Fe^{3+} and

Cr^{3+} clays using a range of solvents to produce methyl-t-butyl ether
(MTBE) as the major product was investigated. MTBE is used as an
alternative non-lead based additive to petrol, to increase its
octane rating. When producing MTBE chosing the correct solvent-
cation exchanged clay system is very important to get the optimum
yield at the lowest temperatures

4.2   Catalysis by Clays

A brief outline of the types of reaction for which solid
acid catalysts have been used is given in Table 1.1 This is a very
short synopsis from a long list of reactions for which clays may
be used. Before examining these reactions in detail it is worth
considering some of the factors influencing the catalytic process.
In most cases the clay appears to be acting purely as a solid
source of protons [9] However to date it has not been possible to
produce a set of guildlines for catalysis by montmorillonites,
which would help to decide whether a particular acid-catalysed reaction
would succeed over a clay or which would suggest procedures to
optimise yields for a partictular reaction. As protons are responsible
for the acidic character of the clay, and are produced by polarization
of interlayer water[30], Adams et al[5] have confirmed experimentally
that M^{3+}-montmorillonites are more active than divalent or
monovalent ion-exchanged clays Consequently Cr^{3+}, Fe^{3+} and Al^{3+}
are the more usual interlayer cations used in catalytic processes.

4.2 1   Reaction Sites

Although the protons necessary for acid catalysis are
produced in the interlayer region, reaction need not occur there.
The mobile proton can easily migrate to a more convenient location
for reaction. It is important to note, that when the water is
polarized about the interlayer cation, it can exert enormous

polarizing power on any molecule in the neighbourhood. Hence,

immediately on production, the proton (H^+) will protonate a molecule

present in the interlayer space and this process may be described

as,

$$M(OH_2)_n^{m+} + H_2O \longrightarrow [M(OH_2)_{n-1}OH]^{(m-1)^+} + H_3O^+$$
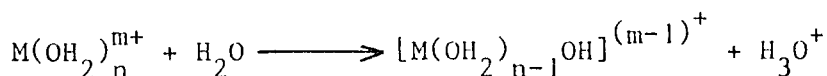
or in the case of an organic molecule being present in the interlayer

then,

$$M(OH_2)_n^{m+} + R \longrightarrow [M(OH_2)_{n-1}OH]^{(m-1)^+} + [RH]^+$$
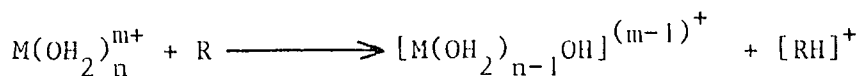
and the protonated species can move to the site where reaction

occurs The relative probability of the foreward reactions occurring

depends on the number of water and organic molecules in the interlayer

space The fact that the reaction need not occur in the interlayer

was demonstrated using cation-exchanged montmorillonite, and the

equivalent heat collapsed clay[8], (ie it has no interlayer region

as the layers have collapsed) When products were formed by the

collapsed clay, this showed that the carbocations [RH]$^+$ can react

at two possible sites, either with (i) oxygenated polar species such

as alcohols and water on the clay surface, or (ii) hydrocarbons

also in the interlayer region. Thus the active sites in the clay

are not confined to the interlayer region exclusively

4 2 11   Solvent Effects

It was first (erroneously) thought that saturated

hydrocarbon solvents should be used in acid catalysed reactions

to avoid the possibility of coordination of the solvents to the

interlayer cations However Adams et al[6] found cyclic ether type

solvents to give comparable yields of MTBE at temperatures ∼30°C

lower than when hydrocarbon solvents are used The lower temperature

minimised the yield of side products, and for the specific

example of 1,4-dioxan, (this was found to give the best result),

it is miscible with all the reactants and products, thus enabling the reaction to proceed more rapidly. Also some displacement of interlayer water by 1,4-dioxan may increase the interlayer acidity. Further to this Adams et al[31] studied the clay catalysed lactonization of cyclo-octene-5-carboxylic acid, a reaction that occurs at temperatures above 100°C. The increased temperature is thought to remove some of the interlayer water, effectively generating a stronger acid. However oxygenated solvents such as 1,4-dioxan reduce the efficiency of reaction by competing with interlayer water for the cation coordination sites, thus reducing the number of free protons. Hydrocarbon solvents such as xylene do not have this effect So above 100°C the cations are not fully hydrated and the clay behaves as a strong acid, (reactions with primary and secondary carbocations occur readily), and saturated hydrocarbon solvents are more efficacious For low temperature reactions, when the cations are fully hydrated, and only a relatively low acidity is required, (protonation to form tertiary or allylic carbocations is feasible), the use of a solvent to promote miscibility (ie 1,4-dioxan) is advantageous.

4 2 111   Clay Catalysed Reactions

Some of the reactions listed in Table 4.1 will be considered here Atkins et al[4] has studied the hydration of alkenes to alcohols using ethylene, to give ethanol. It is suggested that reaction occurs via protonation at a bronsted acid site in the clay, and proceeds via the mechanism.

$$CH_2=CH_2 \xrightarrow{+H^+} CH_3-\overset{\oplus}{CH_2} + H_2O \longrightarrow CH_3-CH_2-\overset{\oplus}{\underset{|}{O}}H \xrightarrow{-H^+} CH_3CH_2OH$$

ethylene   Water   Ethanol
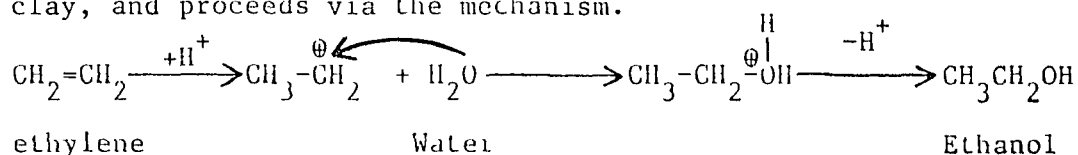
This mechanism may also be written by invoking a lewis acid site within the clay

$$CH_2=CH_2 \xrightarrow{+LA} CH_3-CH_2 + H_2O \longrightarrow CH_3-CH_2 \xrightarrow{-LA} CH_3-CH_2-OH$$
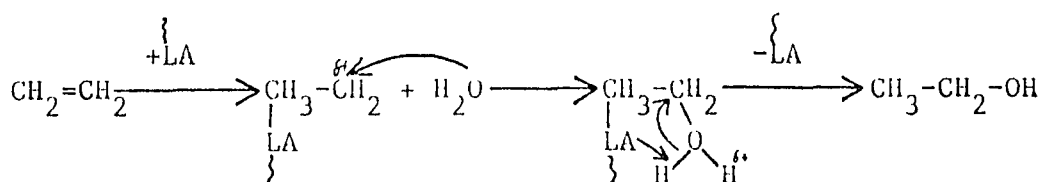
However it should be noted that reactions occur mainly on bronsted sites. It was found that Al^{3+}-montmorillonite gave the highest conversions to ethanol, with the order of reactivity for the cation-exchanged montmorillonites, being $Al^{3+} >> Fe^{3+} > Cr^{3+} > H^+ >$ calcined clay. The poor yields from calcined clays indicated that the reaction is, at least in part, an interlamellar process. Now as the choice of cation influences the polarity of the interlamellar environment and the binding of the alcohol to the cation, two types of interactions are suggested. These are (i) the interaction of the empty electronic orbitals of the cation with the lone pair of electrons of the alcohol molecule, (ii) strength of the hydrogen bonding between the alcohol molecules. Consequently the arrangment of the ethanol about the cation influences the reaction. Hence the overall rate of hydration is effected by the the strength of the alcohol-cation dipole attraction and this may hinder the approach of the reactants to the interlamellar catalytic sites. Hence the observation that different interlayer cations give different yields of product.

The clay catalysed reaction of alcohols with alkenes to give ethers is of some importance, not the least because some sorption studies in this thesis were based on some of the work on this reaction. Adams et al examined the reactions of various alcohols (ie primary alcohols (C_1-C_{18})) with alkenes (2-methyl pent-2-ene) over an Al^{3+}-montmorillonite. However the production of MIBE from methanol and isobutene will be discussed in detail as an example of this group of reactions. The suggested reaction pathways are as follows

CH_3 CH_3
C
CH_2

(1) $+H^{\oplus}$

$+$ CH_3 $C=CH_2$ CH_3

CH_3 CH_3
$C^{\oplus}$
CH_3

$+H_2O$

(3)

(2)

$+$ CH_3OH

CH_3 CH_3
$\oplus C$ $O-H$
CH_3 H

CH_3 CH_3
$C^{\oplus}$ $O-H$
CH_3 CH_3

CH_3 CH_3
C
CH_2
$\oplus C$
CH_3 CH_3

$-H^{\oplus}$

$-H^{\oplus}$

$-H^{\oplus}$

$-H^{\oplus}$

CH_3 CH_3
C
CH_3 OH

t-butanol

CH_3 CH_3
C
CH_3 OCH_3

MTBE

CH_3 CH_3
C
CH
C
CH_3 CH_3

2,4,4-trimethylprop-1-ene

CH_3 CH_3
C
CH_2
C
CH_2 CH_3

2,4,4-trimethylprop-2-ene
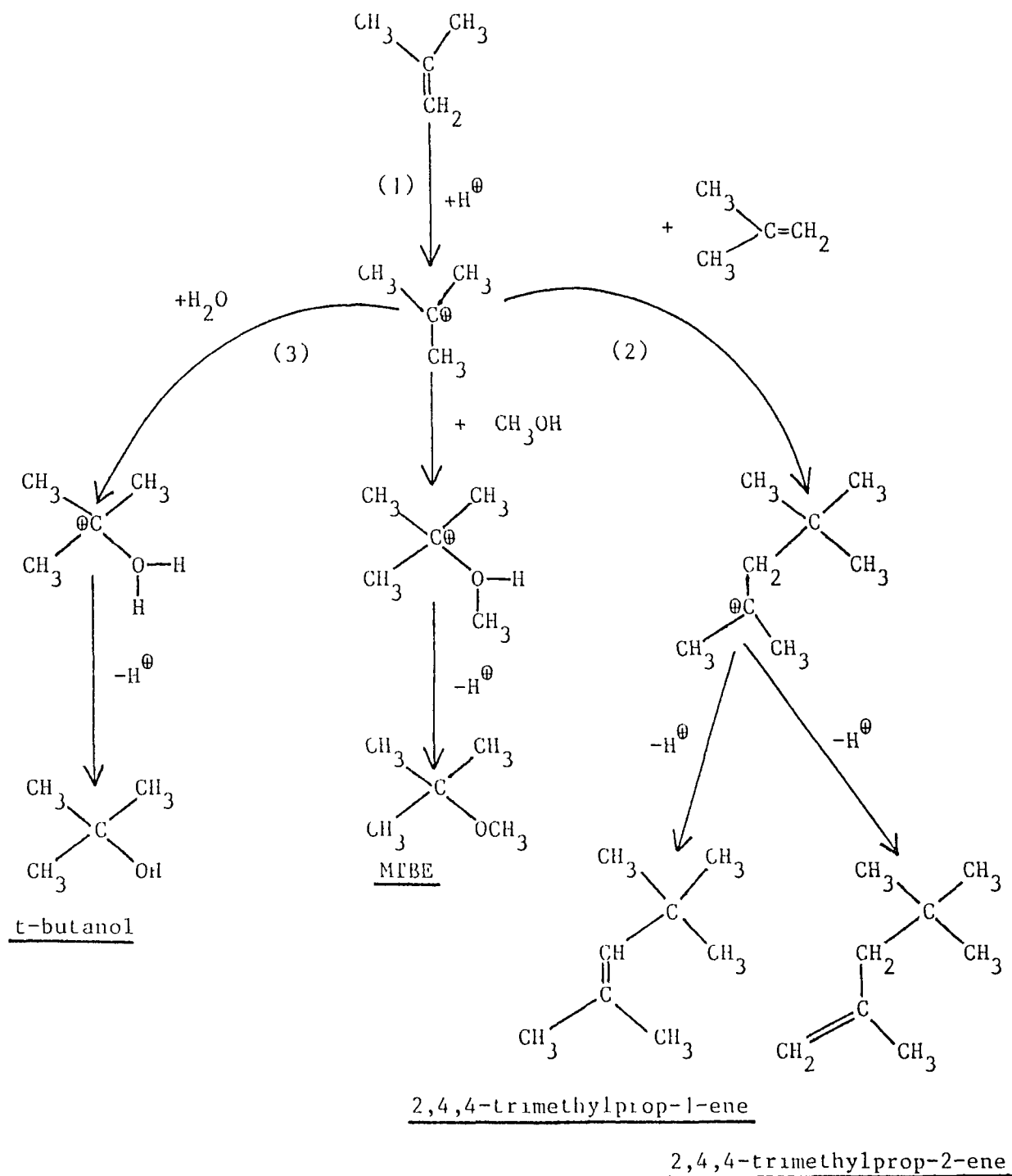
The cation exchanged montmorillonites were compared with some commercially available acid catalysts, which gave good yields of MTBE (>50%), which is not suprising as these catalysts are based on smectite clays. The K10 and KSF catalysts probably have Al^{3+} cations leached from their octahedral sites into the interlayer and consequently behave as Al^{3+}-montmorillonite All three cation exchanged clays Al^{3+}, Fe^{3+} and Cr^{3+}-montmorillonite gave yields of

>50% MTBE with low yields of t-butanol These results were obtained using alkane solvents (eg n-pentane), however further studies with oxygenated solvents (ie tetrahydrofuran, tetrahydropyran (THF, THP), and 1,4-dioxan), demonstrated that they were just as effective, and in the case of 1,4-dioxan and Al^{3+}-montmorillonite, the highest yield of MTBE was obtained.

In the hydration of ethylene, it was shown that an interaction between an organic species (either reactant, solvent, or product molecule) and interlayer cation can influence the reaction yield. In an attempt to elucidate this effect a number of parameters were examined. The basal spacings of the different cation exchanged clays with the solvents, showed the effect was not due to the ease with which the reactant could enter between the layers, because the clay solvent system with the largest basal spacings (Fe^{3+} and Cu^{2+}-montmorillonite with 1,2-dimethoxyethane), gave the lowest yield of MTBE. The miscibility of the reactants and products in the solvent effects their distribution, however this cannot be the sole explanation as the observed effect depends on both solvent and cation, and not the solvent alone. The conclusion was that the effect was due to solvent-interlayer cation interaction, which modifies the efficiency of the reaction It can influence the competition between, water, solvent, reactant and product for sites in the hydration shell of the active cations.

Adams et al[7] invetigated this reaction further by studying the reaction of alcohols (methanol, propanol, and i-propanol) with t-butanol to produce t-butylethers at low temperatures (<100°C), using Fe^{3+}-montmorillonite and 1,4-dioxan as the solvent. It was found that the yield of t-butylethers from the alcohols was of the order methanol>propanol>i-propanol>>t-butanol. This trend

correlates well with the rate of diffusion for these molecules
within the clay, or inversly with the steric hinderance which
would occur during the reaction step when the alcohol attacks
the carbonium ion, (see MTBE reaction pathway) So based on these
studies, the investigations in this thesis were carried out. The
rate of diffusion of the alcohols (methanol, i-propanol and t-butanol)
upon various cation exchanged montmorillonites (Al^{3+}, Cr^{3+} and Fe^{3+})
were measured to see if the rate of reaction was controlled by the
diffusion coefficient of the alcohol, (which would be expected to
depend on steric factors) Also the diffusion of the solvents (THF,
THP and 1,4-dioxan) upon Cr^{3+} and Al^{3+}-montmorillonite was examined.
This was to see if diffusion of these solvent molecules, could
influence the rate of reaction by propping the layers apart, for
the smaller reactant molecules to enter the active sites more easily.
Also infared studies of both the alcohols and cyclic ether solvents
were used to see how these molecules may interact with the clay
surface and interlayer.

Gregory et al[10] investigated the addition of acids to
to alkenes to produce esters or more specificially

$$CH_2=CH_2 \quad + \quad CH_3COOH \quad \xrightarrow[\text{Catalyst}]{\text{Clay}} \quad CH_3COOC_2H_5$$
Ethylene   Acetic Acid   Ethyl Acetate
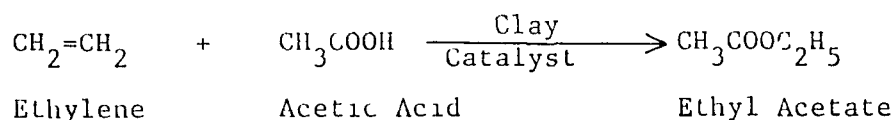
This reaction is known to occur in the interlayer region, since
little or no product is formed using a collapsed clay catalyst.
The reaction mechanism is thought to begin by protonation of an
ethylene molecule at a bronsted acid site (1), and the carbocation
then reacts with an acetic acid molecule within the interlayer
region.

(1) $CH_2=CH_2 \quad + \quad H^{\oplus} \quad \xrightarrow{\hspace{2cm}} \quad CH_3\overset{\oplus}{C}H_2$

      Ethylene   Proton   Carbocation

(2) $CH_3\overset{\oplus}{C}H_2$ + CH_3COOH ⟶ $CH_3COOC_2H_5$ + $H^{\oplus}$

    Carbocation   Acetic Acid   Ethyl Acetate   Proton
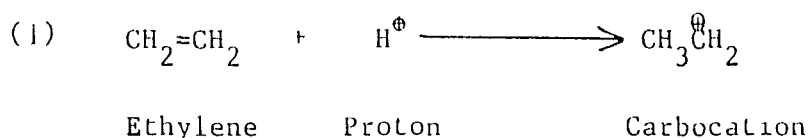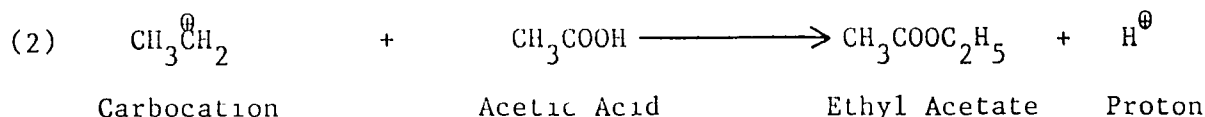
Also the selectivity for conversion to ethyl acetate was >99% for

each of a range of ion-exchanged bentonite (H^+, Al^{3+}, Fe^{3+}, Cr^{3+},

Cu^{2+}, and Na^+). Further to this Ballantine et al[9] studied the

addition of acids to a range of alkenes. The conclusion was that

ion-exchanged clays were highly efficient for reactions with alk-1-enes,

when compared with sulphuric acid catalysed reactions, and the clays

have a high selectivity for a specific product, eg the above reaction

of ethylene with acetic acid over Al^{3+}-montmorillonite will yield

ethyl acetate as the sole product.

Ballantine et al[13] have also been investigating some

elimination reactions involving clay catalysts. One of the interesting

features of these elemination reactions, is that they are novel

clay catalysed reactions, and have no counterparts in proton catalysed

solution chemistry, (although similar reactions have been observed

using finely divided nickel, palladium and ruthenium catalysts).

A range of solid acid catalysts have been examined, (Al^{3+}-montmorillonite,

Al^{3+}, H^+, and NH_4^+-bentonite), and two of the reactions studied were

the elimination of ammonia from (i) alkyl-1-amines, and (ii) cyclo-

alkylamines. The reaction mechanism is as follows.

(i) $R-CH_2-NH_2$ $\xrightarrow{+H^{\oplus}}$ $R-CH_2-\overset{\oplus}{N}H_3$ $\xrightarrow{-NH_3}$ $R-\underset{\underset{R-CH_2}{\overset{|}{\overset{\oplus}{N}H_2}}}{C}H_2$ $\xrightarrow{-H^{\oplus}}$ $R-\underset{\underset{R-CH_2}{\overset{|}{NH}}}{C}H_2$

                                 + $R-CH_2-NH_2$
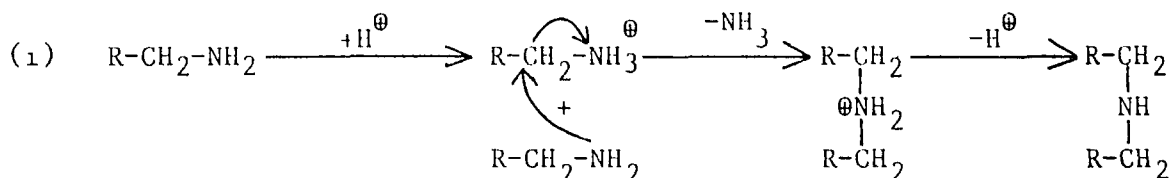
This type of reaction involves the use of an unprotonated amine

to act as a nucleophile to displace ammonia from a protonated amine

molecule, and such reactions are quite unknown in solution chemistry.

The source of highly acidic protons in the interlayer region,

___

(reaction occurs at >200°C),ensures that both protonated and unprotonated species can co-exist in proximity close enough for substitution reactions to occur, making clay catalysts almost unique for this type of reaction.
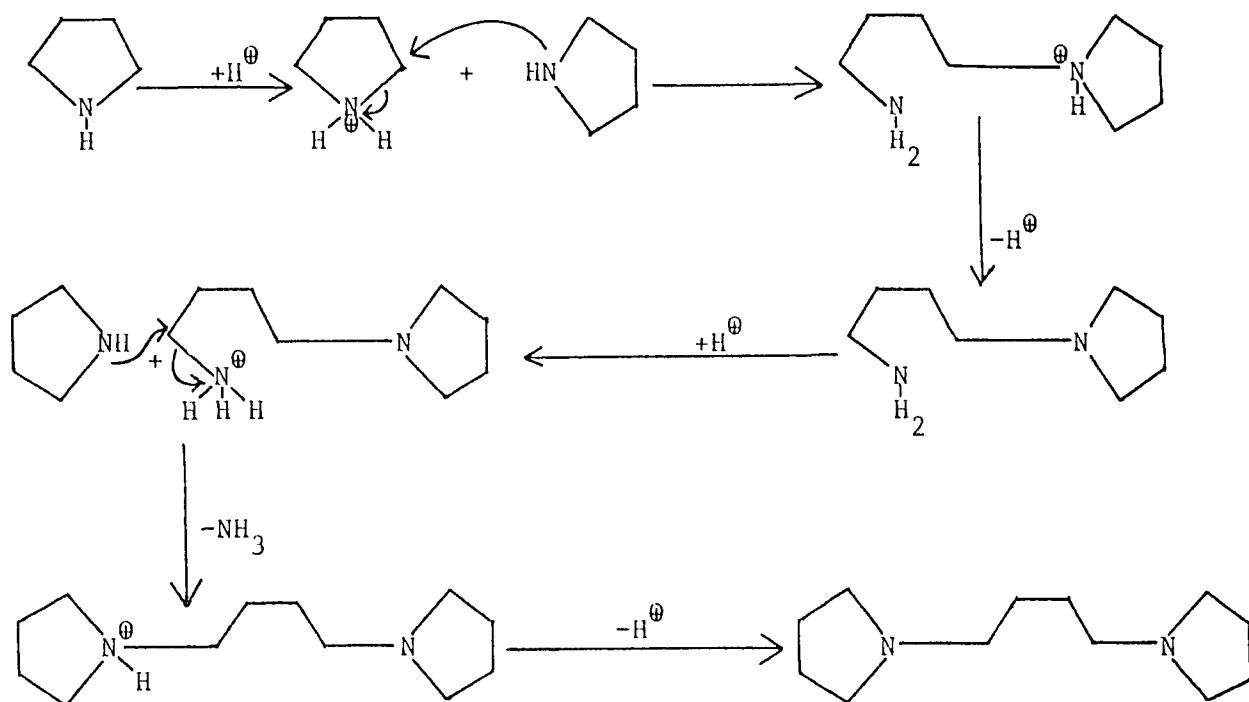
Similar reactions involving the elimination of hydrogen sulphide from thiols have also been reported[15], and these reactions are similar to the amine reactions in almost every respect, eg.
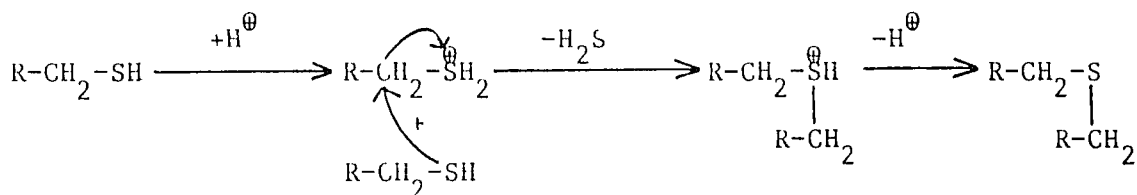
Catalysis of diels-alder cycloaddition reactions by ion-exchanged montmorillonite, have been reported[11] It was found that while Cr^{3+} and Fe^{3+}-montmorillonite were effective catalysts non-transition metal ions such as Na^+, Mg^{2+} and Al^{3+} were not. Where as it has been suggested that the clays are not acting as lewis acid or proton donor catalysts, but rather a one electron transfer process is involved, leading to a radical cation catalysed process.

As an example the dimerization of cyclopentadiene using Fe^{3+}-K10,

(see page 48), Fe^{3+} and Cr^{3+}-montmorillonite catalysts will be considered.
The reaction may be described as follows.
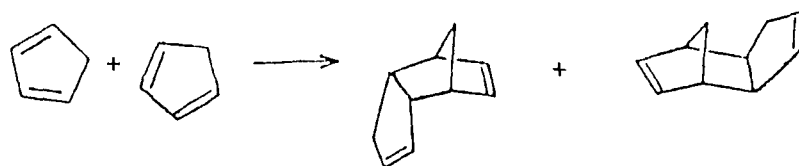
It was found that Fe^{3+} and Cr^{3+} have activities similar to that of
Fe^{3+}-K10 even though this material has a much larger nitrogen
surface area, (250 compared with $50m^2g^{-1}$). So it appears that the
reactions are not catalysed solely by surface Fe^{3+} or Cr^{3+} cations,
but must also involve those cations in the interlayer region of
the K10 or montmorillonite (note, the cation exchange capacities
of these materials are similar). If this is true, it implies that
diffusion between the clay layers is not the rate determining process.
The fact that transition metal cations are active, while Al^{3+} cations
are not, suggests that one electron processes are as important here as
they are in radical cation catalysed diels alder reactions. One
further observation is that reactions catalysed by Fe^{3+}-K10 and
Fe^{3+}-montmorillonite contained numerous unidentified by-products,
but Cr^{3+}-montmorillonite gave a much 'cleaner' product yield.
Indicating that the acidity of the clay appears to effect the product
yield and purity.

In conclusion, cation exchanged montmorillonites may be
used to catalyse a great variety of reactions, and the clay can
behave as a solid source of protons, or it may be involved in

electron transfer process catalysis The choice of interlayer

cation can influence the activity of the clay for a specific reaction,

and it can also effect the selectivity for, and purity of the

product required. The temperature and solvent used can influence

the acidity of the clay,(usually by displacing interlayer water),

and so effect the reaction. Clay catalysts are easy to use, efficient,

selective and in some cases unique acid catalysts for synthetic

organic reactions.

4.3. Acidity of Clays.

The proton-donating or acid-catalysing abilities of a

cation exchanged montmorillonite is one of its most significant

fearures. It is this acidic nature that has led to the use of ion-

exchanged clays as solid acid catalysts. The acid catalytic reactions

are thought to take place at active sites within the clay structure,

and these may be divided into two types of site[32], the bronsted

acid site and the Lewis acid site. The bronsted acid sites, basically

behave as a bronsted-lowcry acid which may be defined as a substance

which supplies protons. Therefore any substance that increases the

concentration of hydrated protons (H_3O^+) above that due to the

autodissocation of the water, is an acid[33]. In the case of an ion-

exchanged montmorillonite, it is the effect of the polarizing power

of the interlayer cation upon its sphere of hydration that polarizes

the water molecules generating a source of protons within the clay

interlayer. So generally bronsted acid sites are associated with

the interlayer cations of the montmorillonite[30,34] Bronsted acid

catalysis is involved in reactions where nucleophilic attack on a

protonated species occurs[28], and although these reactions primarily

occur within the interlayer space, when polar oxygenated species

are involved, reaction may also occur on the surface of the clay.

In the case of ion-exchanged montmorillonite catalysed reactions,
bronsted acid sites are thought to be the major source of the clays
acidity, although in some cases the second type of acid site is
thought to be involved The lewis acid sites, may be defined as a
lewis acid, which is a general definition of an acid , as an electron
pair acceptor[33]. (this definition includes the bronsted-lowry
definition as a special case). This definition includes many systems
where protons are not involved at all. In the case of montmorillonite
the lewis sites are associated with the Al^{3+} and Fe^{3+} cations within
the octahedral sheet of montmorillonite, and the coordination
sphere of these cations is likely to be made up of water and
hydroxyl groups, when they are exposed at crystal edges[28] Lewis
acid sites are thought to be involved in reactions where the clay
is heated in excess of 100°C and so dehydrated. (also when the
clay is dehydrated by vacuum) It is possible that the lewis
sites may be more significantly involved in catalysis due to the
lack of water as a source of protons for the bronsted sites.

The ability to measure the acid strength of a clay catalyst,
in the same way the PH of a liquid can be measured, is a useful
tool when applying these acids to various catalytic reactions.
So a very brief mention of the various methods that have been
developed over the years will be given. It should be noted that
these methods are not specifically for ion-exchanged montmorillonites,
but apply equally well to most solid acid catalysts, (ie zeolites,
silica-alumina oxides, kaolins, etc.).

One of the earliest methods was the use of Hammett
indicators, (developed by Hammett and Deyrup in 1932[35]). These
work like a conventional acid base indicator , by forming a coloured
complex with the acidic clay and changing colour when the clay

is mixed with a strong base such as an amine. (n-butylamine is

- commonly used[36,37]). The colour change occurs once the amine

has filled all of the acidic sites on the clay, (ie is in an

excess). This method however is cumbersome to perform and it is

difficult to accurately note the colour change on a dark medium

such as a clay. Although in the 1960's Drushel and Sommers[38]

developed a system of fluorscent indicatois where the acid-base

change in the indicator could be measured using a spectrometer.

More recent instrumental methods include a temperature programed

desorption technique, developed by Nelson et al[39], although today

a more commonly used technique is infa red spectroscopy (IRS).

This has the advantage of not only being fast and easy to use

but it can distinguish between bronsted and lewis sites within

the clay[40,41]

4.4   The Interaction of Organic Molecules with Acid Catalysts.

Adams et al[6,31] has shown that for catalytic reactions

involving cation-exchanged montmorillonites, the nature of the reactant,

product and solvent molecules, influence the overall reaction dynamics.

An understanding of how these molecules interact with the clay surface

would help in determining how the choice of these molecules can

influence the diffusion rate, product formation, and overall reaction

rate. For the purpose of this study the discussion will be restricted

to the interaction of alcohols, ethers and alkenes with the catalyst

surface, (as these are the type of molecules of primary interest

this study). For this work the most commonly used techniques are

infared spectroscopy and temperature programmed desorption, as they

complement each other, which aids in interpreting the data.

Throughout the literature very little work has been done on

the interaction of alcohols, ethers and alkenes with trivalent cation-

exchanged montmorillonite. The work in this area has centered mainly

on Ca^{2+}, Na^+, and Cu^{2+}-montmorillonite, although some work has been

carried out on Al^{3+}-montmorillonite. By examining the mechanisms of

interaction of various clay-organic systems, it is hoped that this

will aid in the intrepretation of the data for the adsorption of the

alcohols and cyclic ethers on the various trivalent cation-exchanged

montmorillonites studied in this thesis.

When the intercalation of alcohols in montmorillonite is

considered several general trends begin to become apparent:

(i) The alcohols are adsorbed by displacement of water molecules in

the primary hydration shell of the cations[61]

(ii) Primary aliphatic alcohols form single-layer complexes in the

interlayer, but smaller molecules such as methanol and ethanol can

form double-layer complexes[66]

(iii) For these small alcohol molecules, the cation-dipole interactions

are far more important than any surface-molecule interaction.

(iv) For larger alcohol molecules (ie longer carbon chain),

Van der Waals interactions with the silicate surface become more

significant.

The application of these principles is evident in Dowdy and

Mortlands[62] study of the adsorption of ethanol on Na^+, Ca^{2+}, Al^{3+} and

Cu^{2+}-montmorillonite, using infared techniques. When considering the

Al^{3+}-montmorillonite, it was suggested that the ethanol interacted

with the water and hydroxyl groups of the Al^{3+}-hydration sphere,

and that the $Al(OH_2)_6^{3+}$ octahedral complex undergoes

spontaneous hydrolysis to $Al(OH)_x(H_2O)_{6-x}^{(3-x)+}$ so that the ethanol

be bonded as shown in Fig 4.1. The mechanism of interaction shown is

suggested by the infared data. The C-H streching frequencies of ethanol

at (2984, 2936, and $2898cm^{-1}$), are not detectably lowered on adsorption,

hence C-H----O hydrogen bonding of the alcohol to the silicate surface

seems unlikely.
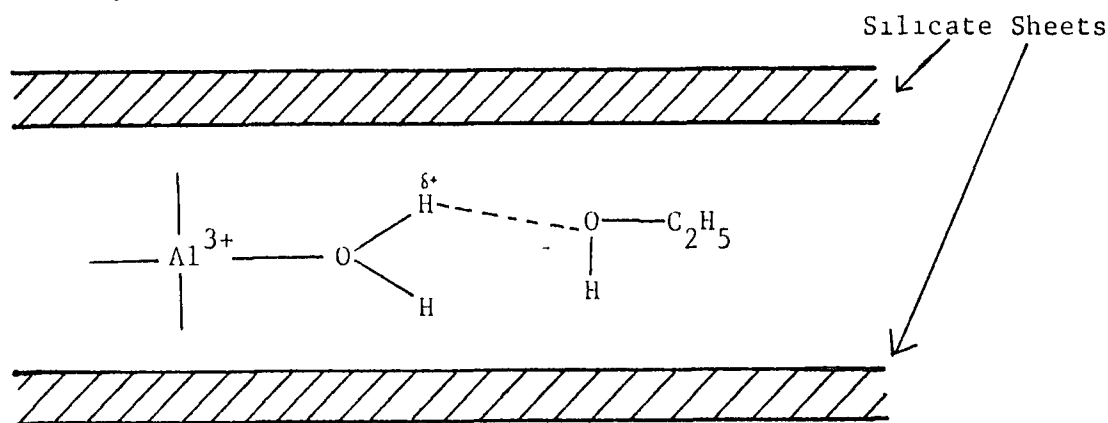
Fig 4.1. A schematic diagram of the interaction of ethanol with

the Al^{3+}hydration sphere in Al^{3+}-montmorillonite.

Also the deformation band of water at $1635 cm^{-1}$ shifted to a higher

frequency in Al^{3+}-montmorillonite on exposure to the ethanol vapour

suggesting the above mechanism of interaction.

This emphasizes the importance of the cation-dipole

interaction in adsorption on cation-exchanged montmorillonites. However

if the interaction of n-propanol on Na^+-montmorillonite is considered,

a further type of interaction appears to occur[63] The n-propanol is

thought to form a single-layer complex of molecules orientated

perpendicularly to the silicate sheets in the interlayer space.

The n-propanol interacts with the surface oxygens via OH-----O hydrogen

bonds, and also simultaniously interacts with the interlayer Na^+ ions

via its oxygen atom At the other end of the molecule the methyl

groups are thought to interact with the surface via Van der Waals

interactions and hydrogen bonds, (Fig 4.11.). For branched chain

alcohols the situation is similar with single-layer complexes being

formed[64].

To summarise the adsorption of alcohols on montmorillonite

is influenced by both cation-dipole and surface-dipole interactions,

as there is an insufficient number of cations to which organic molecules

can coordinate so surface interactions (OH-----O-Si) can and most

probably do occur.
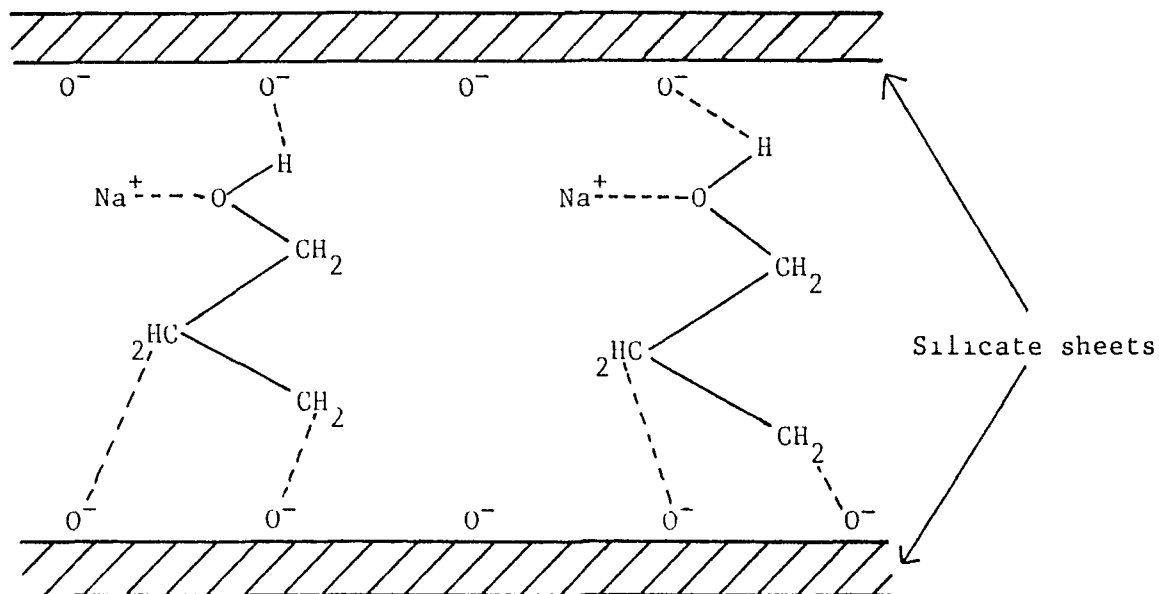
Fig 4.11. A schematic diagram of the interaction of propanol with

Na$^+$-montmorillonite (- - - - = Van der Waals interactions).

Studies of the intercalation and interaction of ethers with

cation-exchanged montmorillonites are not well documented in the

literature, however studies on the interactions of glycols have been

carried out. If ethylene glycol is taken as an example, it resembles

1,4-dioxan in that it has an oxygen molecule at each end separated by

a distance of two carbon units.

Ethylene Glycol   1,4-Dioxan
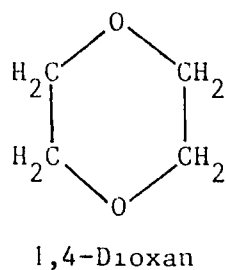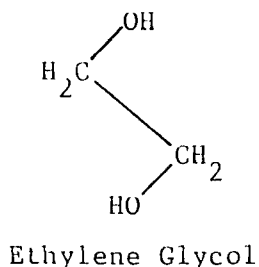
However it does not have the ring structure and overall size of

1,4-dioxan, and this must be considered when drawing analogies between

the two compounds Dowdy and Mortlands'[65] investigation of the

interaction of ethylene glycol with Cu^{2+}-montmorillonite, showed that

ethylene glycol and water compete for the same ligand sites around

the cation. Using the 1632cm^{-1} infra-red water absorption band, they

showed that this band intensified when the clay-ethylene glycol complex

was exposed to atmospheric air for increasing lengths of time, and

the intensity of the bands due to adsorbed ethylene glycol decreased.

Also bands at 2750 and 2650cm^{-1} were attributed to streching vibrations

of the hydroxyl groups in the glycerol molecule which are directly

coordinated to the interlayer copper ion These bands were thought not to be

due to C-H stretching vibrations, as absorption in this region is weak

or absent in the spectra of ethylene glycol complexes with montmor-

illonite containing cations other than copper, and in the spectra of

ethanol-montmorillonite systems Also no lowering of C-H stretching

frequencies was observed on adsorption, as may be expected if the

methyl groups were interacting with the surface, so based on this the

suggested mechanism of interaction for ethylene glycol is as follows[104],
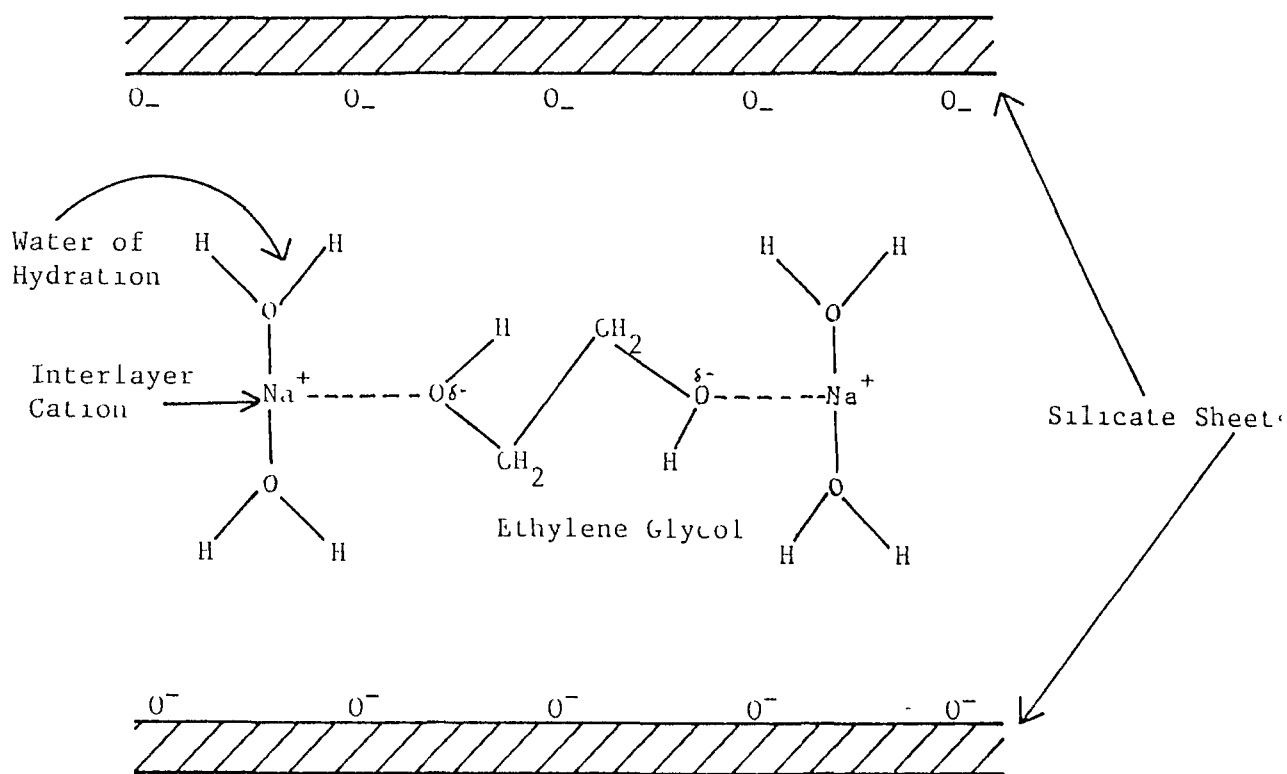
A single-layer complex with the plane of the carbon chain perpendicular to the silicate sheets, and based on the C-H stretching data above no C-H-----O-Si interactions are thought to occur. Also the ethylene glycol is known to form a double-layer complex via a similar mechanism under certain conditions[69]

In general for ethers, one or two layer complexes can exist with cation-exchanged montmorillonite, and for the specific example of 1,4-dioxan a single layer complex is formed[64,70], with the plane of the ring lying normal to the plane of the surface, and again for ethers the interaction is primarily a cation-dipole and not a surface-dipole interaction.

Finally a brief mention of the interaction of alkenes with montmorillonite. Not a great deal is known about the interaction of these molecules with cation exchanged clays. However it is known that unlike polar organic species, they do not occupy similar sites to water at the silicate surface or satisify the coordination requirments of the interlayer cations Non-polar compounds are thought to be adsorbed by relatively weak, non-specific London Van der Waals forces, and ion-dipole effects are not generally important The π electrons of the alkene double bond are thought to interact with the clay surface so enhancing adsorption, (this effect is well known for benzene type compounds (ie they have large π electron groups)), making π electron interactions an important mechanism in the intercalation of alkene molecules[81-83].

In conclusion it appears that cation-dipole interactions are of primary importance for intercalation on cation-exchanged montmorillonite, and interactions with the silicate surface are only of secondary importance Also the packing of the diffusivative or the number of layers formed, depends greatly on the actual diffusing

molecule, (its size, shape, and polarity), and on the specific cation-exchanged form of montmorillonite being used.

4.5. Diffusion in Clays

The diffusion or sorption uptake of various organic compounds in cation-exchanged montmorillonite was investigated for this thesis, however very little work of this nature has been published. In a brief overview, some of the of the studies to date are as follows.

In an early study by Barrer and MacLeod[71] in 1954, the sorption of polar (methanol, ethanol and pyridine), and non-polar (oxygen, nitrogen and benzene), gases were studied. The results showed that both polar and non-polar molecules could be intercalated by montmorillonite, and that greater than monolayer coverage of the surface could be obtained if a sufficiently high pressure was used. Later in the 1960's Palmer and Bauer[72] in a paper on the sorption of amines by montmorillonite, reached some conclusions that still hold today. Using weight uptake measurments they found the sorption rate to be of the order methylamine > ethylamine > dimethylamine >> trimethylamine, so confirming that steric hinderance influenced the rate of sorption Also an average local temperature increase of 1°C upon sorption in the sample was noted, and the effect of the heat of sorption on the rate was suggested, (ie. the uptake occurs under non-isothermal conditions). Finally the authors were examining the effect of particle size in the rate of sorption, but this work was incomplete and no firm conclusions were reached. More recent studies have tried to determine the rate limiting step of diffusion in montmorillonites and in a review by Breen et al[73], it is suggested that at lower partial pressures of water, the rate limiting step is the rate of diffusion of the vapour in the lower spacing intercalate, (ie in the system studied two basal spacings were found to exist 23 3, and 14.4Å respectively).

It is clear that a number of factors influence diffusion.

in cation-exchanged montmorillonites, however due to the lack of
studies on montmorillonite it will be necessary to consider some
studies on zeolites. Similar factors (ie molecular size, polarity and heat
of adsorption) effect diffusion in zeolites, and a considerable number of
studies have been carried out A detailed examination of this work should
provide a good basis for interpreting the results for the diffusion in
montmorillonite studied in this thesis.

Montmorillonite clays have a lamellar sheet structure, that
may be expanded by intercalation of organic molecules. Zeolites on
the other hand have a series of channels and pores, that provide a
robust network, which allows no loosening or opening of the framework
upon sorption The two major types of zeolite considered here, are
zeolite A and zeolite Y The difference between the framework of
these zeolites is that zeolite A has an eight membered oxygen ring
window, with a free diameter of about 4 2Å in the unobstructed Ca^{2+}
or Mg^{2+} form (5A zeolite), and the channels do not contain cations.
The 4A zeolite has a smaller free diameter as the channels are
obstructed by Na^+ cations The Y zeolite has a window constructed of
a twelve membered oxygen ring, making its free diameter larger, so
it can intercalate larger molecules It is worth noting that the two
very different structures of zeolite and montmorillonite minerals,
mean that direct comparisons of the sorption rates for the two
systems are not possible The diffusing molecule must diffuse through the
zeolite window to enter the pore, and this will remain a constant
obstacle throughout the sorption process. In montmorillonites however
the initial diffusing molecules must prise open the silicate sheets
to reach the interlayer This process becomes progressively easier
as more molecules diffuse in and prop the layers apart, until the
clay is saturated. Hence direct comparisons of the diffusion coefficients

for the two systems are not possible, but the diffusion processes may be similar.

As with montmorillonites it is possible to have different cation exchanged forms of a zeolite. Barrer and Brook[74] have examined the influence of the exchange cation on the rate of sorption of nitrogen, oxygen, hydrogen, krypton, and argon onto cation-exchanged zeolites. It was found that the cation influence on the sorption rate followed the general trend Ca < K < Ba < Na < Li for all sorbates, and this suggests the radius of the cation influences the rate of sorption, and the interlayer cation is known to influence the equilibrium sorption in montmorillonite also[21].

It is worth considering the effect of steric hinderance, as this can influence the rate of diffusion The structural differences between zeolites and montmorillonite must be borne in mind when discussing the influence of steric hinderance on the sorption rate. Such studies generally consider the size, shape and polarity of the sorbate. Moore and Katzer[75] while studing the counterdiffusion of hydrocarbons in Y zeolite, observed that the movement of the sorbate molecule through the pore aapperture may be the rate limiting step in the diffusion process This observation was confirmed when Barrer and Clarke[76] studing the diffusion of n-paraffins in zeolite A, noted that the diffusion coefficient decreased as the carbon chain length increased, (ie, the $\widetilde{D}$ values decreased $0 26 > 0,19 > 0.11 (10^{17} m^2 s^{-1})$ as the carbon chain length increased $n-C_4H_{10} < n-C_6H_{14} < n-C_9H_{20}$ respectively). So the larger the sorbate molecule the more slowly it passes through the zeolite window. Moore and Katzer's[75] paper also considered the effect of the polarity of the sorbate molecule. While considering the aromatic diffusate-zeolite interactions, they found the effective diffusion coefficient for toluene to be four orders of

magnitude larger than that for phenol, although the critical molecular diameter for the aromatics is the same, (0 64nm). It appears that the polar hydroxyl group of the phenol is in some way interacting with the zeolite and so retarding its progress through the pore channel, thus reducing its diffusion coefficient, and a similar effect might be expected in montmorillonites

The effect of the particle or crystal size on the rate of diffusion in zeolites has also been examined Yucel and Ruthven[51,52] considered this effect using the sorption of CF_4 and $n-C_4H_{10}$ in zeolite 5A[52] and nitrogen, methane, and ethane in zeolite 4A[51] these studies found no significant difference in the diffusion coefficients for the different crystal sizes when the thermal effects were taken into account Bulow et al[76] also looked at the uptake of n-hexane on different crystal sizes of MgA zeolite Here it was noted that for crystals in the size range 33-43um the uptake rate seemed to be limited by intracrystalline diffusion. However some dependence of the apparent diffusion coefficient on zeolite crystal size was observed. In a more recent paper by Bulow et al[77] the effect of crystal size is examined in more detail Using NaX zeolite of different crystal sizes, two factors were noted, (i) the sorption kinetics in larger crystals (120μm) is mostly controlled by intracrystalline diffusion, and (ii) the uptake on the smaller crystals (~18μm) is limited by intercrystalline transport. This study also confirmed the Yucel and Ruthven[51,52] observation that heat transfer effects need to be considered when calculating the diffusion coefficient, $\tilde{D}$.

The effect upon the diffusion coefficient due to the heat of adsorption was observed by Palmer and Bauer[78] in sorption onto montmorillonites. A number of papers have considered this effect and its influence in zeolite sorption. Firstly it is worth considering

how an increase in temperature will influence the rate of sorption.

Barrer and Clarke[76] showed that increasing the temperature of sorption

causes an increase in the measured diffusion coefficient, and a

decrease in equilbrium loading (Q_∞) of the zeolite, (Table 4.1.).

Table 4.1. The diffusion coefficients and equilbrium loadings for the

uptake of some n-paraffins in zeolite A at various

temperatures[76]

Diffusivative	Temperatuic (K)	Equlibrium Loading $Q_\infty(mgg^{-1})$	Diffusion Coefficient D ($10^{17}m^2s^{-1}$)
$n-C_4H_{10}$	348	87.2	0.74
	363	80.2	1.64
	373	73.5	2.60
$n-C_9H_{20}$	373	136.0	0.32
	393	134.2	1.11
	408	132 6	2.40

So any alteration in the local temperature of the zeolite could

influence the observed sorption rate Consequently heat transfer

processes must be properly accounted for in the diffusion coefficient

determination.

Attempts to measure the heat generated during sorption in

zeolites have been made by Egan et al[45] and llavsky et al[79]. Egan and

co-workers measured a maximum temperature rise of 15°C for the

sorption of nitrogen in 4A zeolite, and 50°C for the sorption of

propane in 5A zeolite, and both experiments were conducted isothermally

at −78°C. The effect of this heat of adsorption on the rate uptake

curve was then considered, (Fig 4.111.). When the temperature maximum

occurs early in the uptake process no pronounced effect on the rate

curve is observed (curves A and B, Fig 4,111.), although it would be

erroneous to assume that the data was obtained under isothermal

conditions. However when the temperature maximum occurs later in the

uptake process (curve C, Fig 4.iii.) the uptake curve is altered

(curve D, Fig 4.iii.), so the effect of the heat of adsorption will

influence the observed value of the diffusion coefficient. The authors

note however that the distribution of particle sizes within the sample

could cause a similar effect, ie. the smaller crystals saturate first

and no longer contribute to the rate, so the observed rate is reduced

as the sample approaches equlibrium loading. The Ilavsky[79] study

confirmed much of this work using a different technique. Using

thermocouple wires of 0.1mm diameter, the temperature on the surface

and in the centre of a zeolite pellet could be measured, and for the

sorption of n-heptane on a zeolite, a temperature gradient of more

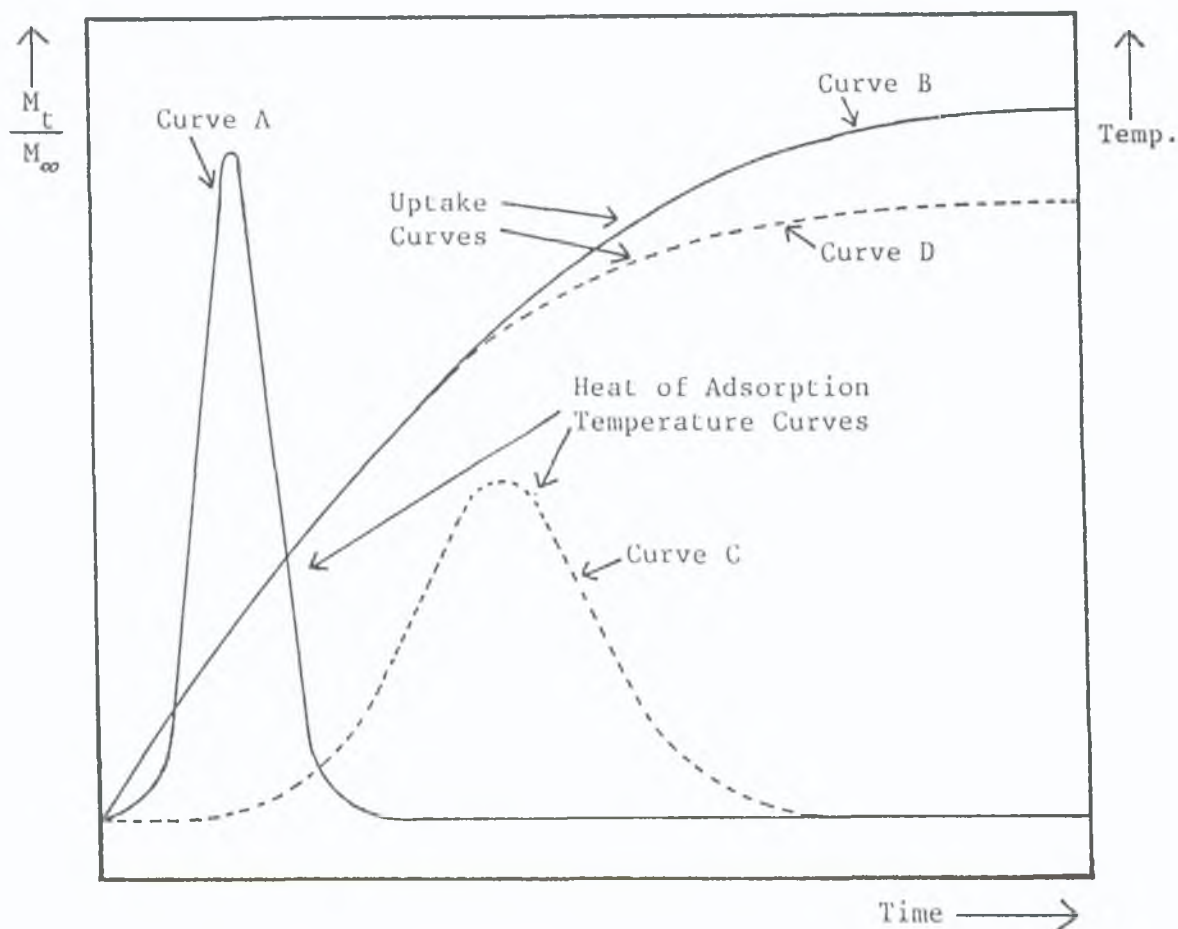than $20^{\circ}C$ above isothermal was observed.

Fig 4.iii.   Diagram illustrating the effect of the heat of

adsorption on the isothermal rate uptake curve.

In recent years the use of nuclear magnetic resonance techniques to measure diffusion coefficients, have been applied to the study of thermal effects in zeolite crystals. Some points worth noting about nuclear magnetic resonance studies are that they have the advantage of not being influenced by thermal effects[53]. Also the mineral samples used for nuclear magnetic resonance studies are previously equilibrated with sorbent, and so they are a study of the sorption dynamics at equilibrium Sorption rate studies use non-equilibrated samples, and so are dynamic studies of a non-equilibrium system. A further point is that the nature of the nuclear magnetic resonance studies, means that the sample and grain size usually have on influence, this however is a problem in sorption rate studies, so the results from the two techniques may not be directly comparable. However Bulow et al[80] found that by comparing nuclear magnetic resonance and sorption rate results, the rate uptake curves deviated from an isothermal uptake curve, being faster in the initial region and slower in the final approach to equilibrium in accord with observations previously made by Egan et al[45] and Lee and Ruthven[55]. This is attributed to thermal effects primarily due to heat transfer from the external surface of the sample. In conclusion diffusion in zeolites may be summarised by the findings of Doelle and Riekert[46]. Processes other than diffusion in crystals, but coupled with sorption, namely flow in the intercrystalline voids and heat transfer, can have considerable influence on the rate of mass transfer between the gas phase and a zeolitic sorbent.

Before discussing the type of diffusion that might occur in a clay system it is worth mentioning counterdiffusion briefly This may be considered as a second molecule diffusing within the clay in the opposite direction to the first, ie the reactant diffusing to

and the product diffusing away from the active site. Moore and Katzer[75]

showed that diffusion of products out of zeolite catalysts may

interact with the reactant molecule and contribute to a reduction in

the rate of diffusion. Such influences on the sorption rate must be

borne in mind when interpreting the data.

Before the experimental results can be evaluated properly

it is important to have an understanding of the diffusion processes

involved in adsorption on clays. When sorption rate studies on zeolites

are carried out the theoretical model can be based on the fact that

each zeolite pellet is a single crystal and may be approximated to a

sphere, consequently a diffusion model may be designed on this basis.

However with clays such as montmorillonite a very different situation

exists (Fig 4.iv.), each grain of clay is comprised of many different

particles of a non-uniform shape and size, and varing diameters. The

grain itself is a non-uniform shape, but by sieving the clay a uniform

size range may be obtained (see chapter 3.) The diffusion model for

a clay must be based on an idealised representation of the actual

packed bed of clay grains. So the physical characteristics of the

clay sample must be borne in mind considering diffusion in such a

system (Fig 4.iv.).

Diffusion in macropores[50a], is known to influence the

overall kinetics of hetrogenous catalytic reactions, and is generally

controlled by a combination of four different diffusion processes.

Two of the four mechanisims will only contribute slightly in the

case of the samples used in the studies here. Molecular diffusion is

when the resistence arise from collisions between the diffusing

molecules, and is dominant whenever the mean free path of the gas,

(the average distance travelled between molecular collisions), is

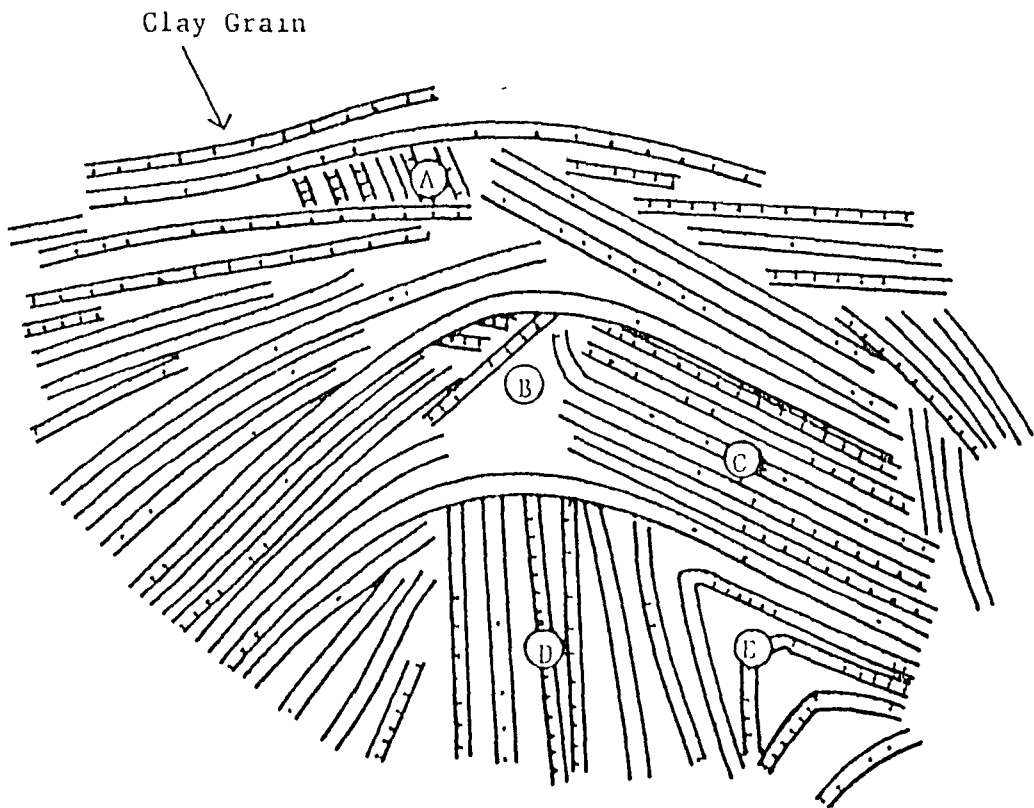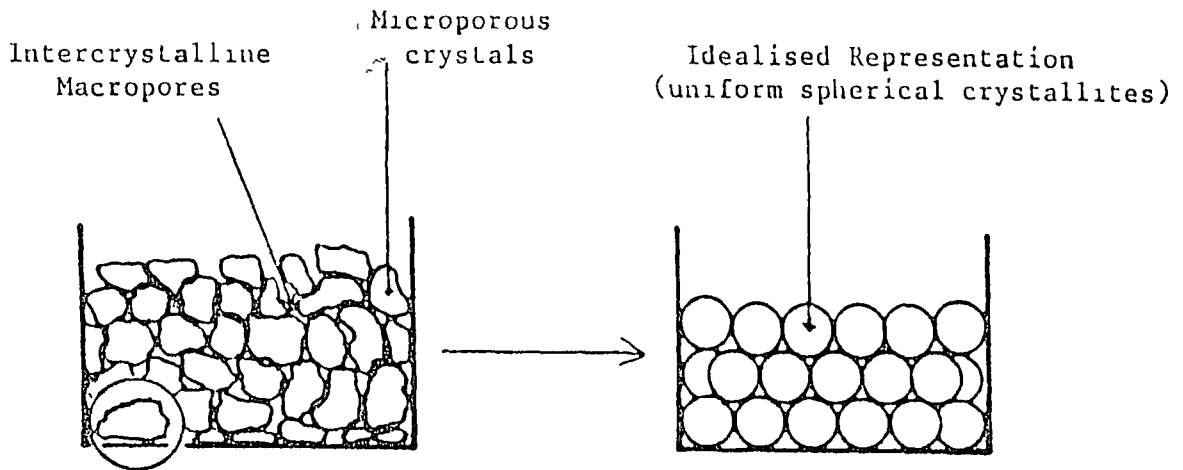small relative to the pore diameter, and with montmorillonites this

Fig 4.iv.   Schematic representation of the structure of a clay grain.

Some of the common structural defects are shown A - E.

Where   A = Edge to face stacking.

B = Voids.

C = Ordered Domains.

D = Regions of disordered stacking.

E = Regions of gross folding.   (adapted from Cebula et al[86]).

is unlikely to be a significant factor. Poiseuille flow is only a
contributing factor, when the differences in total pressure across
a particle directly contributes to the adsorption flux from forced
laminar flow through the macropores This effect is generally
negligible in a packed bed since the pressure drop over an individual
particle is very small, and packed bed systems were used in these
studies.

The two diffusion controlling factors of more interest for
this study are, firstly, Knudsen diffusion, this occurs in low pressure
systems where the mean free path is greater than the pore diameter.
So collisions of the molecules with the pore walls occur more frequently
than collisions between diffusing molecules. The characteristic feature
of knudsen diffusion is its randomness When a molecule strikes the
pore wall it is not bounced off like a tennis ball, rather it is
instaneously adsorbed and re-emitted in a direction random to its
origional direction before collision. Knudsen diffusion may be
estimated from the equation,

$$D_k = 9700u \left(\frac{T}{M}\right)^{1/2} \qquad (cm^2s^{-1})$$

u = the pore radius (cm)
T = temperature   (K)
M = the molecular weight of the diffusing species

One of the features of knudsen diffusion is that each species diffuses
independently so it is independent of composition or total gas
concentration. There is a slight temperature dependence and an inverse
dependence on the square root of the molecular weight. The second
influencing factor is Surface diffusion, as it is a direct contribution
to the flux from transport through the physically sorbed layer on the
surface, and may be applicable in the case of montmorillonite clays.
This effect is temperature dependent, as a temperature above the boiling

point of the sorbed species, would cause the thickness of the adsorbed layer to decrease, so flux through the surface layer becomes small compared with flux through the gas phase. It is also usually concentration dependent as this can influence the adsorbed layer thickness, and as a good general rule, surface diffusion is only significant in small diameter pores in which flux through the gas phase can be attributed entirely to knudsen diffusion.

In conclusion, it is clear that many factors influence diffusion in zeolites and other clay minerals, and these factors will also be important when considering diffusion in trivalent cation-exchanged montmorillonite. So when considering the following studies it is important to bear in mind the effects of size, shape, polarity, and partial pressure of the diffusivative, and its interactions with the clay sheets or the interlayer cations, as these may influence the rate of diffusion Other factors such as the heat of adsorption and the magnitude of such a thermal effect will also influence the rate uptake curve. The clay sample itself is also important, as the nature and type of interlayer cation, and the grain and sample size being used in the packed bed of the sample pan are important So bearing all of these influencing factors in mind a study of the diffusion and interactions of alcohols and cyclic ethers on trivalent cation-exchanged montmorillonite will be considered in the following chapters.

CHAPTER 5

Vapour Phase Sorption Kinetics for Alcohols and Cyclic Ethers on

Cation Exchanged Montmorillonite

5.1 Introduction

The study of sorption dynamics, or the diffusion of organic

compounds towards,and product molecules away from the active sites

of a cation exchanged clay, can play an important role in the rate

of reaction, and may even be the rate limiting stage. In this

investigation the direct measurment of sorption kinetics was used,

as this determines the rates in practical applications. In section

4 5 it was shown that the sorption dynamics are influenced by several

factors, and the effect of these factors on the rate of uptake will be

examined. By using various forms of cation exchanged montmorillonite

such as Al^{3+}, Fe^{3+}, and Cr^{3+}, the effect of size and charge of the

cations will be examined. The cation can influence the selectivity

of the clay for a specific reaction[11], and the cation can interact

with organic molecules in the interlayer[6], thus effecting reactions

occuring in the clay interlayer The physical size of the hydrated cation

will determine the basal spacing of the clay and this can influence the

rate of diffusion of organic compounds to the active sites, as

larger basal spacings can help to reduce steric hinderance in the

diffusion process. Also the choice of cation can influence the number

and yield of side products for a specific reaction[11]

The cationic form of the clay will to a certain extent

influence the geometry and dimensions of the channel network, as will

thermal pre-treatment of the clays. The size shape and flexibility

of the diffusing molecule can be examined using two different solvent

types The alcohols used increased in physical size as methanol<

propan-2-ol< 2-methyl-propan-2-ol, whereas the cyclic ethers used

1,4-dioxan, tetrahydrofuran (THF), and tetrahydropyran (THP), are

all of similar physical dimensions and have no bulky substitutents,

so that all three might be expected to interact with the exchange cation

in a similar manner.

The effect of sample and particle size was investigated by

using clays divided into known grain size ranges and using different

sample sizes of these groups for the studies. Based on studies

by Egan et al[45], and Doelle and Riekert[46], the effect of a temperature

rise caused by exothermic heat of adsorption, on the sorption kinetics

was also measured. Hence the study may be divided into five sections,

(although many of these influencing factors are interrelated).

(i) An investigation of the influence of sample size.

(ii) An investigation of the influence of grain size.

(iii) An investigation of the influence of the cation exchange form

of the clay.

(iv) An investigation of the effect of the molecular size and shape

of the diffusative.

(v) The effect of temperature on the rate of adsorption.

The choice of the compounds for the investigation was too

some extent based on studies by Adams et al[7], where the influence

of steric hinderance on the rate of reaction of methanol, propanol,

and i-propanol with t-butanol was considered, and this suggested the

choice of alcohols for this study. In another study by Adams et al[6]

the influence of the oxygenated solvents THF, THP, and 1,4-dioxan on

the reaction to produce MTBE was considered, and the authors found

1,4-dioxan to give the highest yield of product Hence it was decided

to investigate the diffusion of these cyclic ethers and three of

the alcohols listed above upon various cation exchanged montmorillonites,

$(Al^{3+}, Fe^{3+}, and Cr^{3+})$.

Experimental limitations dictated that the rate of sorption

may only be studied at the room temperature partial pressures of

the diffusing compounds. The vapour pressure considerations allow the

direct comparison of the sorption rates for, 1,4-dioxan, i-propanol,

and t-butanol as one group, and methanol, THF, and THP as the other

group. This allows additional information on the effect of molecular

size and shape on the relative rate of diffusion of these compounds

into clays to be obtained.

5.2. Optimization of the Experimental Conditions.

Before undertaking sorption kinetic investigations it is

important to ensure that the experimental conditions are optimised prior

to making any measurments.

5.2.i. Optimising Vapour Flow Rates

The flow of solvent vapour over the sample essentially generates

a saturated atmosphere about the sample. Fig 5.1. shows that by

increasing the flow rate of the vapour the rate of sorption increased

to a point where increasing the vapour flow any further does not

effect the rate of sorption significantly. If however a flow of

$100cm^3min^{-1}$ had been used the derived rate of sorption, would have

been limited by the concentration of the vapour in the furnace

atmosphere about the sample. Therefore an unsaturated atmosphere

will give an artifically low diffusion coefficient. The trend shown

in Fig 5.1. is for the uptake of i-propanol upon Cr^{3+}-montmorillonite,

and is indicative of the trend for the other clay-vapour systems

studied.

5.2.ii. Optimising the Grain and Sample Sizes.

Fig 5.11. illustrates the influence of grain size on the

rate of adsorption The system illustrated is the sorption of
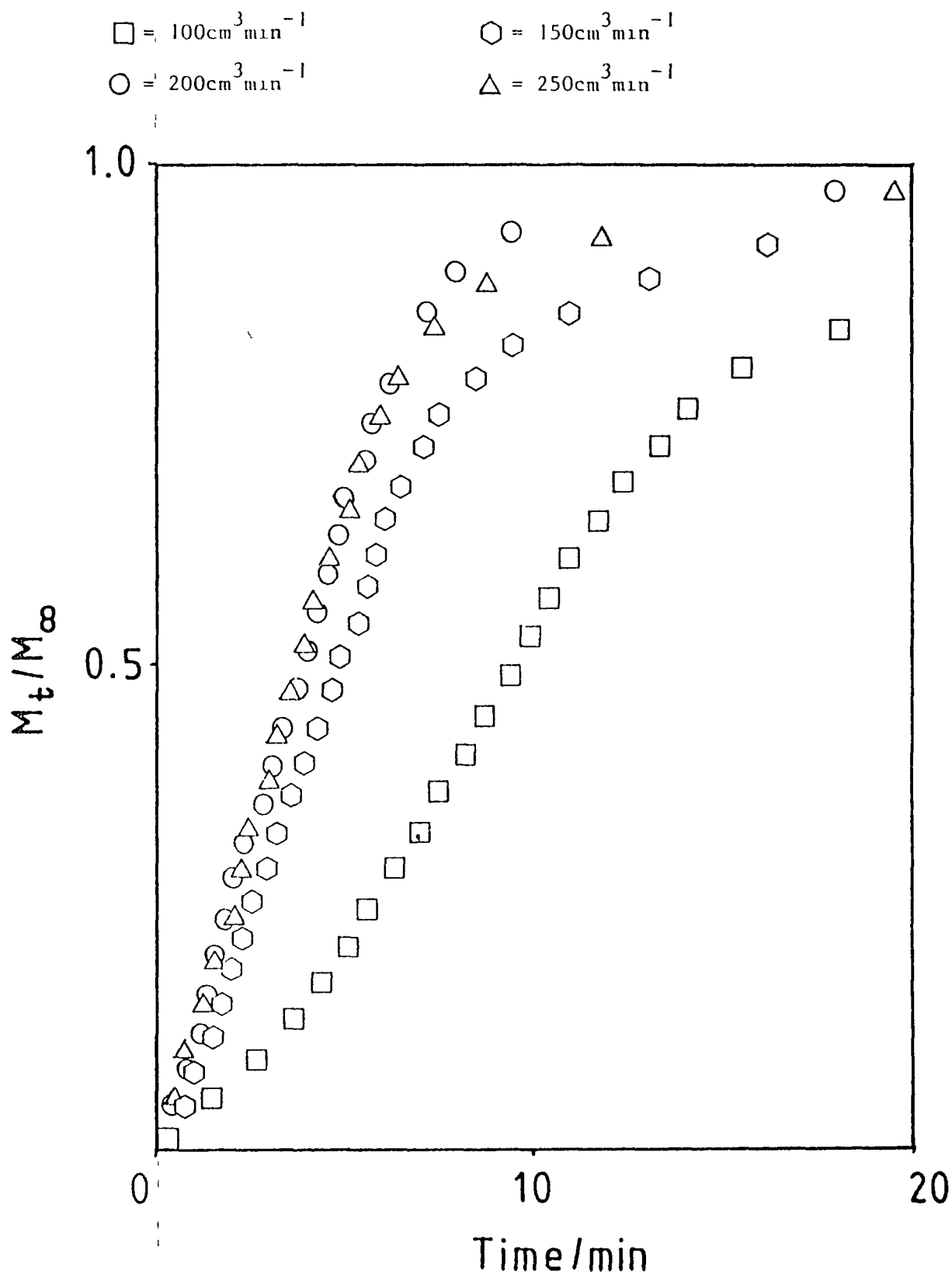
□ = 100cm^{3}min^{-1} ◯ = 150cm^{3}min^{-1}

○ = 200cm^{3}min^{-1} △ = 250cm^{3}min^{-1}

Fig 5.1.   Optimization of the flow rate for the uptake of

1-propanol upon Cr^{3+}-montmorillonite at 18°C.

i-propanol upon Cr^{3+}-montmorillonite at 18°C. The clay was divided
into different grain size groups (see section 3.4.), and the rate of
sorption for each group plotted, (Fig 5 11.). As can be seen the rate
of sorption increased with increasing grain size until a grain size
of <45um was reached, as this was the smallest sieve available at the
time, and this grain size group was chosen as optimium. Using the
<45um grain size the optimium sample size was investigated, using
different sample weights. Fig 5.111. shows that the rate of sorption
increased with decreasing sample size, to a weight of 2.5mg as this
was the minimium weight with which the thermobalance could be operated.
It should be noted that the adsorption of i-propanol upon Cr^{3+}-mont-
morillonite used in these investigations is representative of the
other clay-vapour systems.

Finally Fig 5.iv. illustrates the effect of a mixed grain
size sample on the sorption rate. This shows that for a mixture of
large and small grains the early part of the curve is uneffected,
but the effect is much more pronounced at longer times, with the time
required to reach equilibrium loading significantly longer than that
required by a sample containing the smaller grain sizes only.

5 2.111   Determining the Optimium Thermal Pre-treatment of the Clay.

The hydration state of the clay effects its acidic or
catalytic nature, and was discussed in section 4 3. A fully dehydrated
clay will have a lower amount of bronsted acidity than a partially
dehydrated clay[34]. Ensuring the water content or hydration state of the
clay is reproducible from sample to sample is important. This may be
done by pre-heating the clay to a set temperature before each
experimental run, ensuring a consistent water content each time.
The effect of thermal pre-treatment at a series of temperatures,
on the adsorption of i-propanol upon Cr^{3+}-montmorillonite system,

Δ = 5mg, >250um   ∇ = 5mg, 125-250um   ☐ = 5mg, 63-125um

O = 5mg, 45-63um   X = 5mg, <45um   ● = 2mg <45um
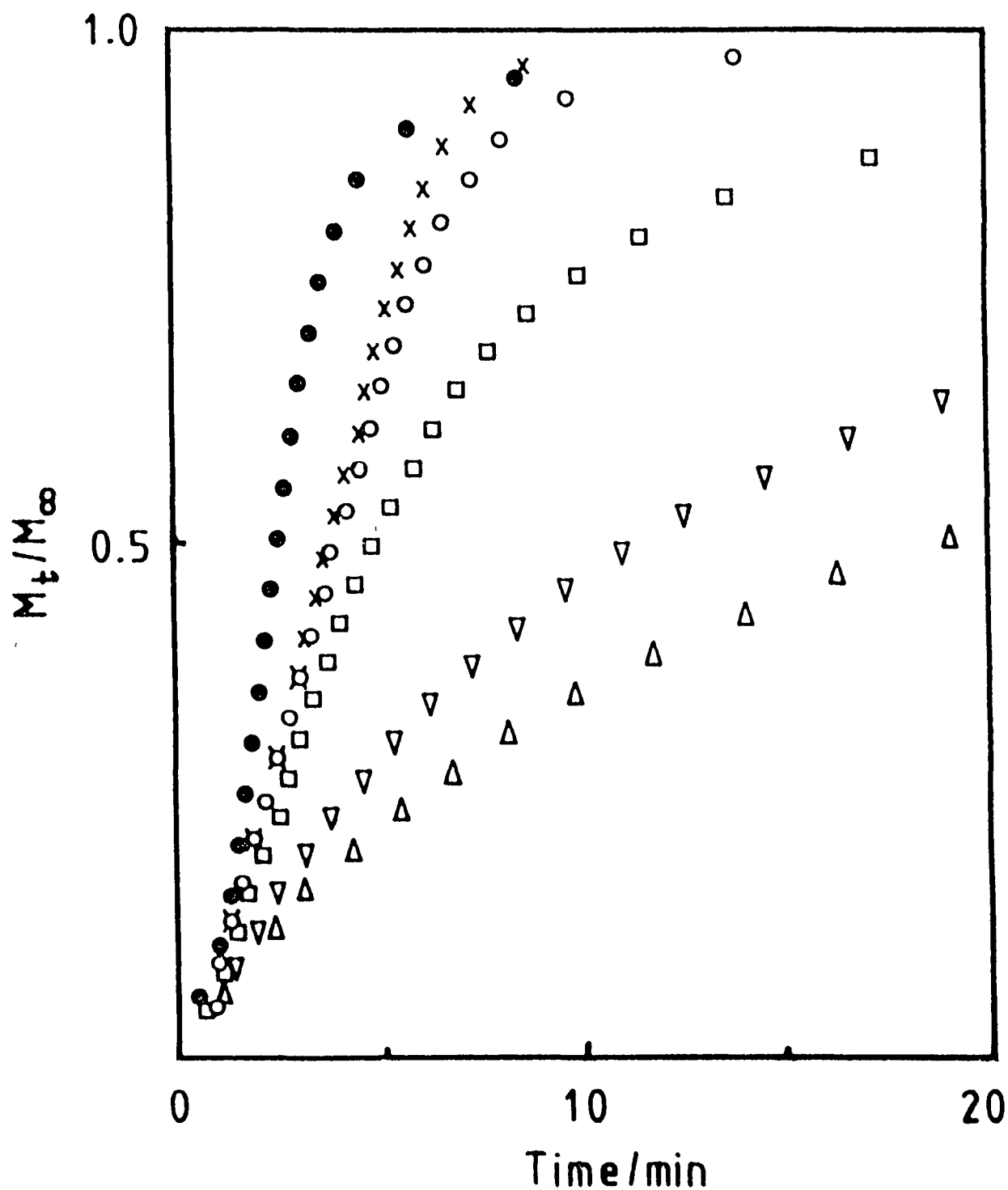
Fig 5.ii. Optimization of the grain size groups using the uptake of 1-propanol upon Cr^{3+}-montmorillonite at 18°C.

Fig 5.iii. Optimization of the sample weight using the uptake of i-propanol upon Cr^{3+}-montmorillonite at 18°C.

$\triangle$ = >250um $\bigcirc$ = 50% <45um + 50% >250um $\bigcirc$ = <45um

Fig 5.iv. Mixed grain size study using the uptake of i-propanol

upon Cr^{3+}-montmorillonite at $18°C$

(fig 5.v.). The rate of sorption decreases as the temperature is

increased beyond 120°C, consequently a thermal pre-treatment

temperature of 120°C was chosen, and again the i-propanol-Cr^{3+}-clay

system is representative of the other vapour-clay systems studied.

Also this pre-treatment ensures that the clays should have a

representitative amount of water in the hydration sphere of the

interlayer cations, thus mimicing the hydration state of the clays

used in catalysis

5.3. Fitting the Experimental Data.

Fig 5.vi. shows a theoretical curve fitted to the experimental

data points. This is done by first plotting the experimental data

on a set of axes, and then different values of the diffusion

coefficient D are supplied to the two-dimensional model of the

uptake process. Using this information the computer plots a curve

for the rate of uptake independent of the experimental data. The

curve is then checked to see if it fits the experimental data

points. If the experimental and calculated curve do not fall on the

same line a better estimate of D is given to the computer, and a

second calculated curve is drawn. This process is repeated until

the two lines coincide. It is important to note that there is an

initial time lag in the uptake data, this is due to experimental

limitations as the furnace atmosphere about the sample does not

become saturated with the vapour instantly upon switching the nitrogen

through the solvent reservoir. This is taken into account when

calculating the best fit curve, a second variable paramater B which

representa the time lag is given to the computer, which then calculates

$\sqrt{B}/D$ the value of which is used to obtain values for the Bessel

functions J_o and J_1, from standard tables and these values are

Fig 5.v. The effect of thermal pretreatment on the uptake of

1-propanol upon Cr^{3+}-montmorillonite at 18°C.

Fig 5.vi. Fitting of the calculated curve to the experimental data
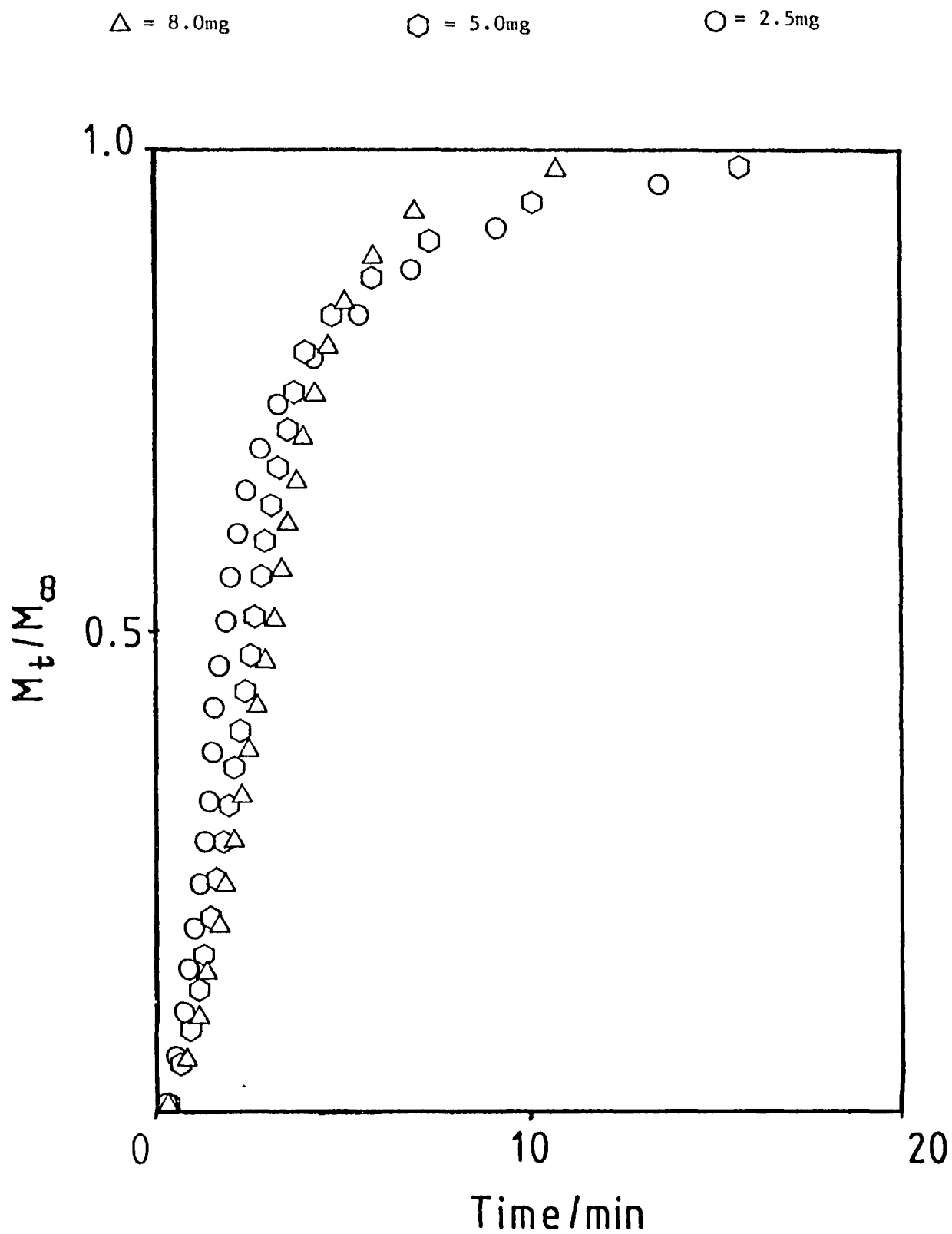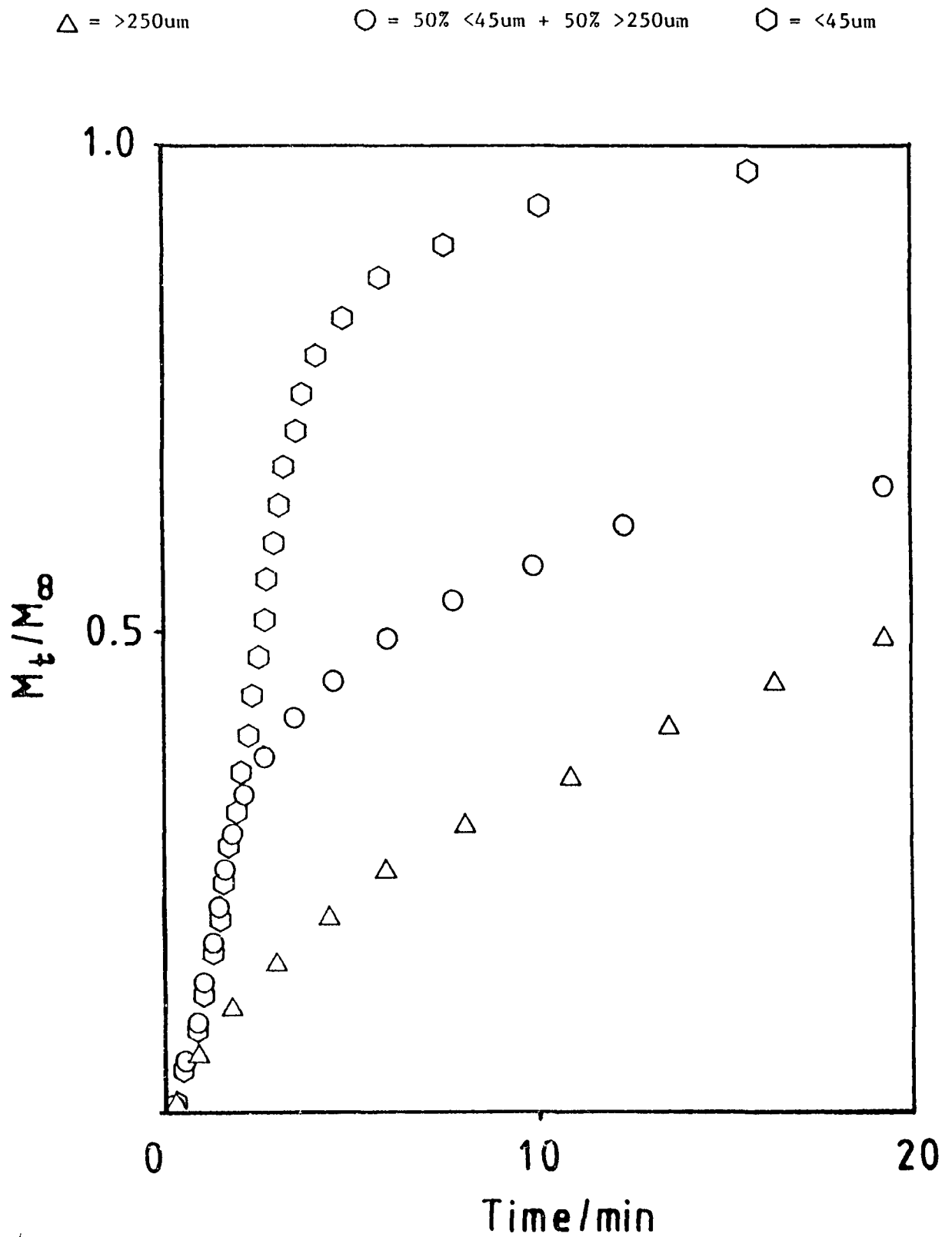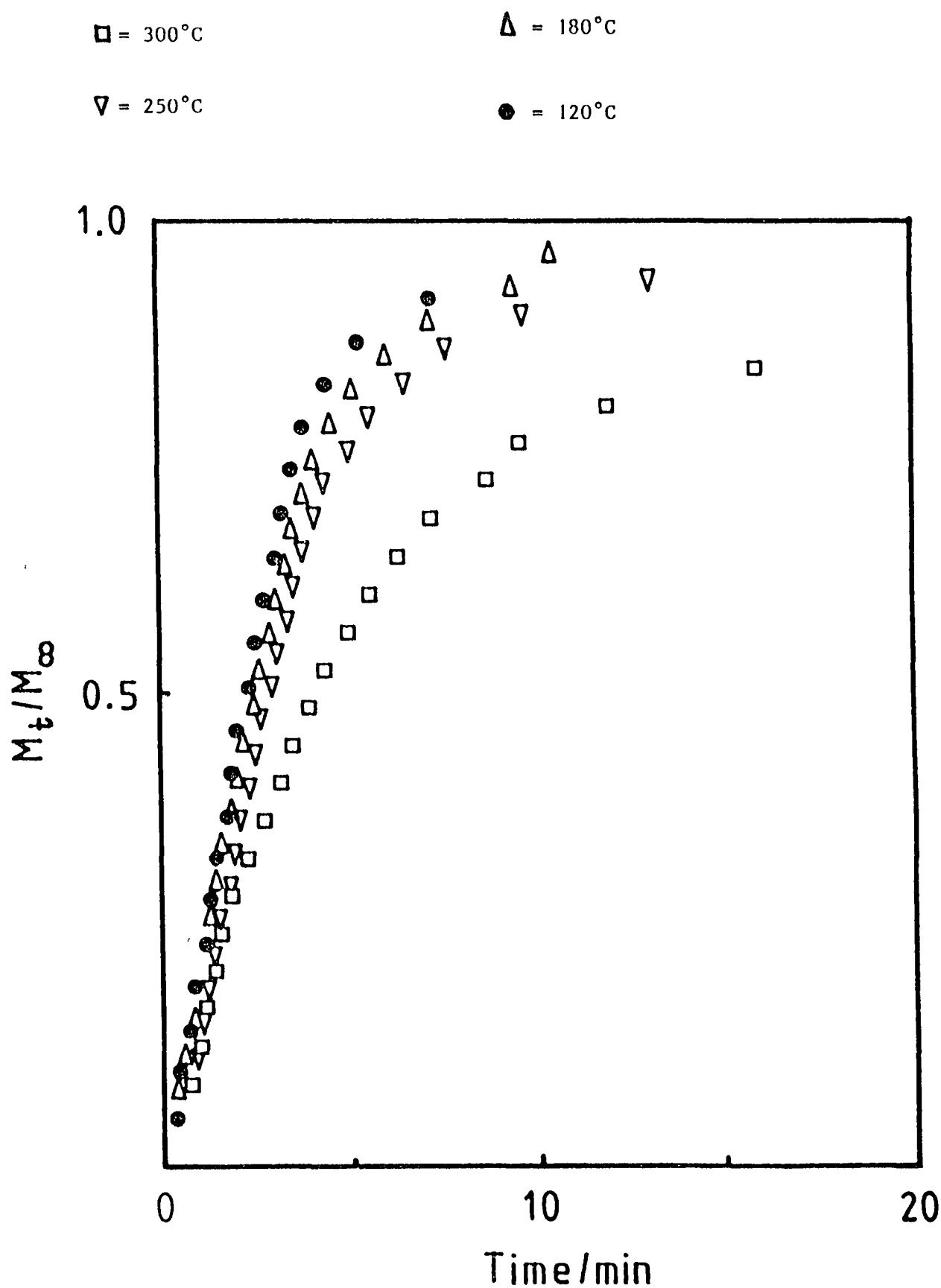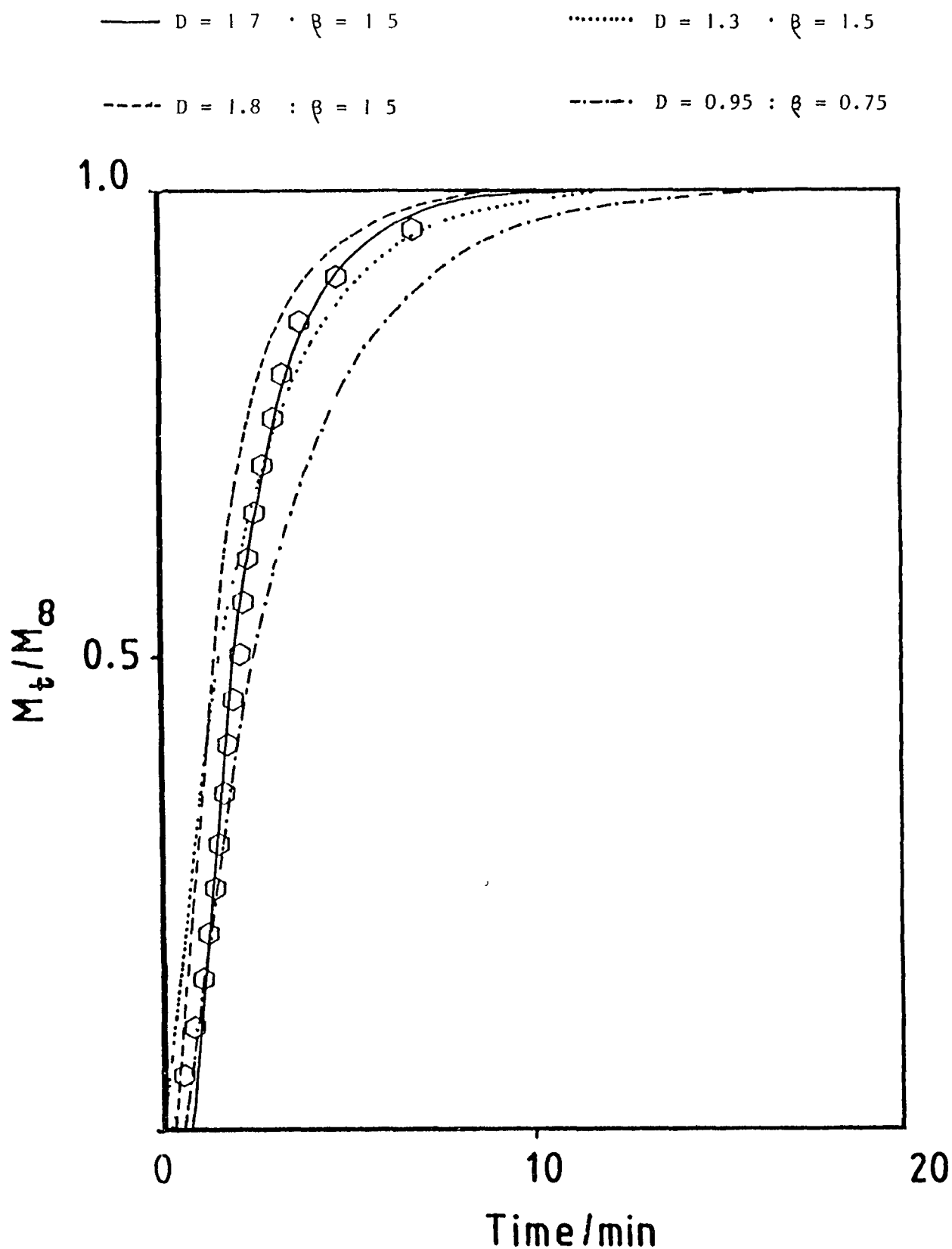
for the uptake of 1-propanol on Cr^{3+}-montmorillonite at 18°C.

inputed to the computer to slightly alter the theoretical curve shape
to fit the experimental data profile more closely, thus obtaining a
more accurate value of $\tilde{D}$. The values of $\tilde{D}$ and corresponding β values are
shown in Fig 5.vi

5.3.i   Experimental Errors on the Data Points.

In order to have some idea as to when a best fit of the
data has been obtained, an indication of the errors involved in the
experimental data points is useful. Fig 5.vii. shows the errors on
the various data points for the uptake curve of i-propanol on
Cr^{3+}-montmorillonite. Taking the error on the measured time to be
10 min. $\pm$ 12sec. which is $\pm$ 2% error, for the weight measurment the
error was taken to be 10mg $\pm$ 0.2mg which is again 2% error, so the
area surrounding the data points in Fig 5.vii. represents a 2% error
on both axes. This error measurment is useful when using the $\tilde{D}$ values
to obtain the activation energies for the clay-vapour systems.

5.3.ii.   The Effect of Particle Size Distribution on Curve Fitting.

As mentioned in section 5.2 the particle size distribution
within a given clay sample can effect the rate of sorption, and
the shape of the uptake curve (Fig 5.iv). The sample which consisted
of 50% <45um grains and 50% >250um grains had an uptake curve that
was uneffected in the early portion but the uptake became much slower
than the <45um sample as time progressed, and the time required to
reach equilibrium loading was much greater.

Fig 5.vii illustrates the particle size distributions of the
clays, and shows that each of the <45um fractions of the different
clay types has a different meaian particle size. From this it might be
expected that the clay types with the larger particle sizes might
deviate slightly from the calculated curves, towards the latter part
of the uptake curve So the uptake curves were the calculated and

• = Experimental data point   ⊢╂┤ = region of error
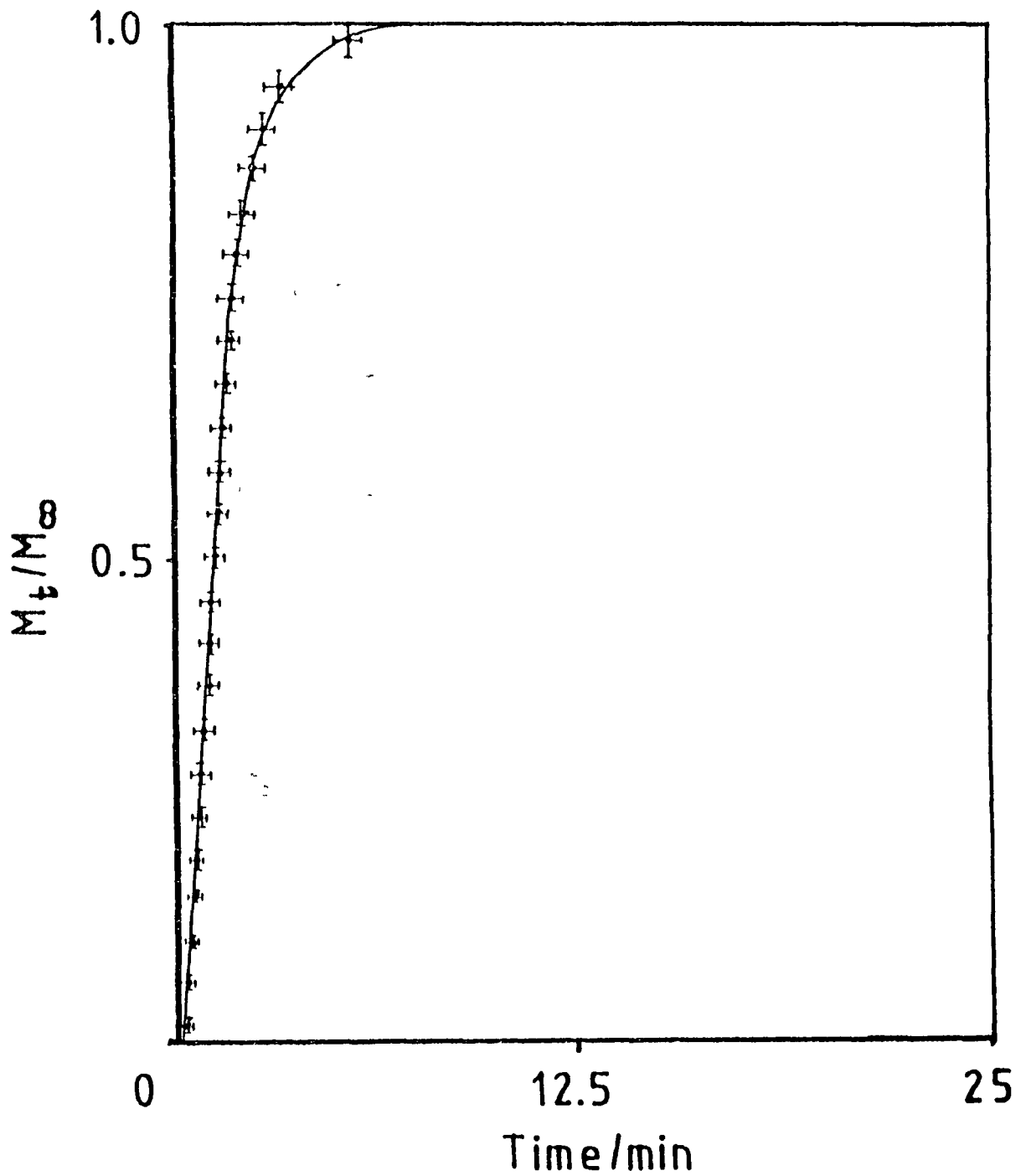
Fig 5.vii. The experimental error bars on the data points for the

uptake of 1-propanol on Cr^{3+}-montmorillonite at 18°C.
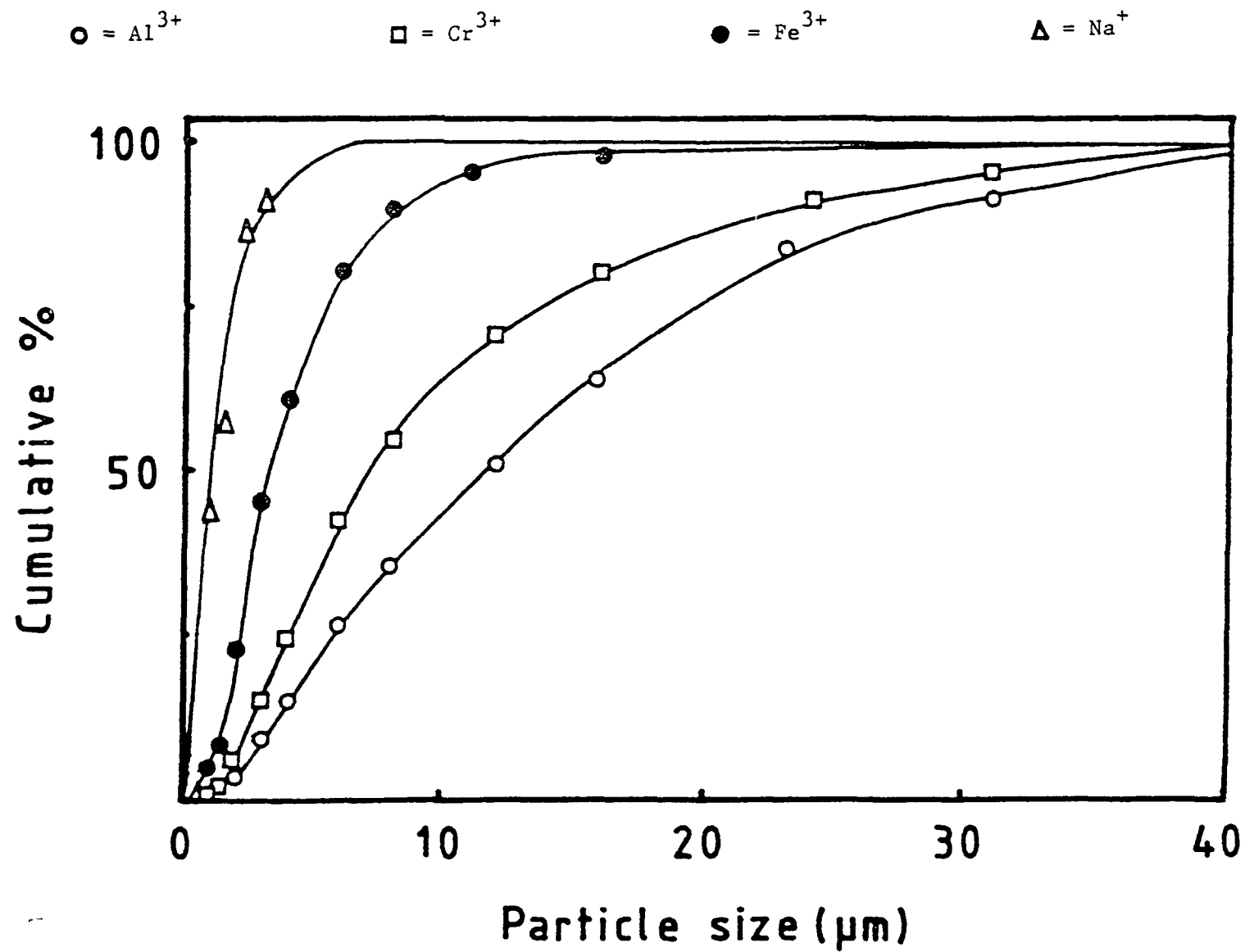
Fig 5.viii. Particle size distribution for the various cation-exchanged montmorillonites.

experimental values which deviate only towards the end of the uptake, may be due to this effect.

5.4   Sorption Kinetics Results.

5.4.1.   The Cation Exchanged Clay Paramaters.

The optimium grain size used was <45um for each of the clay types, and these grains contained a median particle size that increased in the order Na < Fe < Cr < Al (Table 5.1. and Fig 5.viii.). The amount of water lost by the clay when preheated to 120°C is listed in Table 5.ii., and is expressed as a percentage of the total water lost by heating to 500°C, (this temperature is just below the dehydroxylation temperature for the clays). Table 5.iii. lists the basal spacings for the clays after pretreatment at 120°C, cooling in a desiccator, and exposure to the vapour for 16 hours. This gives the equlibrium loading or saturation with vapour of the clay.

Table 5.1.   The median particle size distribution of various

cation-exchanged montmorillonite clays.

Cation	Vapour	Median Particle Size (um)
Al^{3+}	H_2O	11.7
Cr^{3+}	H_2O	7.2
Fe^{3+}	H_2O	2.0
Na^{+}	H_2O	1.2

Table 5.ii. The water loss on preheating at 120°C for various

cation-exchanged montmorillonite clays.

Cation	Vapour	Water removed by 120°C (%)
Al^{3+}	H_2O	70[a]
Cr^{3+}	H_2O	71[a]
Fe^{3+}	H_2O	76[a]
Na^{+}	H_2O	83[a]

note: a = expressed as a percentage of the total water lost by heating
        to 500°C.

Table 5.111.   The saturated vapour basal spacings for various cation-

exchanged montmorillonites over a range of vapours

Cation	Vapour	Basal Spacing (Å)
Al^{3+}	Water	12.5^a
	Methanol	14.0^b
	1-Propanol	14.3^b
	t-Butanol	15.3^b
	1,4-Dioxan	15.6^b
	THF	14.5^b
	THP	15.0^b
Cr^{3+}	Water	12.5^a
	Methanol	15.0^b
	1-Propanol	13.8^b
	t-Butanol	17.4^b
	1,4-Dioxan	15.8^b
	THF	14.3^b
	THP	15.0^b
Fe^{3+}	Water	9.6^a
	Methanol	15.5^b
	1-Propanol	16.0^b
	t-Butanol	17.7^b
Na^+	Water	9.6^a

note· a = 120°C pretreated and cooled in a desiccator prior to analysis.
       b = As for footnote 'a', then exposed to solvent vapour for 16 hours.

5.4.11.   The Rate of Sorption Data.

Sorption kinetics data is usually expressed as plots of,

$$\left(\frac{Q_t - Q_o}{Q_\infty - Q_o}\right) \quad versus \quad Time.$$

Where Q_t = the amount of vapour adsorbed at time t=t.

Q_o = the amount of vapour adsorbed at time t=0

Q_∞ = the amount of vapour adsorbed at time t= equilibrium.

t = time

In this system Q_o was taken as zero, hence this equation may be

written as,

$$\left(\frac{M_t}{M_\infty}\right) \quad versus \quad Time.$$

Where M_t = the mass of vapour adsorbed at time t=t.

M_∞ = the mass of vapour adsorbed at time t= equilibrium.

Using methanol as the vapour the cation dependence of the rate

of sorption was found to increase as $Fe^{3+} < Cr^{3+} < Al^{3+}$ (Fig 5.1x),

and this is representative of the sequence for the other vapours.

The solid lines in the subsequent graphs are the theoretical curves generated

by the computer using the two-dimensional diffusion model, (described in

section 3.10.) The value for the diffusion coefficient was obtained

from the calculated curve, (assuming a particle size of lum), and

is included along with the others derived here in Table 5.1v. The rate

of alcohol uptake observed is shown in Fig 5.x., and the rate of

uptake decreased as methanol $\geqslant$ 1-propanol > t-butanol, and for the

cyclic ethers the observed rate of uptake decreased as THF $\geqslant$ THP >>

1,4-dioxan, (Fig 5 x1). The effect of temperature on the uptake of

methanol on Al^{3+}-montmorillonite is illustrated in Fig 5.x1i., and a

temperature variation in the range 18° to 72°C, has little effect on the

observed diffusion coefficients. This observation was further investigated

using the uptake of 1-propanol on Cr^{3+}-montmorillonite, (Fig 5.x111),

the diffusion coefficients for the uptake at various temperatures,

(18°, 43°, and 72°C) were measured. An Arrhenius plot of these diffusion

coefficients was drawn, and from this the activation energy for the

uptake of 1-propanol on Cr^{3+}-montmorillonite was determined ($\sim$4 kJ mole^{-1}).

The derived activation energy was extremely low, and is indicative of all

of the alcohols Similarly for the cyclic ether vapours, the effect

of varying the temperature on the cyclic ether vapour, the effect

The uptake of THF and 1,4-dioxan on Al^{3+}-montmorillonite was studied,

(Fig 5.x1v.). (note, the solid lines on this figure are not the best

fit of the data points as is usually the case, instead, they represent

the best fit lines for the sorption of THF and 1,4-dioxan on Cr^{3+}-

montmorillonite). This shows that there is little cation dependence

of the uptake of these vapours, when the results from each set of

$\triangle = Fe^{3+}$ $\bigcirc = Cr^{3+}$ $\square = Al^{3+}$
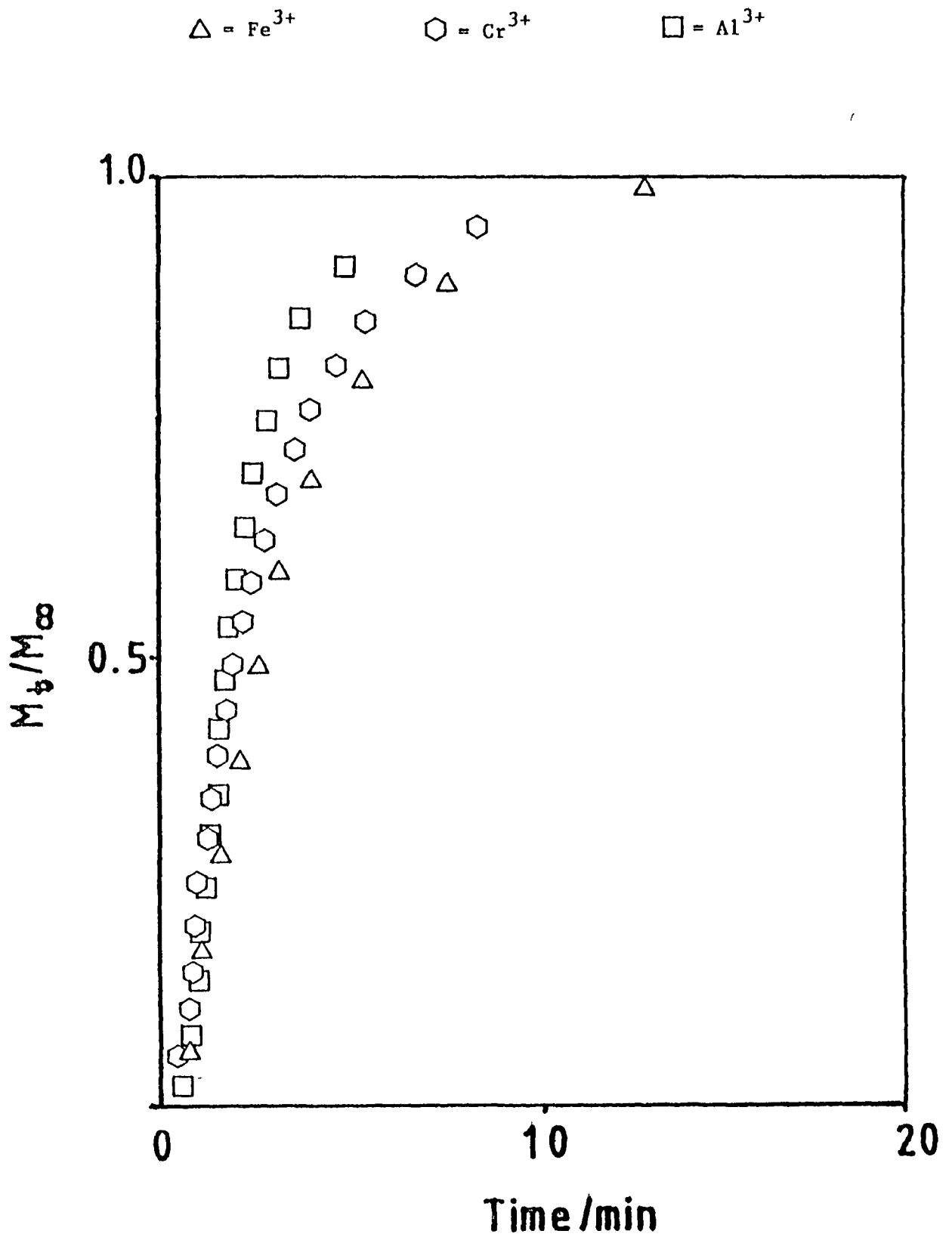
Fig 5.ix.   The cation dependence of the uptake of methanol on the

three cation-exchanged montmorillonites at 18°C.
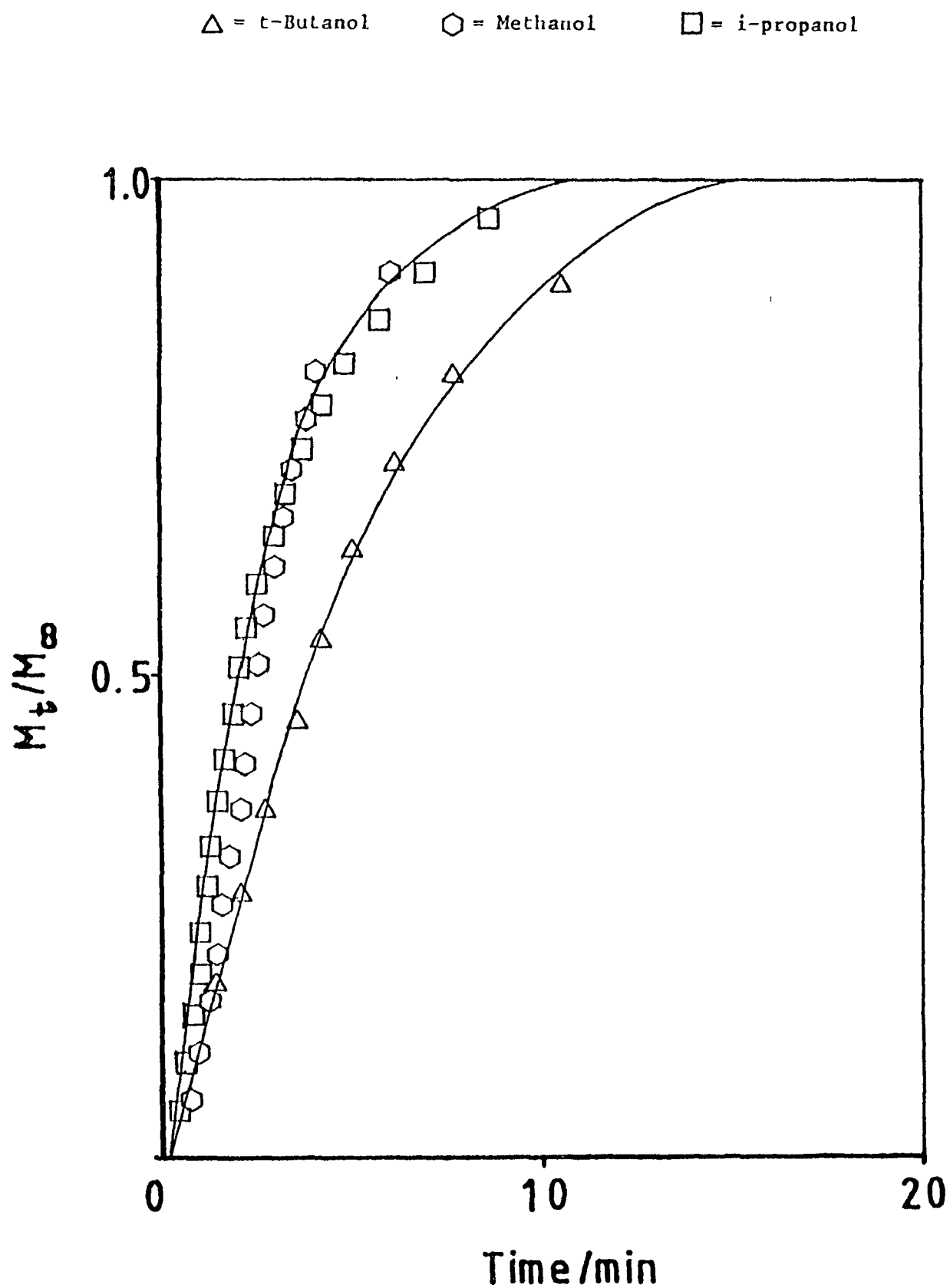
Fig 5.x. The uptake of the three alcohols on Cr^{3+}-montmorillonite at 18°C.
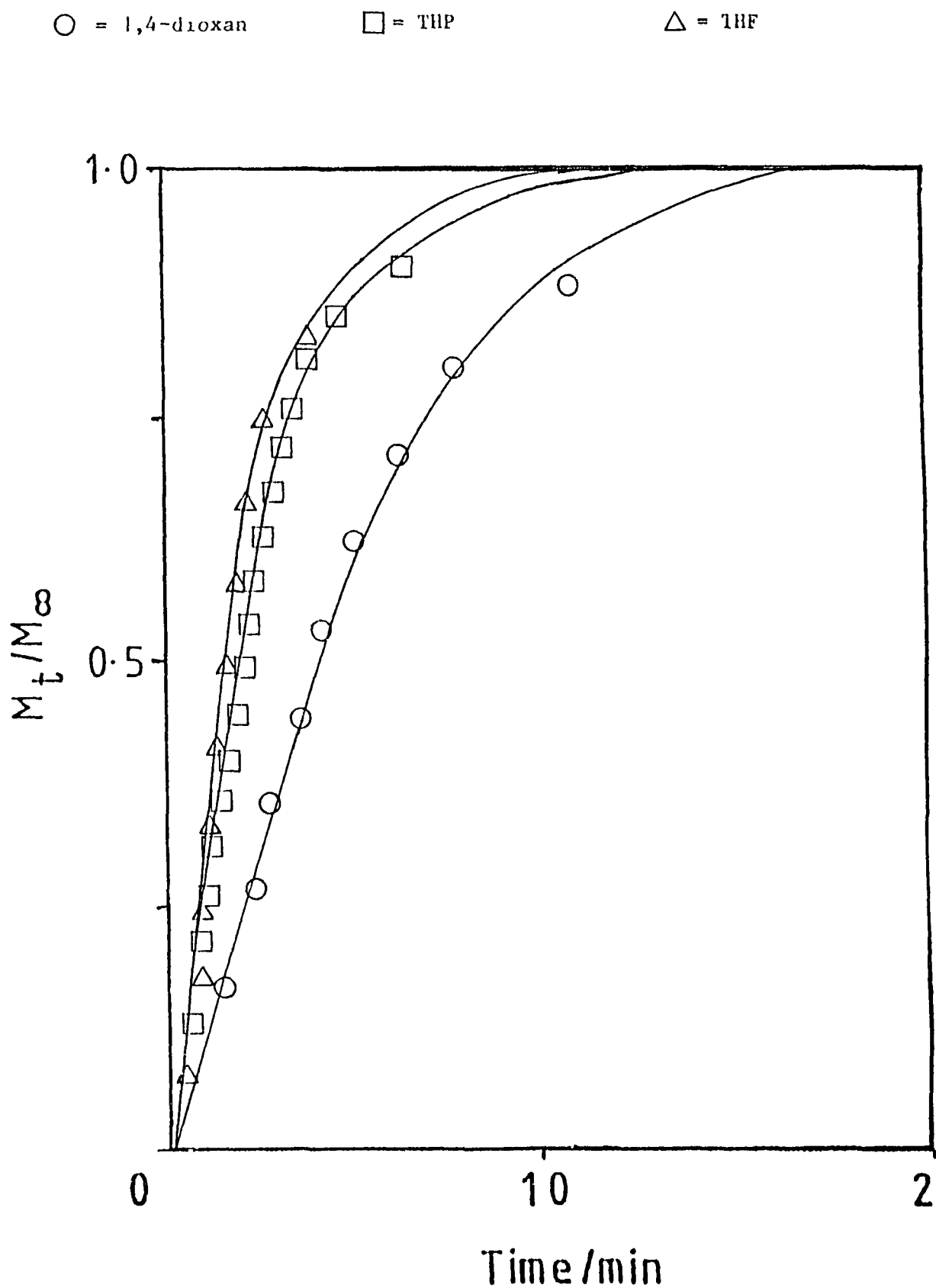
Fig 5.xi. The uptake of the three cyclic ethers on Cr^{3+}-montmorill-onite at 18°C. (The full lines are theoretical curves generated by the two-dimensional model)
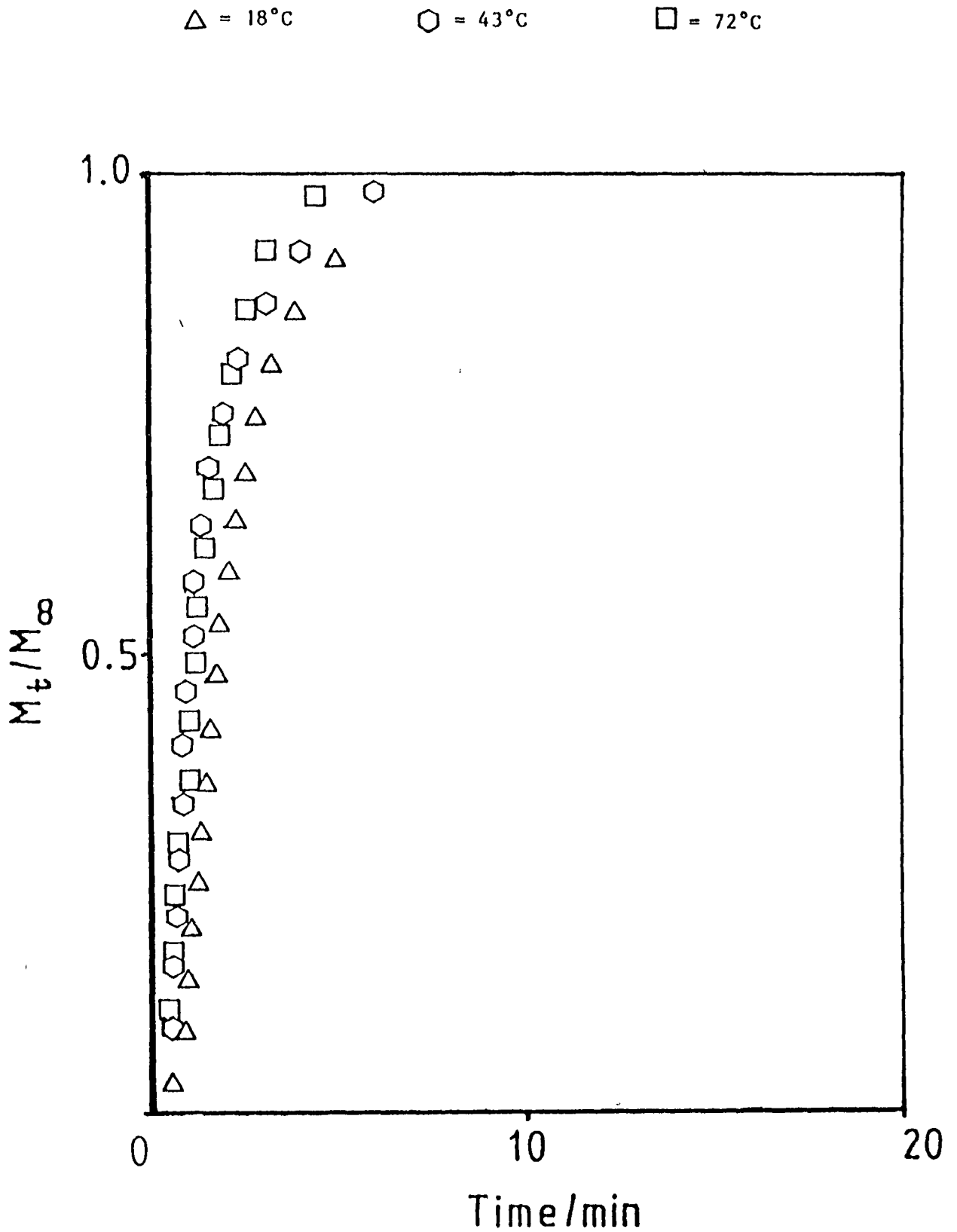
Fig 5.xii. The temperature variation of the sorption rate using the uptake of methanol on Al^{3+}-montmorillonite.
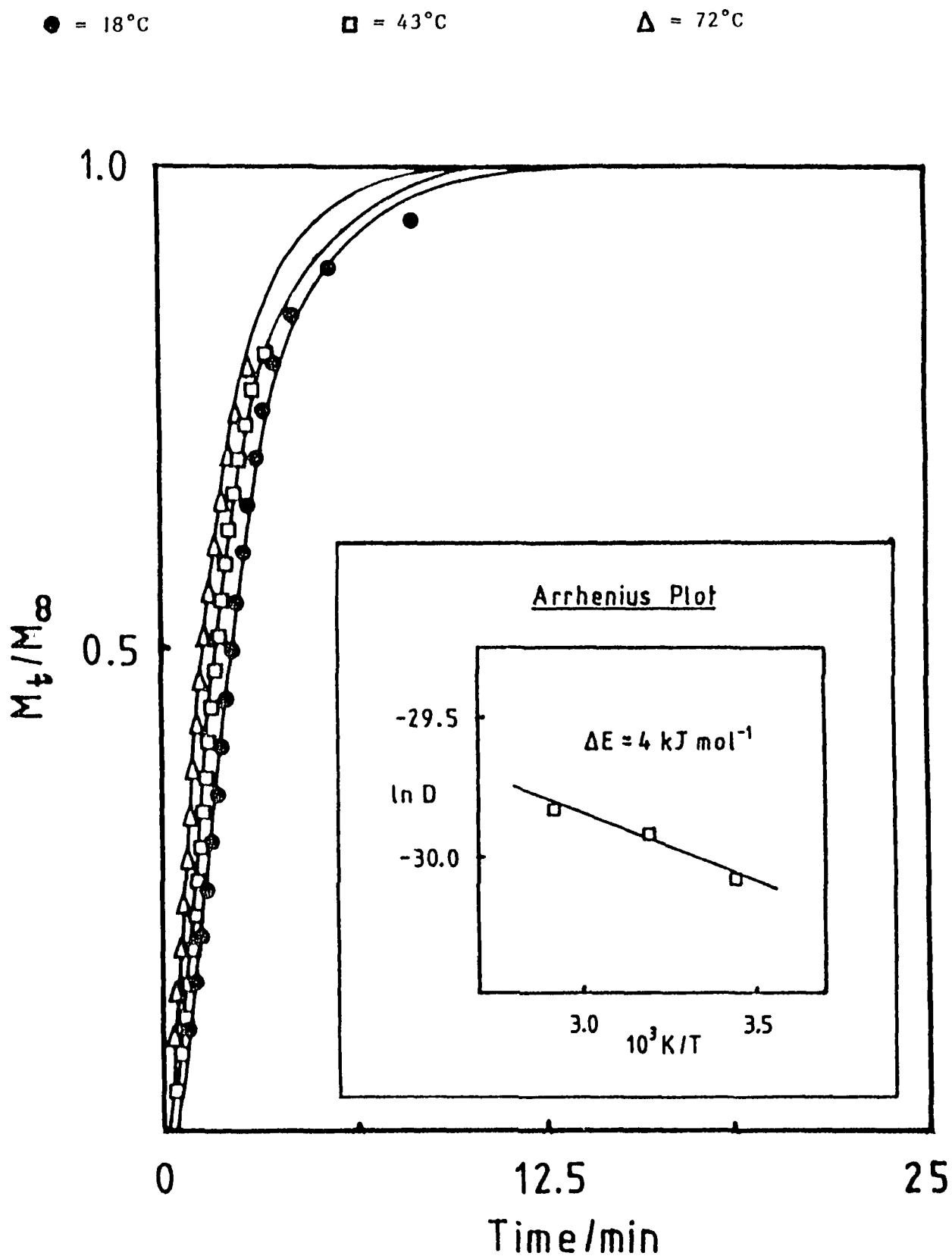
Fig 5.xiii. The effect of temperature on the sorption rate of
1-propanol on Cr^{3+}-montmorillonite. (insert is the
Arrhenius plot of the data, and the full lines are the
theoretical curves generated by the two-dinensional model)

99
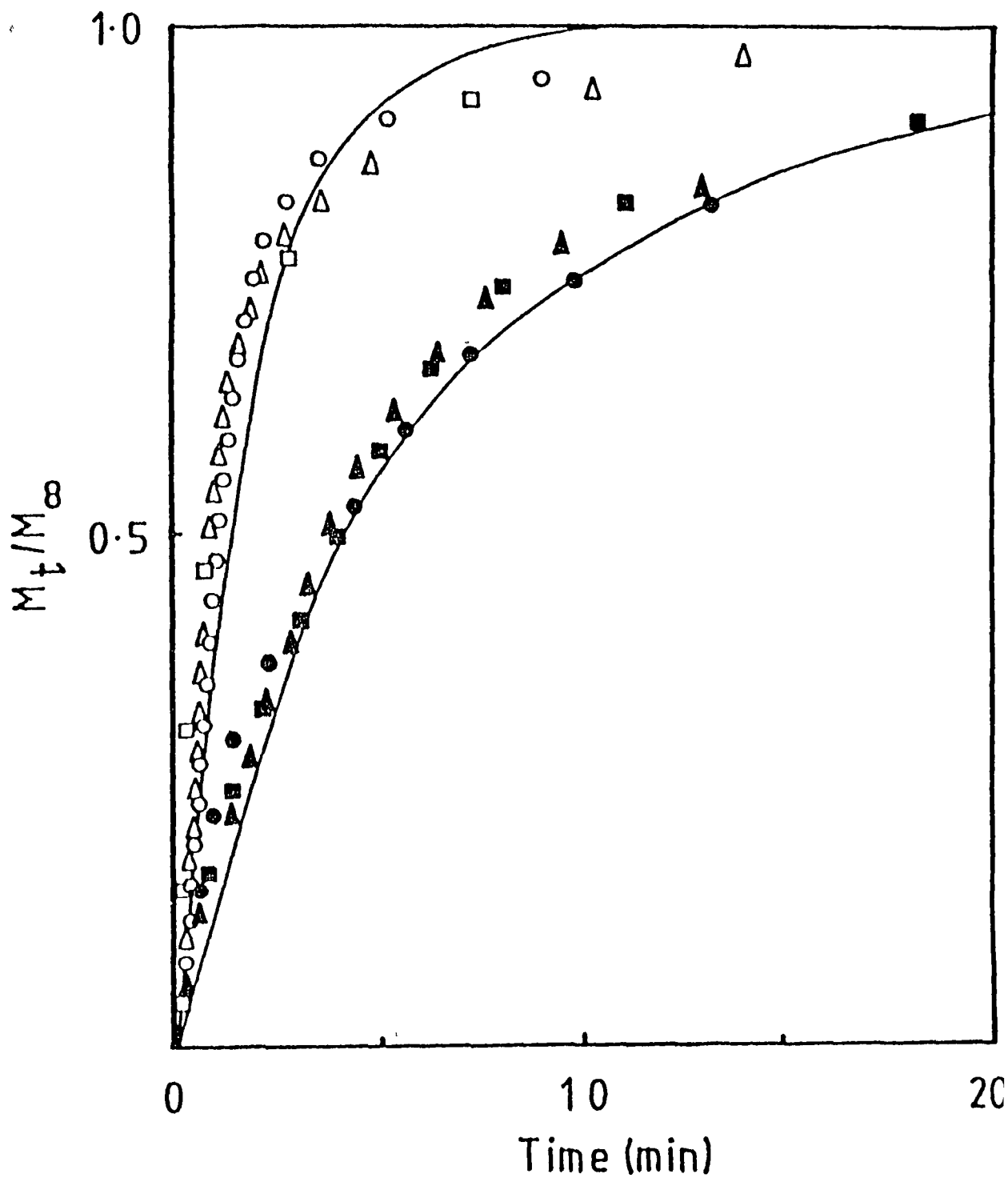
Fig 5.xiv. The uptake of THF and 1,4-dioxan on Al^{3+}-montmorillonite as a function of temperature.

the rate of sorption.

Table 5.v. The peak heat of adsorption data for the uptake of various
vapours on Al^{3+}-montmorillonite at 18°C.

Clay	Vapour	Peak Heat of Sorption (°C)
Al^{3+}-montmorillonite	Methanol	1.0
	1-Propanol	2.0
	THF	3.0
	1,4-Dioxan	0.25

5.5 Discussion of the Experimantal Results.

5 5.1. The Clay Grains.

The use of cation-exchanged montmorillonite clays in
catalysis has been discussed at length in this work, however when
using these clays it is important to ensure that, for example an
Fe^{3+}-montmorillonite is a clay in which the interlayer cations are
actually Fe^{3+}-cations so that a correct interpertion of the results
can be made. It is possible that on heating the clay, the interlayer
enironment of the clay may alter, with some of the cations leaching to
the edges of the clay layers causing the clay to behave as a partially
H^{+}-montmorillonite Hence the basal spacings shown in Table 5 iii.
indicate that thermal pretreatment at 120°C causes the Fe^{3+}-montmorillonite
to essentially collapse, whereas the Al^{3+}-montmorillonite and Cr^{3+}-
montmorillonite are still partially expanded, (ie some H_2O remains
in the interlayer as suggested by Carr[34]). However the results in
Table 5.iii. show that on equilibrium loading during the sorption kinetics
experiments the Fe^{3+}-montmorillonite form is re-expanded to a basal
spacing similar to that of the Al^{3+}, and Cr^{3+}-montmorillonites.
Breen et al[47] have shown that the number of bronsted acid sites increases
following thermal pretreatment at 120°C for all three forms of the clay.
Also Tennakoon et al[21] postulated that upon heating Al^{3+}-montmorillonite
at a temperature as low as 50°C a dimerization and subsequent release

of a proton occurred. Combined with this some mossbauer studies by

Halsen[49] on Fe^{3+}-montmorillonite showed that on drying the iron

percipitated as an oxyhydroxy form between the clay sheets, and

on increased heating this iron diffused to the edge of the platelets

causing the clay to collapse.

Based on this the Fe^{3+}-montmorillonite reported here may behave

as a H^+-montmorillonite with an oxy or oxyhydroxy coating, and the

Al^{3+}, and Cr^{3+}-montmorillonite may be partially H^+-exchanged.

5.5.11. The Effect of Sample and Grain Size on Sorption Kinetics.

In recent studies it has been shown that the rate of sorption

at the surface of a porous solid is usually so high that the overall

rate of sorption is controlled by the heat or mass transfer rather than

by intraparticle diffusion kinetics[50a,50b]. So to confirm the dominance

of intracrystalline diffusion both the sample and grain size must be

varied.

It is now well established that the initial portion of the

uptake curve is sensitive to any resistance to diffusion in the sample

bed, or macropore resistance. As initially the diffusing molecules would

not only be expected to penetrate the clay layers, but also would meet

additional diffusional resistance associated with transport through the

crystal bed[50b], because it is not possible to have a single isolated

particle. The longtime region of the curve is sensitive to the effects

of finite heat transfer resistance and crystal size distribution. As

a buildup of localized heat in the sample can effect the rate of

diffusion. Although as shown in Fig 5.xii. and 5.xiv. the clay-vapour

systems considered here show little variation with temperature and

the peak heats of adsorption (Table 5.v.) are low relative to the

temperature of sorption. Another possible cause of any deviation in the

latter part of the experimental data points from the calculated curve

may be due to the particle size distribution as a grain comprised of

larger particles will have a decreased rate uptake at longer times,

(Fig 5.iv.). Egan et al[45] showed that the rate limiting heat

transfer process in a batch sorption experiment is controlled by the

dissipation of exothermic heat of adsorption from the external surface

of the adsorbent sample, rather than, by conduction of heat through

the sample.

Based on this Fig 5.iii. shows that the rate of sorption

increases with decreasing sample size and this indicates that resistance

to diffusion in the bed is occurring. Also Fig 5.ii. shows that the rate

of sorption increases with decreasing grain size which constituted the

sample bed, suggesting that there is resistance to mass transfer between

the various size particles, (ie Fig 5.vii.), which formed the grain.

Note this trend was observed despite the fact that grains of >63um

packed easily into the sample pan, whereas grains <63um were of a more

powdery nature and increased the physical size of a given sample weight.

This observation removes any concern about the interlayer cation form

(discussed in section 5.5.i.), Since these cations seem to contribute little

to the rate limiting process.

However if Fig 5.ix. is considered the observed cation dependence

of the alcohol sorption rate is difficult to identify, although

the rate parellels the observed sequence of the median size of particles

which contribute to the grains (Table 5.i.). This implies that the

measured rate probably reflects the tortuosity of the channel network

within the grains. Consequently this combination of factors indicate

that inter-particle and not intra-particle diffusion is the rate controlling

influence.

5.5.iii The Sorption Rates of the Alcohols and Cyclic Ethers.

The sorption rate of the alcohols shown on Fig 5.x., generally

decreases as methanol $\geqslant$ 1-propanol > t-butanol and could be due to steric effects, if the rate determining process was interlamellar transport. But as bed diffusion appears to be the rate controlling stage, the sequence conforms to the required $1/\sqrt{mass}$ dependence required if Knudsen diffusion was the major contributor to mass transfer resistance. Knudsen diffusion occurs where resistance to the flow arises from collisions between diffusing molecules, and is independent of concentration with only a slight dependence on temperature, but it is inversely dependent on the square root of the molecular weight.

$$D_k = 9700u\left(\frac{T}{M}\right)^{1/2} \qquad (cm^2 s^{-1})$$

Where u = the pore raduis (cm)
       T = temperature (K)
       M = molecular weight of the diffusing species.

When the cyclic ethers are studied the sorption rate decreased as THF $\geqslant$ THP >> 1,4-dioxan, (Fig 5.xi.). However the sequence does not conform to the $1/\sqrt{mass}$ dependence required for the limiting Knudsen diffusion. This trend may reflect a concentration dependence of the sorption rate insofar as THF and THP yield higher vapour pressures than 1,4-dioxan Also it may simply be that the 1,4-dioxan sorption process is retarded due to bidentate coordination of the ether to the Al^{3+}-ions at the clay edges. A similar binding for methyl acrylate which inhibited its reaction with cyclopentadiene is discussed by Adams et al[28]. Also the difference between the alcohols and cyclic ethers is reflected in the cationic dependence of the alcohol group, which increased as $Fe^{3+} < Cr^{3+} < Al^{3+}$, (Fig 5.ix.), whereas no cationic dependence of the cyclic ether sorption rate was observed, (Fig 5.xiv.).

The values for the effective integral diffusion coefficients $\widetilde{D}$ for the alcohols and cyclic ethers were of the same order of magnitude, (Table 5.iv.). This combined with the temperature independence of the sorption rate (Fig 5.xii. and 5.xiv.), and small temperature increase

associated with the sorption process indicates that bed diffusion is
also the rate controlling influence in the sorption of cyclic ethers.

If the diffusion rates for cation-exchanged montmorillonites
are compared to those for zeolites in the literature, the zeolites would
be expected to have slower diffusion rates than montmorillonites, due
to the restrictive nature of the zeolite channel network (section 4.5.).
This was found to be the case as diffusion in zeolites of molecules of
a similar size and shape to those used in this study, gave diffusion
rates considerably slower[51-54] than those for the montmorillonites.

5.5.iv.   Other Factors Influencing the Sorption Process.

The temperature variation of the sorption rates for i-propanol
on Cr^{3+}-montmorillonite (FIG 5.xiii.), is just disernable, and the
Arrhenius plot to calculate the associated activation energy is
also shown. The activation energy was found to be $\sim$4kJmole^{-1}, and for
such a small potential barrier, the sorption process should have been
almost instancous However for all the clay-organic systems studied
several minutes were required for the clays to reach equilibrium loadings.
The reason for this may well be explained by the inter-crystalline
macropore diffusion resistance (section 5.5.ii.). This delayed time to
reach equilibrim loading could also be due to the finite time required
to dissipate the exothermic enthalpy of intercalation of the vapour
molecules.

This may be examined as follows, if the dissipating time is
wholly or partly rate limiting, it would effect the uptake curve in
two ways. Firstly the initial uptake rate would be increasd due to the
temperature difference of the diffusivity, and secondly, the latter part
of the sorption rate would be retarded due to the temperature dependence
of the equilibrium position[55]. Table 5 v. shows that experiments
conducted to quantify the temperature rise associated with the sorption

106

A = 1,4-Dioxan   ● = i-Propanol   ▇ = THP

Δ = t-Butanol   O = methonal   □ = THF
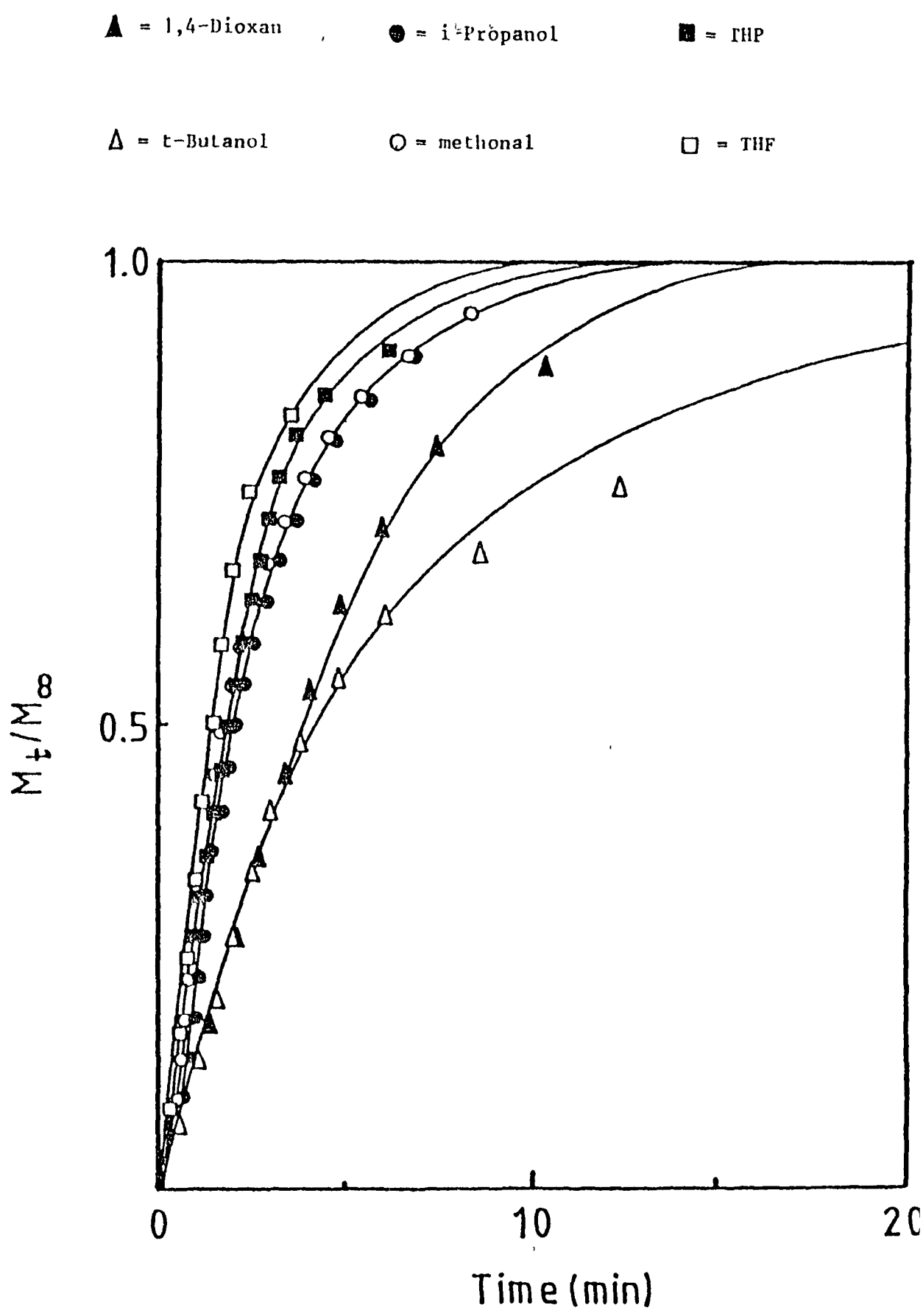
Fig 5.xv. A comparison of the sorption rates for the cyclic ethers and alcohols on Cr^{3+}-montmorillonite at 18°C.

$\triangle$ = Reservoir temperature 17°C $\hexagon$ = Reservoir temperature 19°C

Furnace temperature 15°C   Furnace temperature 15°C
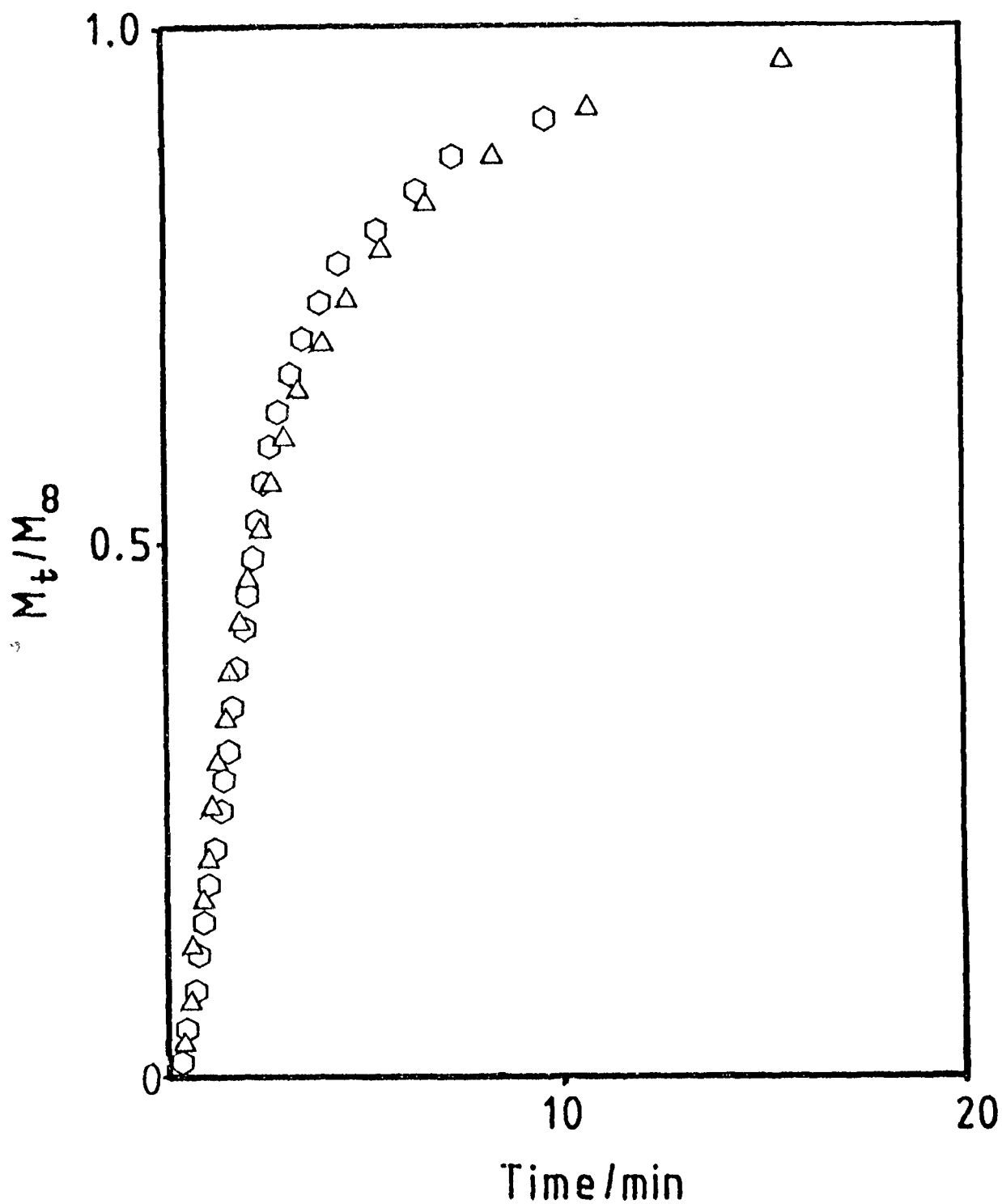
Fig 5.xvi   A comparison of the effect of a temperature differance between

the liquid reservoir and the furnace on the uptake of THF

on Al^{3+}-montmorillonite at 18°C.

of the vapours on various cation-exchanged montmorillonites, however

yield values of up to 3°C (this is the largest value). These temperature

increments are negligible compared with the values of 50°C for the

sorption of propane on synthetic 5A zeolite at $-78°C^{45}$, and 15°C for

butane on synthetic NaX zeolite at $25°C^{46}$, and, thus, confirm the overall

isothermal nature of the uptake process. However when considering

this, it is possible that the magnitude of the temperature rise may

reflect the fact that the heat of sorption of the vapour molecule may

in part be utilized to desorb a water molecule. If this were the case the

observed weight change may only be an incremental change equal to

$$\left(Mass_{vap.} - Mass_{water}\right).$$

The effect of different temperatures in the liquid reservoir

and the thermobalance furnace (this is because the running water used

to cool the furnace was often colder than the ambient temperature in

the room). This is especially important for the 18°C sample runs. When

the furnace temperature is lower than the liquid reservoir temperature

the vapour may condense onto the sample and the sample pan causing an

apperent high rate of sorption, (or high rate of mass increase as this

is what is actually measured). However Fig 5.xvi. shows that there does

not appear to be any significant difference in the sorption rates under

these conditions, so the temperature difference between the liquid

reservoir and the furnace does not appear to have any effect.

The equilibrium loading of the clay is a measure of the total

amount of the diffusing compound that has been adsorbed by the clay,

and Table 5.iv. shows that a general trend for equilibrium loading

of the alcohols and cyclic ethers on all three cation-exchanged

montmorillonites used. The equilibrium loading decreased in the order

methanol >> THF > i-propanol > t-butanol > 1,4-dioxan and THP.

The amount of vapour adsorbed depends to a large extent on the packing

of the molecules within the interlayer space. Hence the small compact molecules such as methanol, would be expected to pack tightly into the interlayer space, (methanol in known to form a double-layer complex with cation-exchanged montmorillonites[66]) The progressively larger molecules would be expected to have a lower equilibrium loading due to steric hinderance of the packing, and this is the trend observed in the experimental results, with the exception of THF. THF might be expected to have an equilibrium loading similar to that for THP and 1,4-dioxan as it is similar in physical size, however it has an equilibrium loading similar to that of 1-propanol. This may be explained by the fact that ethers are known to form one and two layer complexes with cation-exchanged montmorillonites, and 1,4-dioxan is reported to form only mono-layer complexes with montmorillonites[64]. So THF may form a double layer and THP may behave like 1,4-dioxan forming a mono-layer and so explaining the observed trend. However if the basal spacings are considered (Table 5.111.) it is similar for all three cyclic ether vapours, and this would not be the case if THF formed a double layer. So the equilibrium loading difference is probably due to some structural difference between the molecules. The most obvious difference is that THP and 1,4-dioxan are six-membered ring compounds, whereas THF has a smaller five-membered ring, and it may be that the smaller ring structure allows a more dense packing of the THF molecules and hence a higher equilibrium loading value. Also it is possible that the THF molecules do not orientate themselves perpendicular to the silicate sheets, but instead lie parallel to the silicate sheets, thus allowing a more dense packing. This combined with the smaller size of THF may account for the higher equilibroum loading on the clay.

The effect of temperature on the equilibrium loading was as expected with the equilibrium loading decreases as the temperature

increased. This is because increasing the temperature would impart

greater mobility to the adsorbed compounds owing to an increase in

thermal energy, and the weakening of the intermolecular Van der Waals

attractions. Also since the adsorption process is an exothermic process

increasing the temperature would disfavour an exothermic process and the

equilibrium loading would be expected to decrease. This was

observed for all six compounds on the various cation-exchanged

montmorillonites used.

Finally the overall significance of the diffusion results

will be considered The rate uptake curves for all six diffusivatives

on Cr^{3+}-montmorillonite at 18°C are shown in Fig 5.xv. The observed

sequence in this diagram reflects the general trend for all the montmoril-

lonites and is THF $\geqslant$ THP > methanol $\geqslant$ i-propanol > t-butanol > 1,4-dioxan

with respect to the sorption rate. If these vapours are grouped by

comparable vapour pressures, the following trends are revealed,

THF $\geqslant$ THP $\geqslant$ methanol in one group and i-propanol > t-butanol > 1,4-dioxan

in the other group. However when experimental imprecision is taken

into consideration the vapours fall into two distinct groups each having

about the same sorption rate. Group (i) THF, THP, methanol, and i-propanol

have a faster sorption rate than group (ii) t-butanol and 1,4-dioxan.

If steric factors are considered, t-butanol would be expected to have

a slower sorption rate than the other molecules due to the bulky side

group substitutents on this molecule. However 1,4-dioxan might be

expected to have a sorption rate similar to that for THP and THF, since

1,4-dioxan is known to interact with the clay surface and the interlayer

cations[6,31], it is possible that these interactions slow down the rate

of sorption, and it falls into the same group as t-butanol and is not

in the group with THF and THP.

In this study a better distinction between the sorption rates

of the six diffusivatives would have been expected, as methanol is a

very different molecule to THP in terms of its size and shape, and so

methanol would be expected to diffuse faster than THP, however this was

not found to be the case. This assumption is based on the fact that the

molecules are diffusing between the silicate sheets of the montmorill-

onite, (ie intraparticle diffusion). Since the rate controlling

influence is bed diffusion (see section 5.5.iii.), this may not

necessarily be the case. Hence only very bulky molecules such as

t-butanol or molecules that interact with the clay, 1,4-dioxan

might be expected to have a significantly different sorption

rate. It is also worth noting that the cyclic ether compounds show

some evidence of a slight concentration dependence, (ie the sorption

rate for the THP and THF was faster than for 1,4-dioxan, and THF

and THP have a higher partial pressure than 1,4-dioxan). This

may influence the observed trend in the sorption rates to some

extent, as a reduced concentration of 1,4-dioxan in the furnace

atmosphere due to its lower partial pressure would cause a reduced

sorption rate to be observed

One final point worth noting is, that cation-exchanged

clay is used as solid acid catalysts, and all clay catalysed reactions

are carried out in the liquid phase, however diffusion coefficients

derived from studies on sorption in the vapour phase may not

apply . However Bulow et al[67] have shown that there are only slight

differences ($\leqslant 10^1$) in the diffusion coefficients for n-decane into

zeolite A, from the liquid and the vapour phase. So the results from

these studies may be applicable to liquid phase studies in certain

circumstances.

CHAPTER 6

The Interaction of Alcohols and Cyclic Ethers with Trivalent

Cation-Exchanged Montmorillonite.

6.1.   Introduction

In chapter 5 the diffusion of alcohols (methanol, i-propanol,

and t-butanol), and cyclic ethers (tetrahydropyran (THP), 1,4-dioxan,

and tetrahydrofuran (THF)), on various trivalent cation-exchanged

montmorillonite, was examined. In this chapter the interaction of

these diffusivatives with the clay surface or in the interlayer space

about the cations will be examined. Again for the purpose of discussing

the results the compounds will be considered in two groups, the

alcohols and the cyclic ethers.

Ballantine et al[12] has shown that primary aliphatic alcohols

such as ethanol, propanol, and butanol when intercalated in Al^{3+}-

montmorillonite react preferentially via intermolecular nucleophilic

displacement of water to give high yields (30-65%) of di-(alk-1-yl)

ethers, rather than undergo competitive intramolecular dehydration

to the appropiate alkenes. In contrast, the reactions of secondary

aliphatic alcohols (propan-2-ol, butan-2-ol, and pentan-2-ol) gave

high yields (~80%) of the corresponding alkene, except for propan-2-ol

which was converted to both the di-(alk-2-yl) ether (30%), and

alkene (40%). The formation of di-prop-2-yl ether has also been

reported by Adams et al[7], but at a much lower yield (~3%). However

the Adams reaction was carried out at 60°C using a Fe^{3+}-montmorill-

onite in the presence of 1,4-dioxan, whereas Ballantine et al[12]

used no solvent, and a reaction temperature of 200°C with Al^{3+}-

montmorillonite. Adams et al[7] suggested that the low temperature

coefficient of the ether forming reaction indicated the possible

involvement of diffusion control in the reaction. However the

studies detailed in chapter 5 of this thesis show that the diffusion coefficients did not exhibit a temperature dependence. Since the alcohols can react within the temperature range of the sorption kinetics study ($18°-105°C$), it was decided to investigate the nature of the sorbed alcohols in the temperature range $18°-800°C$.

This study was not restricted to alcohols alone as Adams et al[6,31] have also established that cyclic ether type solvents give comparable yields of methyl-t-butyl-ether (MTBE) at temperatures $30°C$ lower than if hydrocarbon solvents are used. So the nature of the sorbed cyclic ethers in the temperature range $18°-800°C$ was also investigated. Table 6.1. indicates the efficency of the process, which depends on the specific cyclic ether employed, is optimised if 1,4-dioxan is used as the solvent with Al^{3+}-montmorillonite. However Cr^{3+}- and Fe^{3+}-montmorillonite also gave respectable yields with THF, and THP as the solvents.

Table 6.1   Solvent and cation dependence of yield of methyltert-iarybutyl ether

Cation	Solvent (% yield of MTBE)		
	1,4-dioxan	THP	THF
Al^{3+}	61	4	0
Fe^{3+}	65	35	32
Cr^{3+}	63	42	28

Adams et al[31] suggested that 1,4-dioxan was the optimal solvent because all the molecules participating in the reaction were miscible in it, thereby facilitating the rapid distribution of all the reactants and products between the clay interlayer and the external solution. If Table 5.iv. of chapter 5 is considered it can be seen that the rate at which the three cyclic ethers were adsorbed by the cation-exchanged montmorillonite forms under discussion was of the

order THF > THP >> 1,4-dioxan,with 1,4-dioxan being sorbed almost

six times slower than THP, and THF However the diffusion coefficients

for the cyclic ethers did not exhibit the increase with temperature

expected of a thermally activated process nor did they conform to

the $1/\sqrt{mass}$ dependence for limiting knudsen diffusion, as was found

for the alcohol diffusion coefficients.

Consequently this investigation to ascertain whether the

alcohols or cyclic ethers underwent any transformation in the

temperature region ($18°-105°C$) of the diffusion experiments and was

extended up to 800°C to conform with similar studies by Al-Oswais

et al[84], on the nature of the intercalation of acetic acid on Al^{3+}-

montmorillonite, and Ballantine et al[85] on the interaction of nitrogen-

containing bases such as cyclohexylamine.

6.2.   Temperature Programmed Desorption and Infared Spectroscopy

Results.

6.2 i.   The Temperature Programmed Desorption Results.

Using the experimental methods and techniques detailed in

chapter 3, the following results were obtained. The basal spacing

and percentage weight loss ($18°-800°C$) data for the alcohol saturated

samples is listed in Table 6.11., and confirms that the desorption

profiles reported below arise from intercalated and not surface

species.

Fig 6.1.(i.-iv.) shows the desorption profiles for methanol,

n-propanol, i-propanol, and t-butanol from a range of cation-

exchanged clays, (Na, Ca, Fe, Cr, and Al). The desorption of methanol

from the trivalent cation exchanged and sodium-forms, (Fig 6.1.i.)

was characterized by two peaks at $20°C$ and $110°C$. In addition, the

Al^{3+}-form exhibited a weak broad desorption peak near 300°C, and the

Ca^{2+}-montmorillonite had a sharp peak at $140°C$ which partially masked
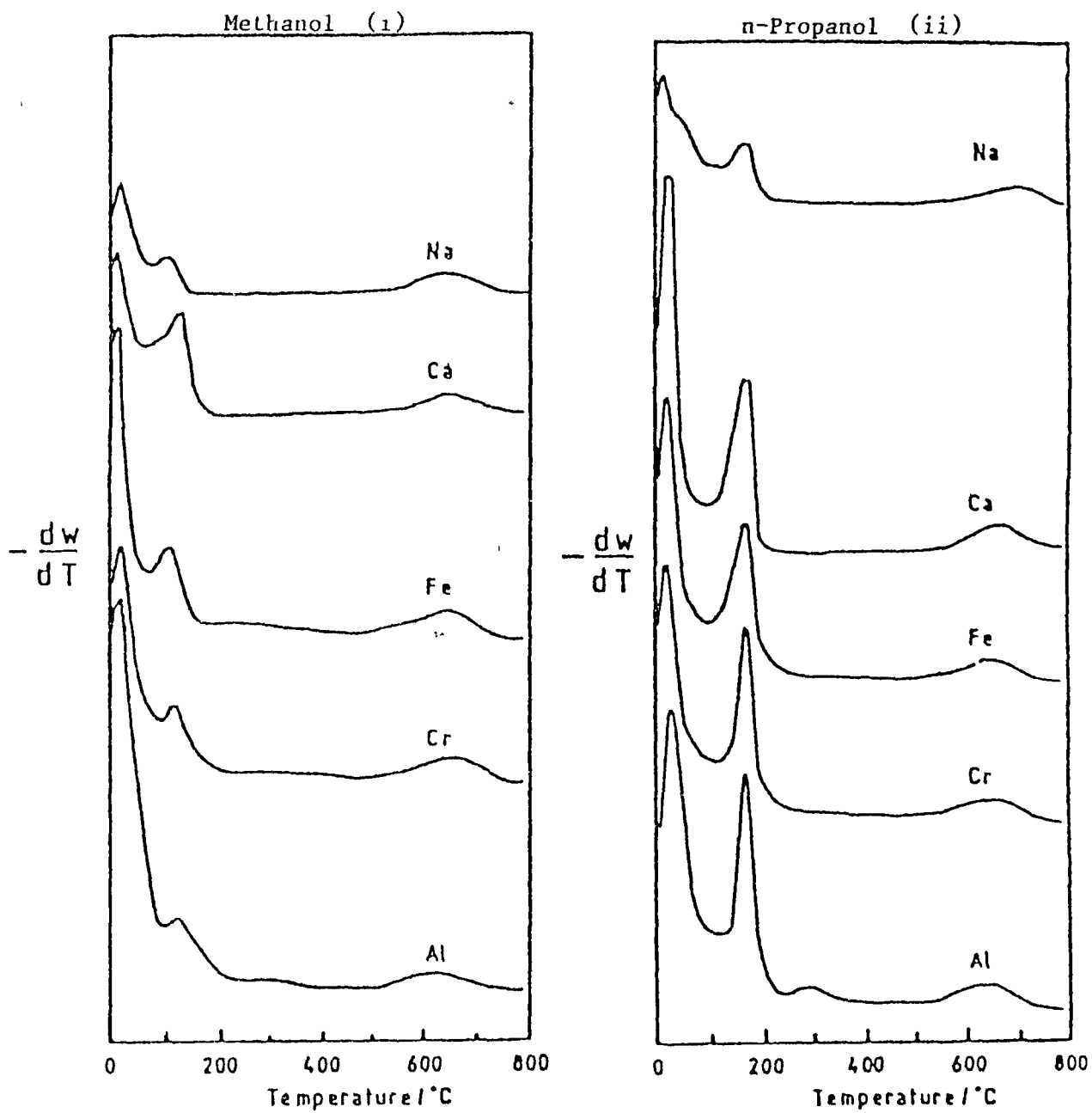
Fig 6.1.(i-ii). Desorption profiles for methanol, and n-propanol from
Na^+, Ca^{2+}, Fe^{3+}, Cr^{3+}, and Al^{3+}-exchanged montmorillonite.
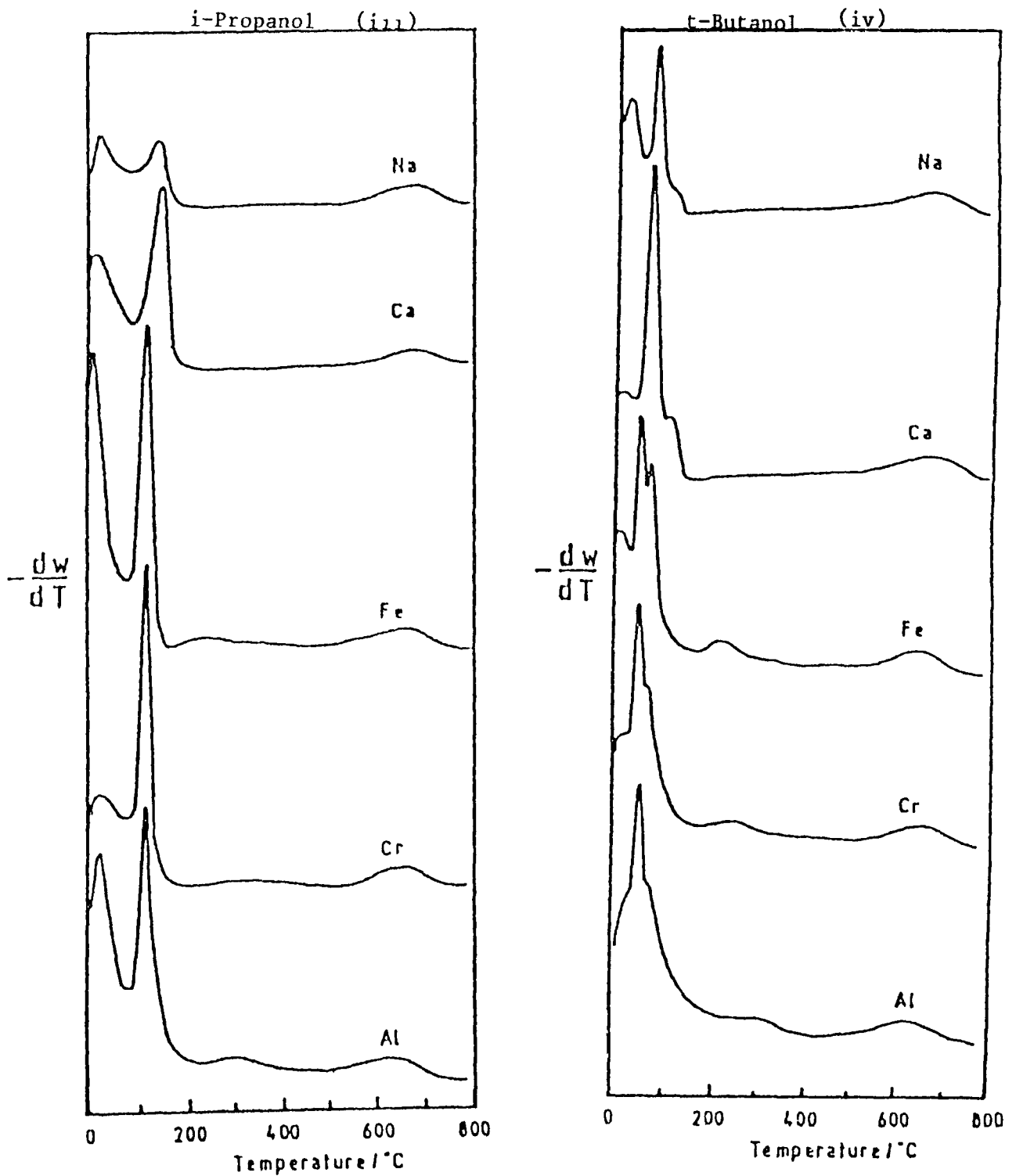
Fig 6.1.(iii-iv). Desorption profiles for i-propanol and t-butanol from Na^+, Ca^{2+}, Fe^{3+}, Cr^{3+}, and Al^{3+}-exchanged montmorillonite.

that at 110°C. The temperature the maxima in the desorption

profiles of n-propanol from all the cation-exchanged forms (Fig 6.1.ii.)

were identical at 30° and 160°C Only the Al^{3+}-form

exhibited a weak desorption peak near 290°C. The desorption profiles

for i-propanol from Na^+ and Ca^{2+}-montmorillonite showed two peaks

near 20°C and 140°C, whilst the higher temperature desorption maximum

in the trivalent cation-exchanged forms occurred at the lower

temperature of 100°C (Fig 6.1.iii.). Furthermore all the trivalent

cation-exchanged forms exhibited some deviation from baseline in

the region 200-400°C and it was most noticeable for the Al^{3+}-exchanged

form. The desorption profiles for t-butanol (Fig 6.iv.) contained the

lowest temperature desorption peaks in this study with three poorly

resolved peaks occurring at or near 30, 50 and 70°C in the M^{3+}-

exchange forms and 30, 90 and 110°C in the Na^+ and Ca^{2+}- montmorillonite.

Once again deviation from the background was observed in the region

200-400°C of the Al^{3+}-, Cr^{3+}-, and Fe^{3+}-montmorillonite desorption

profiles.

Table 6.11. Weight loss (%) by 800°C and basal spacings at 20°C for
the cation-exchanged montmorillonite-alcohol systems.

Cation	Solvent	Weight Loss (%)	Basal Spacing (Å)
Al^{3+}	Methanol	36	14.0
	n-Propanol	26	----
	i-Propanol	27	14.3
	t-Butanol	23	15.3
Cr^{3+}	Methanol	26	15.0
	n-Propanol	24	----
	i-Propanol	24	13.8
	t-Butanol	21	17.4
Fe^{3+}	Methanol	25	15.5
	n-Propanol	27	----
	i-Propanol	25	16.0
	t-Butanol	24	17.7
Ca^{2+}	Methanol	17	----
	n-Propanol	22	----
	i-Propanol	19	----
	t-Butanol	16	----

Fig 6.2.(i.-iii) show the desorption profiles for THP, THF,
and 1,4-dioxan, respectively, from a range of cation exchanged forms.
In complete contrast to the desorption profiles for the alcohols, there
was little uniformity in the position of the desorption maxima from
the different cation-exchanged forms. Consequently the temperatures
at which the major pre-dehydroxylation events occurred are presented in
Table 6.iii.

Table 6.iii. The position of the peak maxima in Fig 6.2.(i.-iii.), ($^{\circ}$C).

Cation	1,4-Dioxan	Tetrahydropyran	Tetrahydrofuran
Al^{3+}	30, 150, 240	30, 130, 275	20, 120, 220
Cr^{3+}	30, 150, 270	30, 110, 300	20, 90, 180
Ca^{2+}	10, 45, ---	30, 120, ---	30, 145, ---
Na^{+}	10, 75, 115	30, 110, 160	30, 130, ---

Nonetheless some tentative trends were observed. Desorption from
Ca^{2+}-montmorillonite always occurred in two distinct processes, the
second of which was broad enough to encompass the two higher temperature
maxima exhibited in the desorption profile of THP and 1,4-dioxan
from Na^{+}-montmorillonite. Desorption from trivalent cation-exchanged
forms always occurred in three steps, the second of which generally
occurred at higher temperatures in the Al^{3+}-form, whereas the highest
temperature desorption maxima were usually observed in the Cr^{3+}-form.

When interpreting the infared spectra for both alcohols and
the cyclic ethers it was noted that the trends were similar for all
the cation-exchanged forms of the clay used. So the Cr^{3+}-montmorillonite
spectra will be used to demonstrate the alcohol results as it is
representative of all the M^{3+}-montmorillonites used.

6.2.ii.   Infra-Red Spectroscopy Results.

Fig 6.3.(i-iv). shows the changes in the 1300-1800cm^{-1} region
of the infra-red spectrum caused by outgassing the alcohol saturated

Tetrahydropyran (i)

Fig 6.2.1. Desorption profiles for THP from Na^+, Ca^{2+}, Cr^{3+}, and Al^{3+}-exchanged montmorillonite.

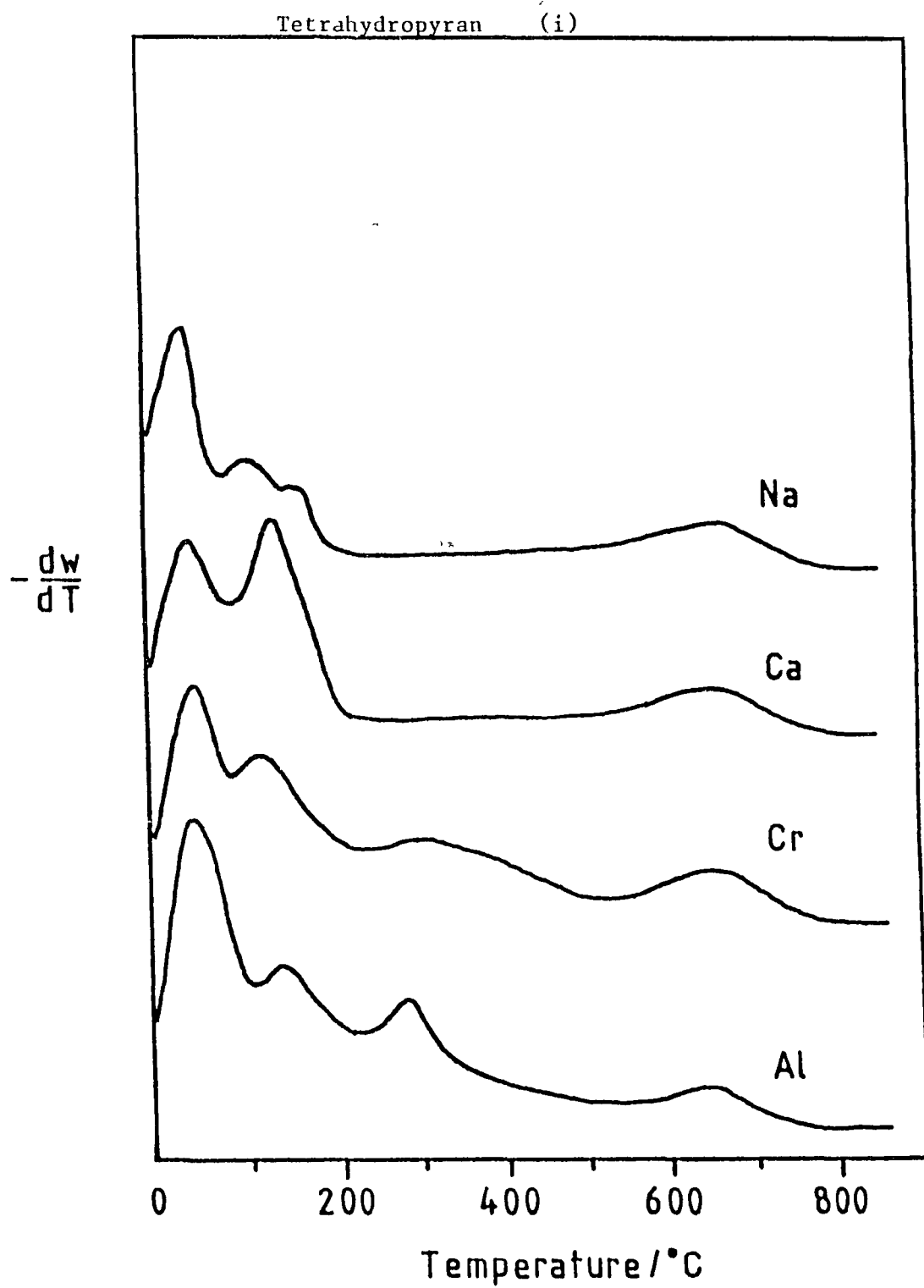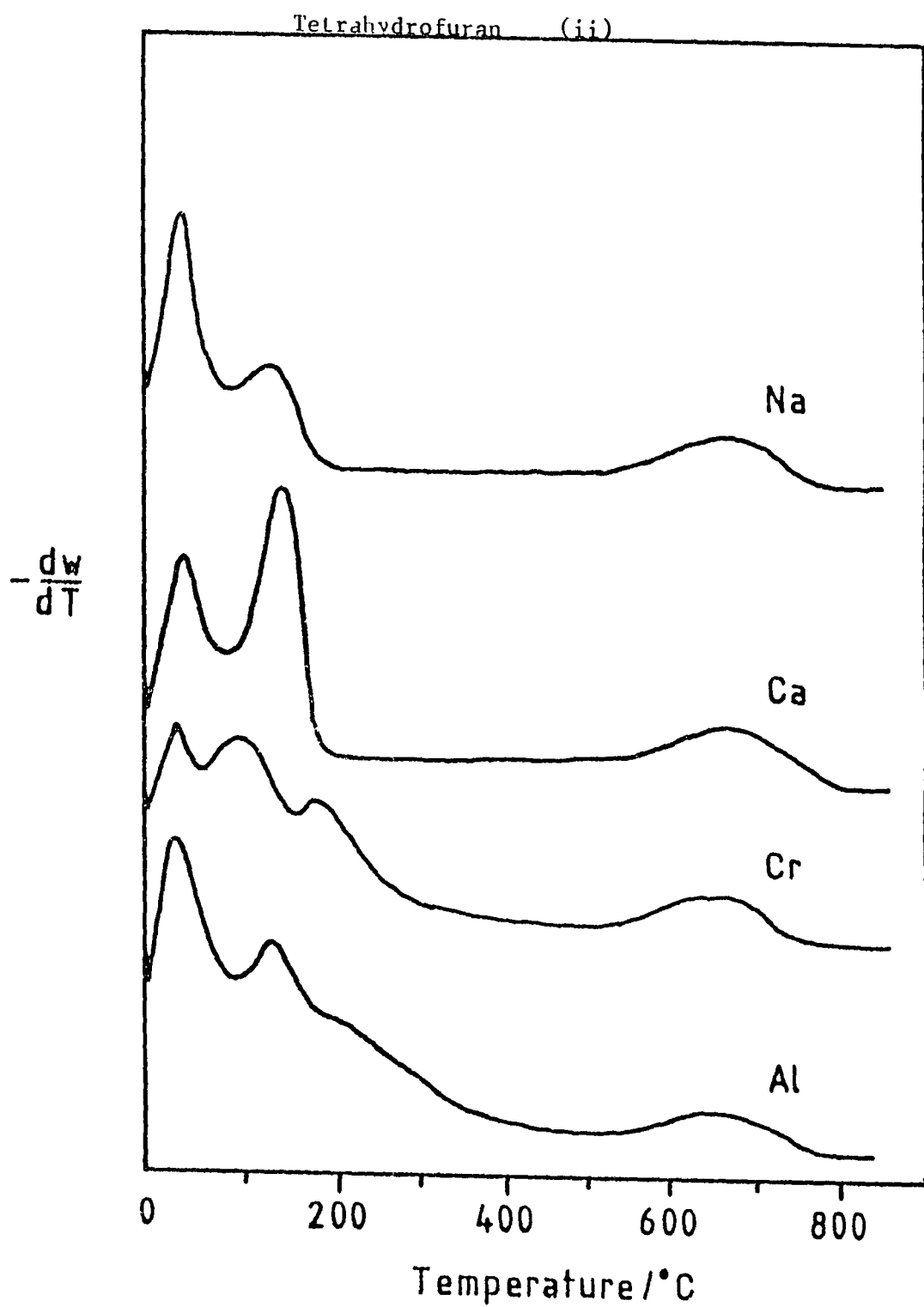Fig 6.2.ii. Desorption profiles for THF from Na^+, Ca^{2+}, Cr^{3+}, and Al^{3+}-exchanged montmorillonite.
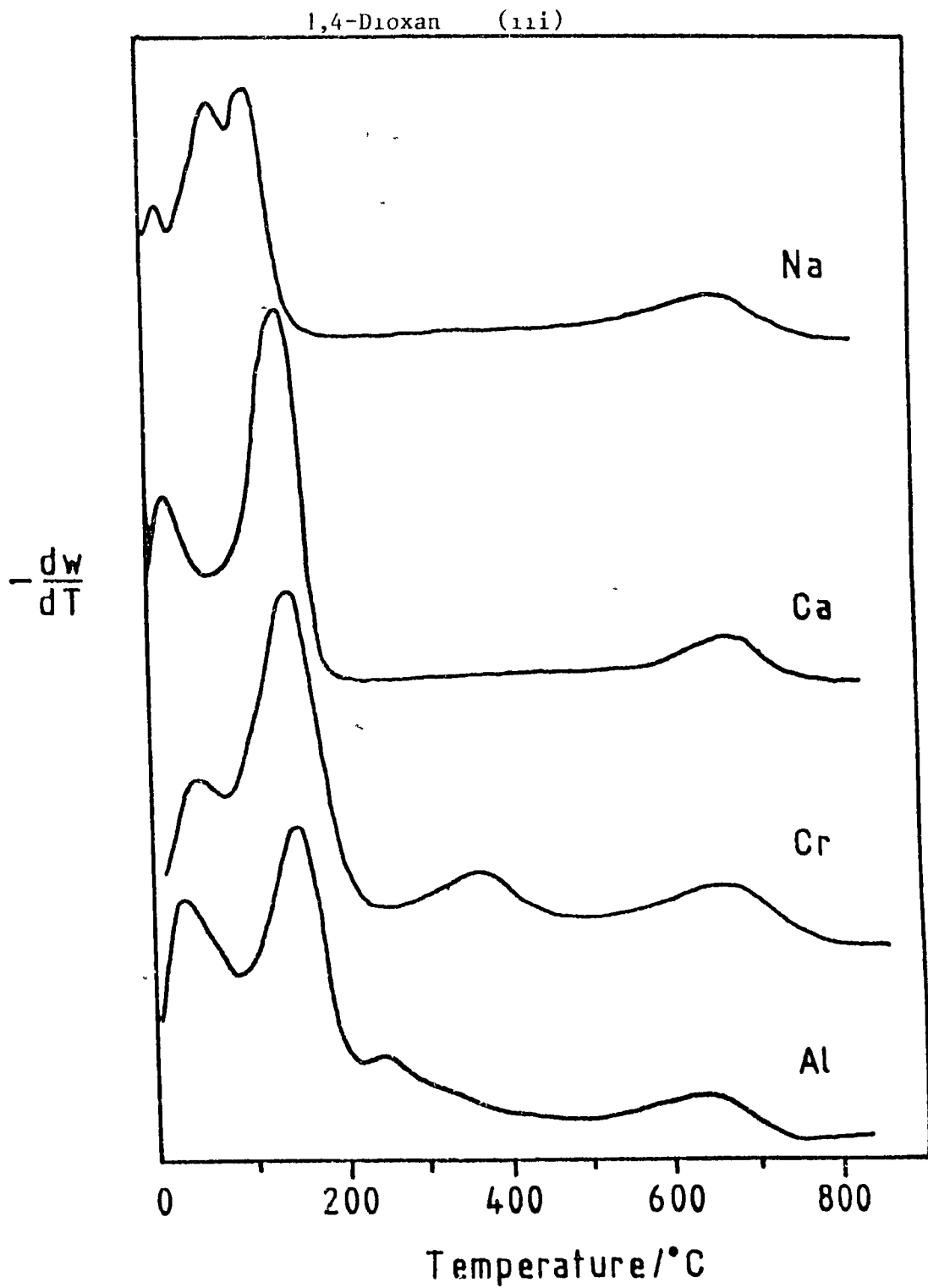
1,4-Dioxan (iii)

Fig 6.2.iii. Desorption profiles for 1,4-dioxan from Na^+, Ca^{2+}, Cr^{3+}, and Al^{3+}-exchanged montmorillonite.

Cr^{3+}-montmorillonite at progressively higher temperatures 20°, 50°, 100° 150°C. The infra-red spectrum of the Cr^{3+}-montmorillonite/n-propanol intercalate (top spectra Fig 6.3.(i-iv)) changed little as the outgassing temperature was increased. The CH_3 deformation band at 1475cm^{-1} was maintained up to 150°C, whilst the C-H band at 1397cm^{-1} and the OH band at 1625cm^{-1} became progressively weaker up to this temperature. In contrast the infra-red spectrum of Cr^{3+}-montmorillonite/ i-propanol system (middle spectrum Fig 6.3.(i.-iv.) exhibited a marked change as the outgassing temperature was increased from 50°-100°C, (Fig 6.3.ii. and 6.3.iii.). The characteristic doublet at 1391 and 1377cm^{-1} is lost and the bands at 1626 and 1457cm^{-1} became the dominant feature of the spectrum. At 150°C (Fig 6.3.iv.), poorly resolved bands at 1435 and 1427cm^{-1} were observed, together with a weak doublet at 1375 and 1363cm^{-1}. Increasing the outgassing temperature to only 50°C caused considerable changes in the spectra of the Cr^{3+}-montmorillonite /t-butanol system (bottom spectra Fig 6.3.(i.-iv.). The 1376cm^{-1} band was considerably reduced in intensity and the bands at 1626, 1464, and 1363cm^{-1} dominated the higher temperature spectra. Figs 6.4.(i.-iii.) illustrate the changes that occur in the C-H streching region of the n-propanol, i-propanol, and t-butanol saturated Cr^{3+}-montmorillonite as the outgassing temperature is increased. The important feature to note is that the change in the characteristic absorption band profile occurs at progressively lower temperatures, 150°C for n-propanol (Fig 6.4.i.), 100°C for i-propanol (Fig 6.4.ii), and 50°C for t-butanol (Fig 6.4.iii.). Thus reinforcing the changes observed in the 1300-1800cm^{-1} region of the respective spectra.

Fig 6.5.(i-iii) shows the infared spectra obtained from air-dried Al^{3+}-montmorillonite exposed to THP, THF, and 1,4-dioxan,
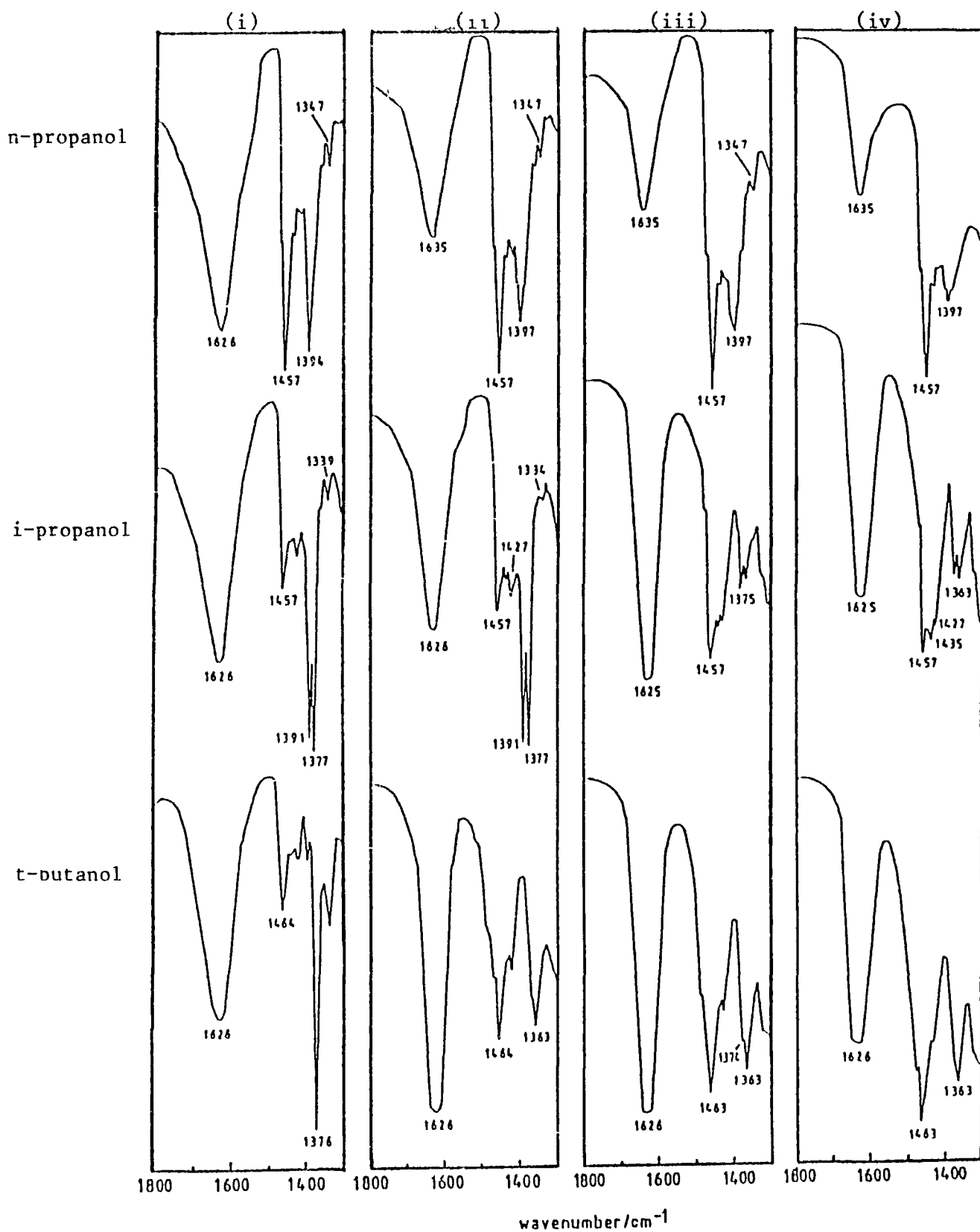
Fig 6.3.(i-iv). Effect of outgassing temperature on the IR spectra of Cr^{3+}-montmorillonite/alcohol intercalates (i) 20°C, (ii) 50°C, (iii) 100°C, and (iv) 150°C.

124
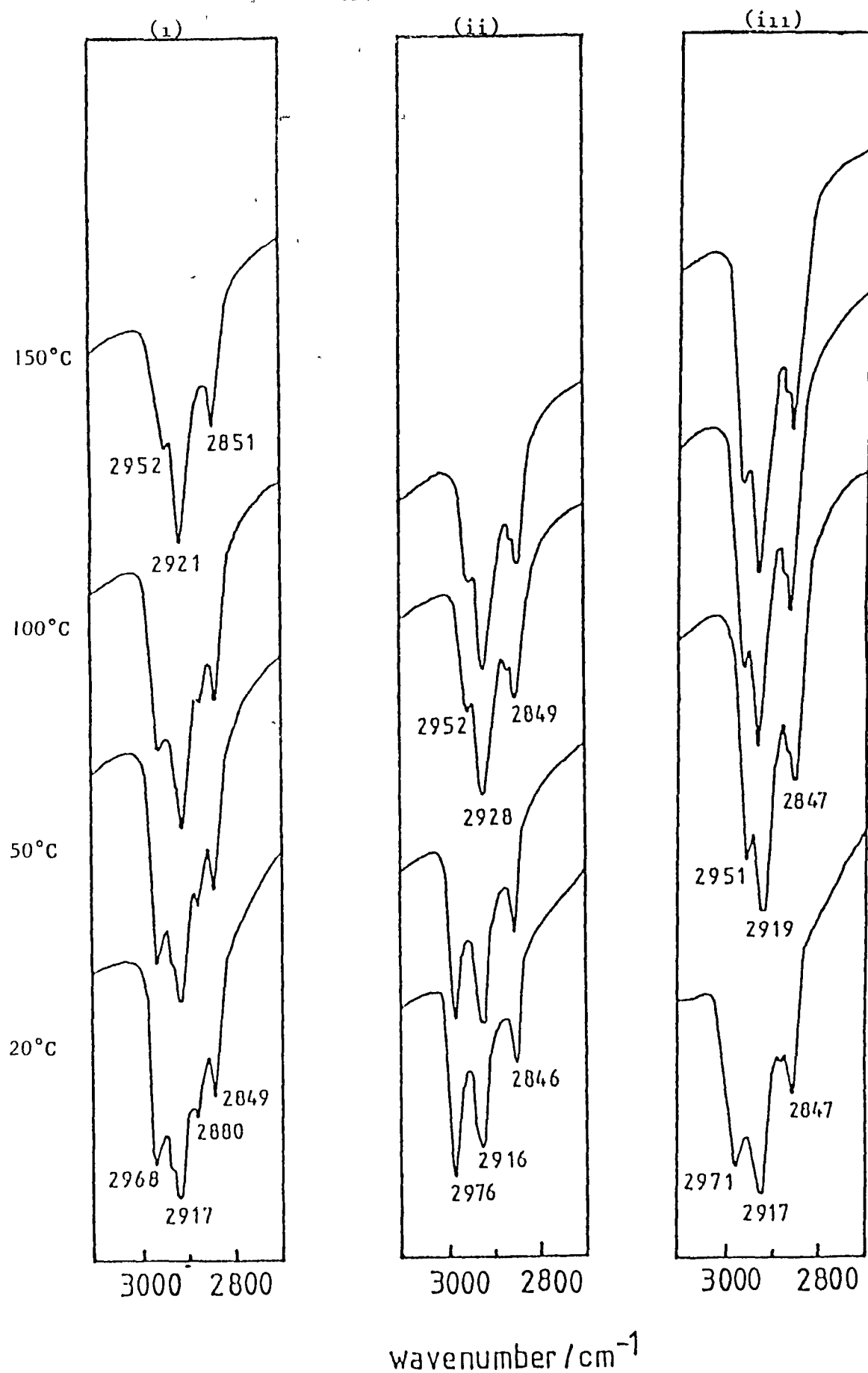
Fig 6.4.(i-iii). Effect of outgassing temperature on the C-H stretch region of the IR spectra of (i) n-propanol, (ii) i-propanol, and (iii) t-butanol.
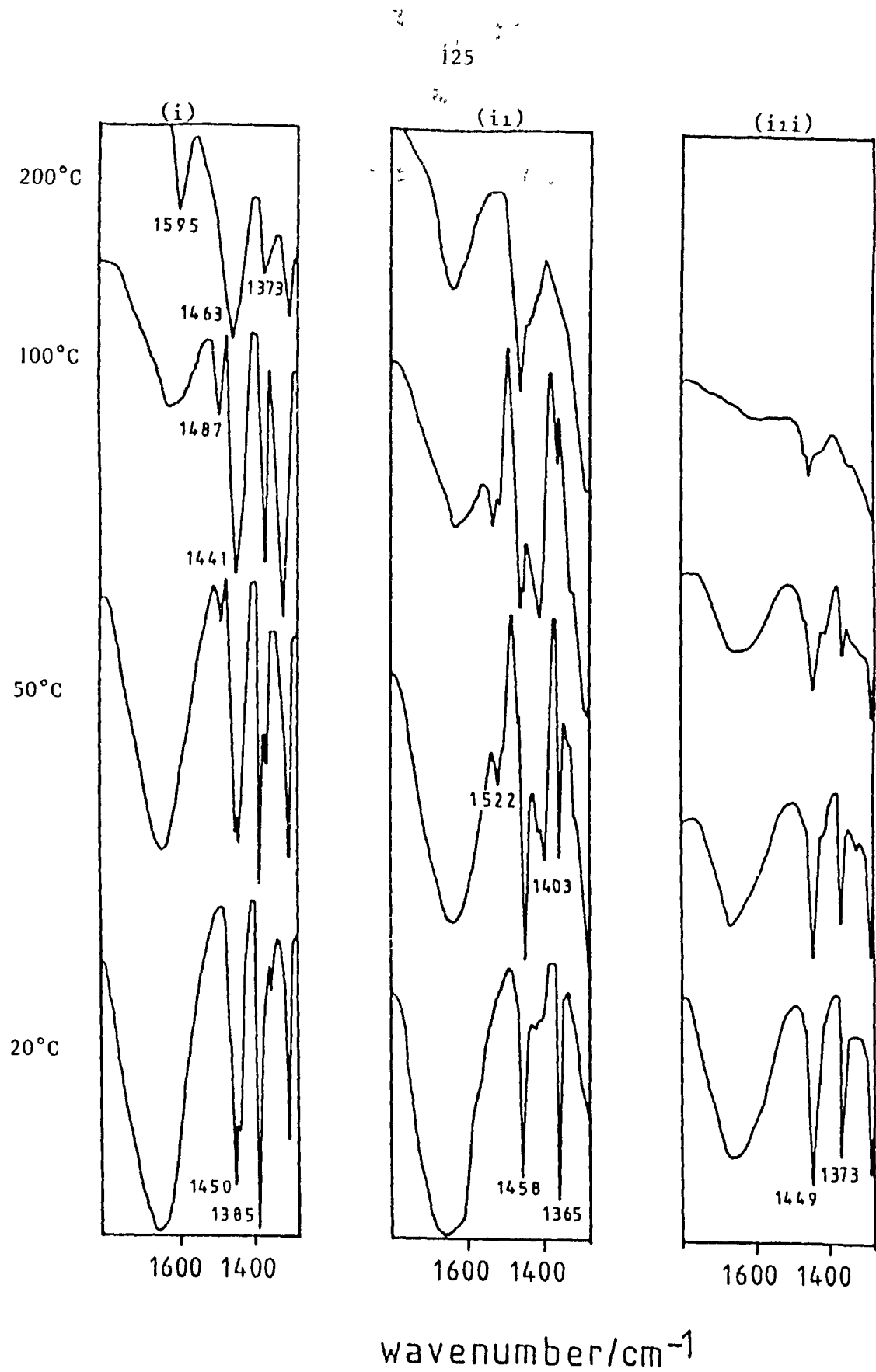
Fig 6.5.(i-iii). Effect of outgassing temperature on the IR spectrum of Al^{3+}-montmorillonite saturated with (i) THP, (ii) THF, and (iii) 1,4-dioxan.

respectively, and were representatitive of the desorption from the Cr^{3+}-form except that the desorption of THF occurred at lower temperatures in the latter. The bottom spectra Fig 6.5.i., obtained after degassing at room temperature, shows that the major absorption bands attributed to THP occurred at 1450, 1440, 1385, and 1303cm^{-1}, together with bands at 1275 and 1258cm^{-1}which are not illustrated. As the temperature was increased through 50° to 100°C the bands near 1440 and 1365cm^{-1} increased in intensity and then replaced the bands at 1450 and 1385cm^{-1}. Furthermore a band near 1487cm^{-1} appeared and grew in intensity but this disappeared upon heating to 150°C although the other bands were unaffected. The top spectrum Fig 6.5.i. shows the bands remaining at 200°C were centered near 1595, 1463,1373, and 1309cm^{-1}. The bottom spectra in Fig 6 5.ii., obtained after degassing at room temperature, shows the two absorption bands for THF at 1458 and 1365cm^{-1}. Heating at 50°C for one hour resulted in the appearance of further bands at 1522, 1415, and 1403cm^{-1}. After one hour at 100°C the sharp, characterictic band near 1365cm^{-1} was much reduced in intensity whilst the bands at 1522 and 1404cm^{-1} were unaffected The 1404cm^{-1} band was still in evidence after degassing at 150°C. But subsequent to heating at 200°C (top spectrum Fig 6.5.ii.) the predominant band was at 1456cm^{-1}. Interestingly, in contrast to the corresponding spectrum in Fig 6.5.i. the band at 1626cm^{-1}, normally attributed to water in these systems had survived.

The absorption spectrum of 1,4-dioxan adsorbed on Al^{3+}-montmorillonite subsequent to degassing at room temperature (bottom spectrum Fig 6.5.iii.) exhibited bands near 1449, 1373, and 1293cm^{-1}, together with a band at 1256cm^{-1} which is not illustrated. The position of these bands were unchanged as the temperature was increased up to 100°C. The 1373cm^{-1}band was removed on heating at 150°C and replaced

by a broad, unresolved absorption near $1350cm^{-1}$ and appears much the same as the top spectrum in Fig 6.5.iii. obtained at 200°C.

6.3. Discussion of the Experimental Results.

6.3.1. The clay alcohol interactions.

The maxima at 20°C in the desorption profile of methanol from the various cation-exchanged forms Fig 6.1.(i.-iv.) could be removed by passing dry nitrogen gas through the system and can thus be attributed to physisorbed alcohol, as can the peaks in the 20°-30°C region for the desorption of n-propanol, i-propanol, and t-butanol, from the cation-exchange forms, (Fig 6.1.(ii-iv)). The maximium at 110°C in the desorption profile of methanol from the various cation-exchanged forms (Fig 6.1.i.) corresponds closely to the values of 117°-140°C and 130°C reported for the desorption of methanol adsorbed,(i) on the surface hydroxyls of silica-magnesia mixed oxides[42] and, (ii) in zeolite H-ZSM-5 reported by Ison and Gorte[57], respectively. However Ison and Gorte[57] observed a second desorption maximum near 180°C which they attributed to the desorption of a single methanol molecule from each cation site in H-ZSM-5, but there is no evidence of such an interaction in this study. Moreover, the exchange cation present in the interlayer space has no influence on the temperature of the desorption maxium at 110°C.

The higher temperature maximum at 160°C in the desorption profile for n-propanol from the various cation-exchanged forms (Fig 6.1.ii.) similarly exhibits no cationic dependence. However, the corresponding maximum for i-propanol (Fig 6.1.iii.) occurs at 140°C in the Na^+- and Ca^{2+}-forms but at 110°C in the trivalent cation-exchanged montmorillonite, and the reason is not immediately obvious. The results in Table 6.11. indicate that several processes can occur, which may be in competition.

128

Table 6.ii Product distribution (weight %) for reactions of alcohols with M^{3+}-montmorillonite.

Reactant	Reactant Recovered	Ethers	Alkenes
Methanol	- a , - b	- b , (2)	-
n-Propanol	22	63 c	3
i-Propanol	29	30 d, (3) d	40
t-Butanol	3	-	97 e, (8) f

Note: Figures in parantheses taken from Adams et al[87], using 1g Fe^{3+}-montmorillonite, 50mmol. of reactant alcohol, and $3cm^3$ of 1,4-dioxan at 60°C.

Other values are from Ballantine et al[12], using 0.5g of Al^{3+}-montmorillonite at 200°C for 4 hours.

a = Not reported by Adams et al[87].

b = Not reported by Ballantine et al[12].

c = Yield of di-prop-1-ylether.

d = Yield of di-prop-2-ylether.

e = 18% alkene, 50% alkene dimer, and 29% alkene tetramer.

f = Alkene Dimer.

These reactions may be summarised as follows,

(i) ROH_{ads} ⇌ ROH_g

(ii) ROH_{ads} ⇌ $alkene_g + H_2O_g$

(iii) $2ROH_{ads}$ ⇌ $R-O-R_g + H_2O_g$
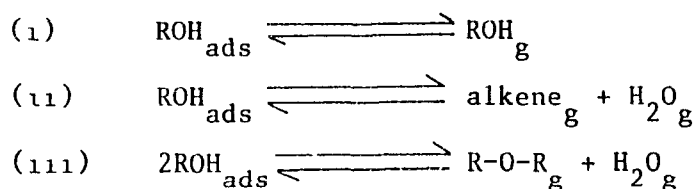
Where ads = an adsorbed molecule.

g   = a vapour phase molecule.

The problem is further complicated in steps (ii) and (iii) because the products may not desorb at the same temperature that they are produced. However, if situation (i) pertains then the higher desorption temperature of 160°C for n-propanol compared to 110°C for i-propanol could be attributed to the higher volatility and greater steric hinderance of i-propanol. Moreover, primary amines are known to desorb at higher temperatures than secondary amines[58], but this approach does not

explain the higher desorption temperatures of i-propanol from Na^+- and Ca^{2+}-montmorillonite.

If equation (ii) describes the desorption process then it is necessary to ascertain whether one or both products are desorbed upon formation. Noller and Ritter[42] found that propene formed by the acid-catalysed dehydration of i-propanol on silica-magnesia desorbed at least 65°C below that formed from n-propanol and that the alkene was desorbed upon formation.

Finally, if the reaction and desorption sequence follows scheme (iii) then once again volatility and steric considerations suggest that di-prop-1-ylether would desorb at a higher temperature than di-prop-2-ylether.

Unfortunately, no single reaction sequence explains why the desorption of i-propanol from the M^{3+}-exchange forms occurred at a lower temperature than that from Na^+- and Ca^{2+}-montmorillonite, whilst the desorption of n-propanol exhibits no cationic dependence. The explanation lies in the lower desorption temperature of the species generated in the M^{3+}-montmorillonite/i-propanol system. The maximum at 110°C must be attributed to the desorption of propene from i-propanol whereas, by analogy with methanol intercalates (Fig 6.1.1.), the peak at 140°C is due to the desorption of unchanged i-propanol. In contrast the desorption of n-propanol is governed by scheme (iii). In the M^{3+}-exchanged montmorillonite some or all of the n-propanol is converted to the corresponding di-prop-1-ylether and both the alcohol and the ether desorb at 160°C. Breen et al[47] have reported that amines such as n-butylamine and the corresponding di-but-1-ylamine desorb at the same temperature, although due to their greater basicity this desorption occurs at 410°C in M^{3+}-montmorillonite.

It is known that tertiary carbonium ions can be formed from

the protonation of species such as isobutene or the acid-catalysed dehydration of t-butanol at temperatures as low as $60°C$[31]. Consequently if alkenes formed from alcohols do desorb at lower temperatures than the alcohol from which they are derived then the peaks in the desorption profile of t-butanol from the M^{3+}-exchange forms should occur at lower temperatures than those from the Na^{+}- and Ca^{2+}-forms. This is clearly the case (Fig 6.1.iv.). Moreover, as Table 6.ii. indicates, dimeric and tetrameric alkenes can be produced from t-butanol which may account for the complex nature of the desorption profiles. Furthermore, given the ease of dehydration of t-butanol and the relative stability of the tertiary butyl ion it is possible that the peak at $110°C$ in the desorption profile of t-butanol from the Na^{+}- and Ca^{2+}-exchange forms may be due to the desorption of alkene.

Corroborative evidence for the chosen interpretation of the temperature programmed desorption profiles can be inferred from Fig 6.3. and 6.4. Unfortunately, the main C-O streching region ($1000 - 1300cm^{-1}$) is obscured by the alumino-silicate lattice absorption so definitive interpretations concerning the presence of alcohol versus ether are not available However, Grady and Gorte[59] observed similar changes to those reported here, in the infared spectrum of i-propanol adsorbed on H-ZSM-5 and attributed a marked change in the $2800 - 3000cm^{-1}$ region, to the complete loss of the C-H band at $1380cm^{-1}$ together with an increase in the intensity of the band at $1630cm^{-1}$ (due to the elimination of water) to the formation of propene. Their interpertion was confirmed by mass spectroscopic determination of desorbed propene. Furthermore, there can be no question that the temperature at which the infra-red change in Figs 6.3. and 6.4. closely parallel the events in the temperature programmed desorption profiles and that the effect of temperature on these spectra indicate that i-propanol and t-butanol

undergo very similar changes to give peaks of similar intensities near 2950, 2925, 2848, 1626, 1460, and 1360cm^{-1}.

The results of Ballantine et al[12] reported in Table 6.11. indicate that i-propanol should form the di-prop-2-ylether in addition to the alkene. However, their study was conducted in a sealed vessel of 20cm^3 capacity containing 0.5g of Al^{3+}-montmorillonite and 5g of i-propanol. The results reported here suggest that the alcohol once converted to the alkene does not encounter an i-propanol molecule with which to react. Consequently, an attempt was made to produce the di-prop-2-ylether in the experimental apperatus used for this study by subjecting the Al^{3+}-montmorillonite/i-propanol sample to a flow of i-propanol saturated nitrogen gas whilst it underwent the normal temperature ramp used to obtain the desorption profile. The resulting differential thermogram is presented in Fig 6.6.iii. together with the desorption profiles from i-propanol (Fig 6.6.i.) and n-propanol (Fig 6 6.ii) saturated Al^{3+}-montmorillonite samples. In addition to the propene desorption peak at 110°C, there is an alcohol/ether desorption peak at 160°C and the maximum at 300°C is enhanced. Indicating that di-prop-2-ylether appears to be forming in the interlayer.

6.3 ii   The clay-cyclic ether interactions.

Again all the maxima below 50°C in the desorption profiles in Fig 6.2.(i-iii.) were removed by a prolonged flow of dry nitrogen proving that they arose from physisorbed species. The nature of the bonding or the transformation mechanism giving rise to the higher temperature desorption peaks is not easy to elucidate.

The infared spectrum of THP-saturated Al^{3+}-montmorillonite Fig 6.5.(i-iii). shows that after degassing at 100°C noticeable changes have taken place, in partictular the appearance of the 1487cm^{-1} band. Subsequent degassing to 200°C results in the appearance of bands at
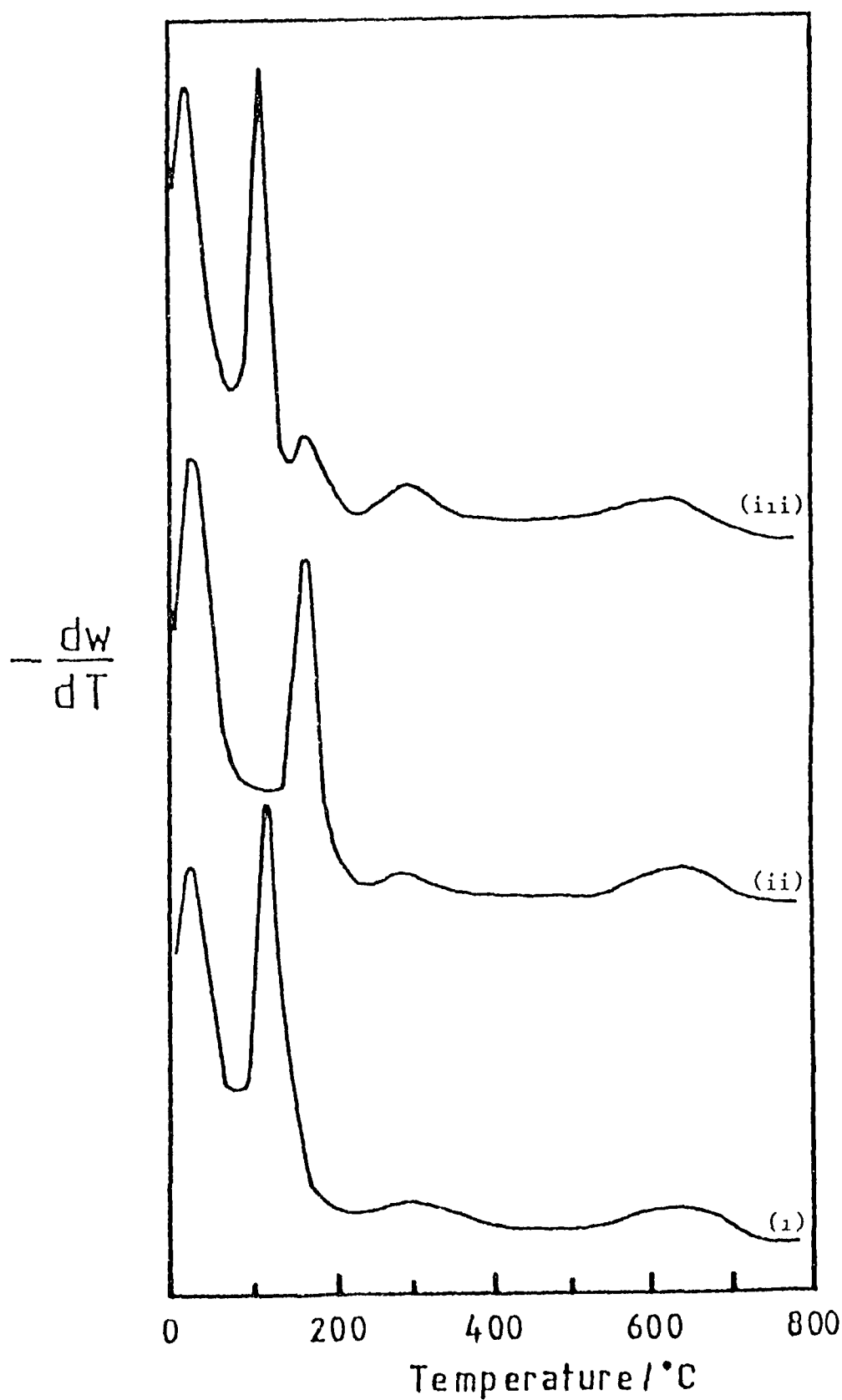
Fig 6.6.(i-iii). Comparison of the desorption profiles of (i) i-propanol
and (ii) n-propanol sorbed on Al^{3+}-montmorillonite,
(iii) Al^{3+}-montmorillonite/i-propanol subjected to
nitrogen/i-propanol flow.

1595, 1463, and 1373cm^{-1} Dalka[88] attributed bands near these

frequencies to the formation of oligomeric moeities derived from the

transformation of but-1-ene on dehydroxylated Y zeolite at room

temperature. The formation of alkenes from THP is not unlikely insofar

as the acid-catalysed ring opening of THP and THF over HY zeolites

has been observed[89,90], and a similar mechanism has been suggested to

explain the formation of 2-methyl-1,3-dioxalane from 1,4-dioxan[91].

The most likely product following acid-catalysed ring opening is the

diol, which could then be dehydrated to yield alkenes. These alkenes

could then oligomerise.
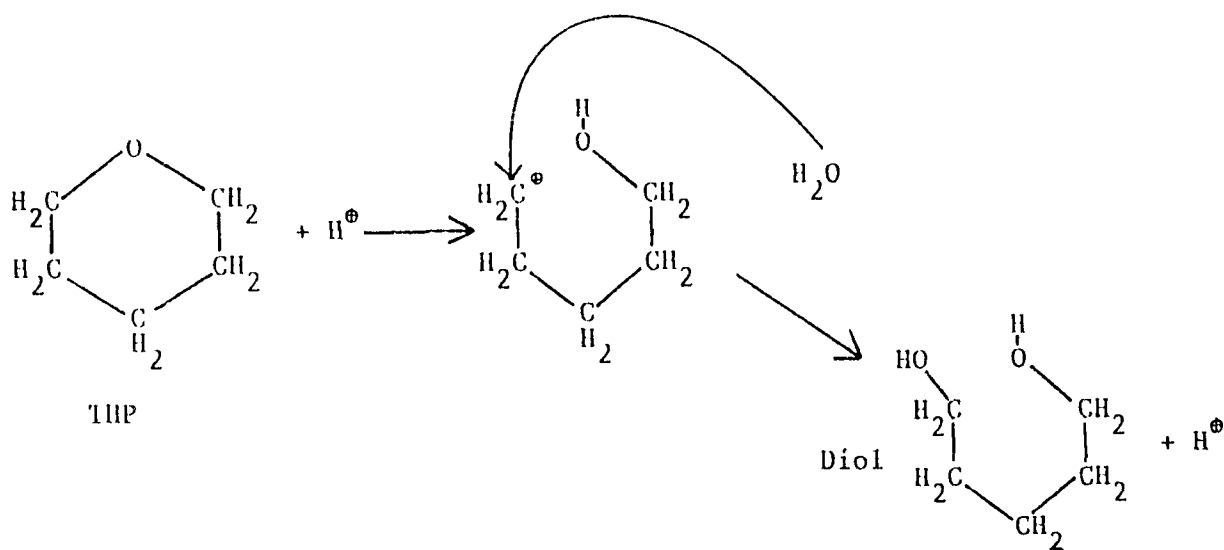
Correlation of the infared and temperature programmed desorption results

for the desorption of THP from the trivalent cation-exchanged forms

suggests that the loss of THP in its unmodified form occurred at or

before 200°C,thereby implying that the maxima near 300°C in the TPD

profiles (Fig 6.2.i.) must be attributed to the desorption of the

oligomeric species or a component thereof.

In the case of THF (Fig 6.2.11.) the changes in the infared

spectrum were not so drastic, although the interim formation of bands

near 1520 and 1403cm^{-1} require consideration. Haber et al[92] in an

extensive study of the transformation of alcohols on HY and H-Z-79

zeolites attributed the band near 1520cm^{-1} to the formation of aromatic

surface structures. However Grady and Gorte[59] preferred, in the absence

of aromatic compounds in the mass spectrum of the desorbed products,

to assign it to a C-C double bond If the latter interpretation pertains

here then it would reinforce the proposed formation of alkenes

following acid-catalysed ring opening However, the infra-red evidence

suggested that the transformation of THF to oligomeric species was not

as extensive in the case of THP, since the OH absorption band at $1626cm^{-1}$

was still present at 200°C suggesting the presence of water or alcohol

molecules. Nonetheless the possibility does exist that this absorption

was of a C-C double bond although there was no evidence of the $1590cm^{-1}$

band which is indicative of the formation of oligomeric species[88].

The desorption thermogram of THF from Cr^{3+}-montmorillonite

(Fig 6.2.iii.) exhibited three desorption maxima at 20, 90, and 180°C,

the latter two of which occurred at temperatures some 30° or 40°C

below those in the desorption profile of THF from the Al^{3+}-form.

This temperature difference agrees well with the infra-red observations

and the tenacity of the band at $1626cm^{-1}$, is similar to that in the

desorption of alcohols discussed above, and may imply that the high

temperature maximum was due to the desorption of an alcohol molecule.

The desorption of 1,4-dioxan from Al^{3+}-montmorillonite was

quite uneventful by comparison. Neither shifts in the peak positions

nor the appearance of new bands in the infra-red spectra were recorded

suggesting that most of the 1,4-dioxan was desorbed without modification.

This observation agrees with the temperature programmed desorption

profiles in Fig 6.2.iii. in that the major desorption of 1,4-dioxan

occurred at 150°C for the Ca^{2+}, Cr^{3+}, and Al^{3+}-exchanged forms. The

pre-dehydroxylation peaks above 200°C in the desorption profiles for

1,4-dioxan from Al^{3+} and Cr^{3+}-montmorillonite may be due to the

desorption of oligomeric entities or strongly bound ether molecules

but there is little infared evidence to support either suggestion.

It is interesting to once again find that 1,4-dioxan behaves in a different manner to the other two cyclic ethers. Adams et al[31] reported that 1,4-dioxan was the optimum solvent for the formation of methyl t-butyl ether. Breen and Deane[93] in their studies on the sorption of methanol from binary solution with 1,4-dioxan, THF and THP, found that although the amount of 1,4-dioxan adsorbed exceeded that of THP and THF the ratio of 1,4-dioxan:methanol was lower than that of THP:methanol. The result of which is that the solvent 1,4-dioxan, allows more of the reactant, methanol, into the interlamellar space which contains the active, or acidic site. Finally it has been shown in chapter 5 that the rate of uptake of 1,4-dioxan onto Al^{3+}- and Cr^{3+}-montmorillonite, was considerably slower than that of the alcohols, (methanol, i-propanol, and t-butanol), and that of the cyclic ethers, (THF and THP). Therefore, in both a dynamic and an equilibrium sense 1,4-dioxan allows more of a reactant molecule, such as an alcohol, to approach the active sites. Furthermore, the evidence in this study suggests that it is relatively stable towards acid attack in these systems.

CHAPTER 7

Conclusions

7.1.   The Sorption Rate Studies.

The sorption rate was found to increase with decreasing sample and grain size, indicating that resistance to diffusion in the bed and to mass transfer between the various size particles which form the grain control the rate of uptake. The rate of uptake for the alcohols (methanol $\geqslant$ i-propanol > t-butanol) parallels the observed median size of particles which contribute to the grains. So implying that the measured rate reflects the tortuosity of the channel network within the grains.

Bed diffusion is the rate controlling stage for the alcohol sorption, and the sequence conforms to the $1/\sqrt{mass}$ required for knudsen diffusion as the major contributor to the mass transfer resistance. For the cyclic ethers the sorption rate decreases as THF > THP >> 1,4-dioxan, and this does not conform to the $1/\sqrt{mass}$ required for knudsen diffusion. This may be due to some concentration dependence as THF and THP have higher vapour pressures than 1,4-dioxan, or an alternative explanation may be that the 1,4-dioxan sorption rate is retarded due to bi-dentate coordination of the ether to Al^{3+}-ions at the clay edges. Moreover, the sorption rate for the cyclic ethers shows no cationic dependence, whereas, the alcohols have a cationic dependence which increases as $Fe^{3+} < Cr^{3+} < Al^{3+}$. The integral diffusion coefficients for both the alcohols and the cyclic ethers are of the same order of magnitude which may reflect the fact that bed diffusion and not intracrystalline diffusion is the rate influencing factor.

The relatively low activation energy for the sorption process indicates that the sorption should have been almost instaneous. However,

this was not the case. The time required to reach equilibrium loading

probably reflects the fact that intercrystalline macropore diffusion

resistance and the finite time required to dissipate the exothermic

enthalpy of interaction of the vapour molecules retard the overall

sorption rate. However, the contribution from the latter may be minimal

since it was shown that the overall sorption process is virtually

isothermal as little heat of adsorption is generated (in the clay-

organic systems studied here) relative to the sorption temperature

The equilibrium loading found to decrease of the order

metanol >> THF > i-propanol > t-butanol > 1,4-dioxan and THP. This

sequence may be explained by the fact that small molecules such as

methanol have a more dense packing in the interlayer space (ie double-

layer complex is formed[66]), and so a higher equilibrium loading is

obtained. This loading decreases as steric hinderance of the diffusing

molecule increases. THF has a higher equilibrium loading than the other

two cyclic ethers, and this may be attributed to its smaller size,

which allows it to orientate or pack more densely into the interlayer

space. The equilibrium loading decreases as the temperature increases

because an increased temperature disfavours exothermic processes such

as the adsorption processes occurring here.

The overall diffusion rates were of the order THF $\geqslant$ THP >

methanol $\geqslant$ i-propanol > t-butanol > 1,4-dioxan. If the partial pressures

of the vapours and the experimental imprecision are taken onto account,

two groups each having about the same sorption rate (i) THP, THF,

methanol, and i-propanol, and (ii) t-butanol, and 1,4-dioxan, become

apparent. The fact that no clear distinction between the sorption

rates for the various compounds can be seen is probably due to the

fact that the rate controlling influence is bed diffusion, so

significant differences in the uptake rate due to steric hinderance

are less important.

7.2. Clay-Diffusivative Interaction Studies.

In the desorption profiles of the various compounds, low temperature peaks below 40°C are attributed to physisorbed species. n-Propanol was found to exhibit no cationic dependence in the desorption profiles and the i-propanol was found to desorb from the M^{3+}-exchange forms at a lower temperature than the Na^{+}- and Ca^{2+}-montmorillonite. These observations may be explained in terms of three possible processes occurring, (i) the alcohol is desorbed unchanged, (ii) the alcohol is transformed to an alkene and desorbed, and (iii) the alcohol is converted to a di-propyl ether and then desorbed. For the desorption of n-propanol on M^{3+}-montmorillonite some or all of the n-propanol is converted to the corresponding di-prop-1-yl ether and both ether and alcohol desorb at the same temperature. For t-butanol/M^{3+}-mont-morillonite the peaks occur at lower temperatures than for the Na^{+}- and Ca^{2+}-montmorillonite/t-butanol systems and based on the fact that alkenes formed from alcohols are known to desorb at lower temperatures than the alcohol[31], and that t-butanol can form tetrameric alkenes as well as dimers, this would account for the more complex nature of the t-butanol/M^{3+}-montmorillonite desorption profiles. The low temperature desorption peak in the i-propanol/M^{3+}-montmorillonite system is also most likely to be due to the desorption of the corresponding alkene. These findings are corroborated by the infra-red studies. Finally to reinforce the conclusions reached here an i-propanol saturated Al^{3+}-montmorillonite underwent the normal temperature ramp used for the desorption profiles, while being exposed to a flow of i-propanol saturated nitrogen gas. This resulted in an additional peak in the desorption profile corresponding to an alcohol/ether desorption peak, indicating that di-propyl ethers may well be forming in the

interlayer on adsorption of alcohols, confirming the above conclusions.

For the cyclic ethers the bonding or transformation mechanism was not easy to elucidate. THP may undergo acid-catalysed ring opening to yield alkenes which could undergo oligomerisation prior to desorption. The infra-red and temperature programmed desorption results for THP from M^{3+}-montmorillonite suggests that THP desorbed in its unmodified form at or below 200°C, and is desorbed as an oligomeric species or a component thereof at 300°C. The THF infra-red results are not so drastic and acid-catalysed ring opening of the THF to an oligomeric species was not as extensive as for THP, although little evidence of the formation of oligomeric species from THF was found in the infra-red spectrum for THF/M^{3+}-montmorillonite. The desorption of 1,4-dioxan is quite uneventful by comparison to the other two ethers. The infra-red spectrum suggests that most of the 1,4-dioxan was desorbed without modification, and this observation was confirmed by the temperature programmed desorption profiles as no evidence of the desorption of oligomeric entities or strongly bound ether molecules was found, except for a small maxima in the 200°-300°C region of the desorption profiles.

Once again the 1,4-dioxan is behaving differently to the other two cyclic ethers. Adams et al[31] reported that 1,4-dioxan was the optimum solvent for the formation of MTBE, and Breen and Deane[93], in studies of the sorption of methanol from binary solution with 1,4-dioxan, THF and THP found that although the amount of 1,4-dioxan adsorbed exceeded that of THF and THP the ratio of 1,4-dioxan:methanol was lower than that of THP:methanol. The result of which is that the solvent 1,4-dioxan, allows more of the reactant methanol, into the interlamellar space which contains the active, acidic site. Finally it has been shown

that for the sorption of THF, THP, and 1,4-dioxan onto Al^{3+}-and Cr^{3+}-montmorillonite, the rate of uptake of 1,4-dioxan was considerably slower than that of the alcohols, methanol, i-propanol, and t-butanol, and the cyclic ethers THP, and THF. Therefore, in both a dynamic and an equilibrium sense 1,4-dioxan allows more of the reactant molecule, such as an alcohol, to approach the active sites. Furthermore, the evidence in this study suggests that it is relatively stable towards acid attack in these systems.

Reference Articles.

1. R.E. Grim

   Clay Mineralogy.

   1968,2nd edition, McGraw-Hill, London.

2. C.K Wentworth.

   A scale of grade and class terms for clastic sediments.

   J. Geol. 30: 377-392: (1922)

3. J.T. Way.

   On the power of soil to Absorb manure.

   J. Roy. Agr. Soc. 13: 123-143. (1952)

4. A.A. Damour and D. Salvetat.

   Et analyses sui un hydrosilicate d'alumine trouve a

   Montmorillion

   Ann. Chim. Phys. ser 3. 21: 376-383: (1847)

5. J.M. Adams, J A. Ballantine, S,H, Graham, R.J. Laub, J.H. Purnell,

   P]. Reid, W.Y.M. Shaman and J.M. Thomas.

   Selective chemical conversions using sheet silicate intercalates:

   Low temperature addition of water to alk-1-enes.

   J Catalysis. 58· 238-252· (1979)

6. J.M. Adams, D.E. Clement and S.H. Graham.

   Synthesis of methyl t-butly ether from methanol and isobutene

   using a clay catalyst.

   Clay and Clay Min. 30 129-134· (1982)

7. J.M. Adams, D.E. Clement and S.H. Graham.

    Low temperature reactions of alcohols to form t-butyl ethers

    using a clay catalyst.

    J. Chem. Research. 5: 254-255: (1981)

8. J.M. Adams, D.E. Clement, and S.H. Graham

    Reactions of alcohols with alkenes over an aluminium exchanged

    montmorillonite.

    Clay and Clay Min. 31: 129-136: (1983)

9. J.A. Ballantine, M. Davis, J.H. Purnell, M. Rayanakorn. J.M. Thomas,

    and K.J. Williams.

    Chemical conversions using sheet silicates: Facile ester synthesis

    by direct addition of acids to alkenes.

    J. Chem. Soc. Chem. Comm. 8-9: (1981)

10. R. Gregory, D.J.H. Smith, and D.J. Westlake

    The production of ethyl acetate from ethylene and acetic acid

    using a clay catalyst.

    Clay Min. 18 431-435 (1983)

11. J.M. Adams, K. Martin and R.W. McCabe.
    Catalysis os diels-alder cycloaddition reactions by ion-exchanged
    montmorillonite.
    Proc. Int. Clay Conf. Denver 1985. (L.G. Shultz, H. van Olphen, and
    F.A. Mumpton. eds. The Clay MInerals Society, Bloomington, Indiana,
    324-328: (1987)

12. J.A. Ballantine, M. Davis, J.H. Purnell, M. Rayanakorn, J.M. Thomas,
    and K.J. Williams.
    Chemical conversions using sheet silicates: novel intermolecular
    dehydration of alcohols to esters and polymers.

J. Chem. Soc. Chem. Comm. 427-428: (1981)

13. J.A. Ballantine, J.H. Purnell, M. Rayanakorn, and K.J. Williams.

    Organic reactions catalysed by sheet silicates: intermolecular

    elimination of ammonia from primary amines.

    J. Mol. Catalysis. 30· 373-388· (1985)

14. J.A. Ballantine, J.H. Purnell, M. Rayanakorn, J.M. Thomas, and

    K.J. Williams.

    Chemical conversions using sheet silicates: novel intermolecular

    elimination of ammonia from amines.

    J. Chem. Soc. Chem. Comm. 9-10: (1981)

15. J.A. Ballantine, R.P. Galvin, R.M. O'Neill, J.H. Purnell,

    J.M. Thomas, and M. Rayanakorn.

    Chemical conversions using sheet silicates: novel intermolecular

    eliminations of hydrogen sulphide from thiols.

    J. Chem. Soc. Chem. Comm. 695-696· (1981)

16. U. Hofmann, K. Endell, and D. Wilm.

    Kristallstruktur und quellung und montmorillonite.

    Z. Krist. 86: 340-348· (1933)

17. C.H. Edelman and J.C.L. Favejee

    On the crystal structure of montmorillonite and halloysite.

    Z Krist. 102· 417-431: (1940)

18. S.B. Hendricks.

    Lattice structure of clay minerals and some properties of clays.

J. Geol <u>50</u>: 276-290: (1942)

19. P.F. Low.

    Physical chemisty of clay water interactions.

    Advan. Agron. <u>13</u>: 269-327· (1961)

20. K. Norrish.

    The swelling of montmorillonite.

    Disc. Farad Soc. <u>18</u>.120-134· (1985)

21. D T.B. Tennakoon, R. Schlogl, T. Rayment, J. Klinowski, W. Jones,

    and J.M. Thomas.

    The characterisation of clay-organic systems.

    Clay Min. <u>18</u>· 357-371· (1983)

22. D.M.C. MacEwan

    Complexes of clays with organic compounds.

    Irans. Farad. Soc. <u>44</u>· 349-367· (1948)

23. J.D. Russell.

    Infra-red study of the reactions of ammonia with montmorillonite and

    saponite

    Trans. Farad. Soc. <u>61</u>: 2284-2292: (1966)

24. C.E. Marshall.

    Layer lattices and base exchange clays.

    Z. Krist. <u>91</u>: 433-449. (1935)

25. N. Oyama, and F.C. Anson.

Catalysis of the electro-reduction of hydrogen peroxide by a

montmorillonite clay coating on graphite electrodes.

J. electroanal Chem. 199: 467-470· (1986)

26. W.E. Rudzinski, and A.J. Bard.

Clay modified electrodes part VI· aluminium and silicon pillared

clay-modified electrodes.

J. electroanal Chem. 199. 320-340: (1986)

27. P.A. Diddams, J.M. Thomas, W. Jones, J.A. Ballantine, and J.H. Purnell.
Synthesis, characterisation, and catalytic activity of beidellite-
montmorillonite layered silicates and their pillared analogues.
J Chem. Soc. Chem. Comm 1340 : (1984)

28. J.M. Adams, K Martin, and R.W. McCabe.

Clays as selective catalysts in organic synthesis.

J. Inclusion Phenom. (in press)

29. J M. Adams, K. Martin, R.W. McCabe, and S. Murray.

Methyl-t-butyl-ether production: a comparison of montmorillonite

derived catalysts with an ion-exchange resin.

Clay and Clay Min 34· 597-603: (1986)

30. M.M. Mortland, and K.V. Raman.

Surface acidity of smectites in relation to hydration, exchangable

cation, and structure.

Clay and Clay Min. 16. 393-398· (1968)

31. J.M. Adams, T.V Clapp, and D.E. Clement.

Catalysis by montmorillonites.

Clay Min. 18: 411-421: (1983).

32 M.M. Mortland.

Protonation of compounds at clay mineral surfaces.

9th Int. Cong. Soil Sci. vol. I· 691-699: (1968)

33. F.A. Cotton and G. Wilkinson.

Basic inorganic chemistry.

1976, 1st edt. Wiley, london.

34. R.M. Carr.

Hydration states of interlamellar Cr^{3+}-ions in montmorillonite.

Clay and Clay Min. 33: 357-361. (1985)

35. L.P. Hammett and A.J. Deyrup.

A series of simple basic indicators 1: The acidity function of mixtures

of sulphuric and perchloric acids and water.

J. Am. Chem. Soc. 54: 2721- 2739· (1932)

36. K. Morishige, S Kittaka, S Takao, and T, Morimoto.

Thermal desorption and infared studies of methylamines adsorbed on

dehydrated alkaline earth metal X zeolites.

J. Chem. Soc. Farad. Trans. 1. 80: 993-1003: (1984)

37 A.K. Ghosh and G. Curthoys.

Characterization of zeolite acidity by n-butylamine titration.

J. Chem. Soc. Farad. Trans I. 79· 417-153· (1983)

38   H.V. Drushell and A.L. Sommers.
     Catalyst acidity distribution using visible and fluorscent indicators.
     Anal. Chem. <u>38</u>: 1723-1731: (1966)

39. H.C. Nelson, R.J. Lussier and M.E Still.
     An estimate of surface acidity in amorphous catalysts from temperature
     programmed desorption. A simple tool for catalyst characterization.
     Applied Catalysis. <u>7</u>. 111-121 (1983)

40. A K. Ghosh and G. Curthoys.
     Acidity of de-aluminated mordenites by infared spectroscopy.
     J. Chem. Soc. Farad. Trans. I. <u>79</u>· 805-813: (1983)

41. E.P. Parry.
     An infared study of pyridine adsorbed on acidic solids. Characterization
     of surface acidity.
     J. Catalysis. <u>2</u> 371-379· (1963)

42. H. Noller and G. Ritter.
     Temperature programmed desorption of methanol, ethanol, propan-1-ol, and
     propan-2-ol on silica-magnesia mixed oxides.
     J. Chem. Soc. Farad Trans. I. <u>80</u>· 275-283· (1984)

43. J.A. Ballantine, W. Jones, J.H Purnell, D.T.B. Tennakoon, and
     J.M Thomas.
     The influence of interlayer water on clay catalysis· Interlamellar
     conversions of 2-methyl-propene.
     Chem. Lett. <u>6</u>· 763-766· (1985)

44. H. Bennet and R.A. Reed.
     Chemical methods of silicate analysis.
     1971, Academic Press, London

45. J.P. Egan, B Kindl, and R.B. Anderson.

Kinetics of adsorption on A zeolites, temperature effects.

Adv. Chem. 102: 164-170: (1971)

46. H.J. Doelle and L. Riekert.

Kinetics of sorption, desorption and diffusion in zeolites.

Angew. Chem. Int. Ed. Engl. 18: 266-272: (1979)

47. C. Breen, A.T. Deane, and J.J. Flynn.

The acidity of trivalent cation-exchanged montmorillonites. Temperature

programmed desorption and infared studies of pyridine and n-butylamine.

Clay Min. 22: 169-178: (1987)

48. D.T. Tennakoon, W. Jones, J.M. Thomas, T. Rayment, amd J. Klinowski.

Structural characterization of catalytically important clay-organic

intercalates.

Mol. Cryst. Liq. Cryst. 93: 147-155· (1983)

49. J. Helsen.

Katholicke Universiteit Leuven, B-3030 Leuven (Heverlee), Belgium.

Personal communication to my supervisor. (1985)

50[a] D.M. Ruthven.

Principles of adsorption and adsorption processes. Chapter 5,

'Diffusion in porous media'.

1984, Wiley, New York.

50[b] D M Ruthven.

Principles of adsorption and adsorption processes. Chapter 6,

'Kinetics of sorption in batch systems'.

1984, Wiley, New York.

51. H. Yucel and R.M. Ruthven.

Diffusion in 4A zeolite, (Study of the effect of crystal size).

J. Chem. Soc. Farad. Trans I. $\underline{76}$ 60-70 (1980)

52. H. Yucel and R.M. Ruthven.

Diffusion in 5A zeoilte, (Study of the effect of crystal size).

J. Chem. Soc Farad Trans I $\underline{76}$· 71-83: (1980)

53. J. Karger and P. Volkmer.

Comparison of predicted and nuclear magnetic resonance zeolitic

diffusion coefficients.

J. Chem. Soc. Farad. Trans I. $\underline{76}$: 1562-1568· (1980)

54. J. Karger and J Caro.

Interperation and correlation of zeolitic diffusivities obtained

from nuclear magnetic resonance and sorption experiments.

J. Chem. Soc. Farad. Trans. I. $\underline{73}$· 1363-1376· (1977)

55 J. Crank.

The mathematics of diffusion.

1968, Clarendon Press, Oxford

56. H.S. Carslaw and J.C. Jaeger.

Conduction of heat in solids.

1959, 2nd edt , Oxford Press, Oxford.

57. A. Ison and R.J. Gorte.

The adsorption of methanol and water on H-ZSM 5.

J. Catalysis. <u>89</u>: 150-158· (1984)

58. A.T. Deane

Physicochemical studies of clay-organic interactions.

PhD thesis NIHE Dublin· (1987)

59. M.C. Grady and R.J. Gorte.

Adsorption of 2-propanol and propene on H-ZSM 5.

J. Phys. Chem. <u>89</u>· 1305-1308: (1985)

60 E. Maegdefrau and U. Hofmann.

Die kristalstruktur des montmorillonite.

Z Krist. <u>98</u>· 299-323: (1937)

61. M.M. Mortland.

Clay-organic complexes and interactions.

Advan. Agron. <u>22</u>· 75-117: (1970)

62 R.H. Dowdy and M M. Mortland.

Alcohol-water interactions on montmorillonite surfaces I. ethanol.

Clay and Clay Min <u>15</u>· 259-271· (1967)

63. N.M. Radul and F.D. Ovcharenko.

Method for determining the orientation of adsorbed alcohol molecules

in the interlayer space of montmorillonite.

Ukr. Khim Zh. <u>37</u> 775-777· (1971)

64. D M.C. MacEwan.

Complexes of clays with organic compounds. I. Complex formation

between montmorillonite and halloysite and certain organic liquids.

Trans. Farad Soc. 44: 349-367 (1948)

65. R.H Dowdy and M M. Mortland.

Alcohol-water interactions on montmorillonite surfaces· II. Ethylene

glycol.

Soil Sci. 105: 36-43: (1968)

66. I Barshad

Factors affecting the interlayer expansion of vermiculite and

montmorillonite with organic substances.

Soil Sci. Soc. Am. Proc. 16. 176-182· (1952)

67. M Bulow, P. Struve and L V.C. Rees.

Investigation of the gaseous phase diffusion and liquid phase self

diffusion of n-decane on Ca-, Na-A zeolites.

Zeolites 5 113-117· (1985)

68. W.F. Bradley, E.J. Weiss, and R.A. Rowland

A glycol-sodium vermiculite complex

Clay and Clay Min 10 117-122 (1963)

69 R.C. Reynolds.

An X-ray study of an ethylene glycol-montmorillonite complex.

Am. Mineralogist 50· 990-1001: (1965)

70. W.F. Bradley.

Molecular associations between montmorillonite and some polyfunctional

organic liquids.

J. Am. Chem. Soc. 67: 975-981· (1945)

71 R.M. Barrer and D.M MacLeod.

Intercalation and sorption by Montmorillonite

Trans. Farad. Soc. 50 980-989· (1954)

72. J.M. Adams, A. Bylina and S.H. Graham.

Shape selectivity in low temperature reactions of C_6 alkenes catalysed

by Cu^{2+}-montmorillonite.

Clay Min. 16: 325-332· (1982)

73 C. Breen, J.M. Adams and C. Riekel.

Review of the diffusion of water and pyridine in the interlayer

space of montmorillonite· Relevance to kinetics of catalytic reactions

in clays.

Clay and Clay Min. 33: 275-284: (1985)

74. R M. Barrer and D.W. Brook.

Molecular diffusion in chabazite, mordenite, and levynite.

J Chem. Soc Farad. Trans I 49· 1049-1059 (1953)

75. R.M. Moore and J R. Katzer.

Counterdiffusion of liquid hydrocarbons in type Y zeolite: Effect of

molecular size, molecular type, and direction of diffusion.

J. Amer. Inst. Chem. Eng. 18 816-824· (1972)

76. M. Bulow, P Struve, G. Finger, C. Redszus, K. Ehrhardt, W. Scherimer, and J. Karger

Sorption kinetics of n-hexane on MgA zeolites of different crystal sizes.

J Chem. Soc. Farad Trans 1 76· 597-615: (1980)

77. M. Bulow, P. Lorenz, W. Mietk, P. Struve, and N. Samulevivc.

Sorption kinetics of neopentane on NaX zeolites of different crystal sizes.

J. Chem. Soc. Farad. Trans I 79 1099-1108 (1983)

78. J. Palmer and N. Bauer.

Sorption of amines by montmorillonite.

J. Phys. Chem. 65· 894-895· (1961)

79. J Ilavsky, B Brunovska, and V.H Lavacek.

Experimental observations of temperature gradients occurring in a single zeolite pellet.

Chem Eng Sci 35· 2475-2479 (1980)

80. M. Bulow, P. Struve, W. Mietk and M Kocirik.

Experimental evidence of the influence of sorption-heat release processes on the sorption of benzene in NaX zeolite crystals.

J. Chem. Soc. Farad Trans. I 80 813-822 (1984)

81. L.G. Tensmeyer, R.W. Hoffmann, and G.W. Brindley.

Infared studies of some complexes between ketones and calcium-montmorillonite. Clay-organic studies III.

J. Phys. Chem. 64. 1655-1662. (1960)

82. B K.G. Theng.

Mechanisims of formation of coloured clay-organic complexes A review.

Clay and Clay Min. 19· 383-390: (1971)

83. G.W. Brindley, R. Bender, and S Ray

Sorption of non-ionic aliphatic molecules from aqueous solutions

on clay minerals. Clay-organic studies VII.

Geochim. Cosmochim. Acta. 27 1129-1137 (1963)

84. Al-Owais, J.A. Ballantine, J.H. Purnell and J.M. Thomas.

Thermogravimetric study of the intercalation of acetic acid and water

by Al^{3+}-montmorillonite.

J Mol Catalysis. 35· 201-212· (1987)

85 J.A Ballantine, P. Graham, I. Patel, J H. Purnell, K J. Williams,

and J M. Thomas

New differential thermogravimetric method using cyclohexylamine for

measuring the concentration of interlamellar protons in

clay catalysts.

Proc Int Clay Conf Denver 1985 (L.G Shultz, H. van Olphen, and

F.A. Mumpton Eds The Clay Minerals Society, Bloomington, Indiana.
311-318, (1987)

86. D J. Cebula, R K Thomas, S. Middleton, R.H. Ottewill, and J.W. White.

Neutron diffraction from clay water systems.

Clay and Clay Min. 27· 39-52 (1979)

87. J M Adams, D.E Clement, and S.H. Graham.

Low temperature reactions of alcohols to form t-butyl ethers using

clay catalysts

/

J Chem Research. 5. 234-255 (1981)

88 J. Datka.

Transformations of butenes on dehydroxylated Y zeolites studied

by infared spectroscopy

J Chem. Soc. Farad. Trans I. 77 2633-2643 (1981)

89. K Fujita, K. Hatada, Y Ono, and T. Keii.

Ring transformations of tetrahydrofuran into pyrrolidine over

synthetic zeolite.

J Catalysis 35 325-329 (1974)

90. Y. Ono, K Hatada, K. Fujita, A Halgeri, and T. Keii

Type L zeolites as selective catalysts for the ring transformation

of cyclic ethers into cyclic imines

J Catalysis 41 323-328· (1976)

91. J A. Ballantine, J.H. Purnell, and J M. Thomas.

Sheet silicates· Broad spectrum catalysts for organic synthesis.

J. Mol. Catalysis 27· 157-167 (1984)

92. J. Haber, J Komorek-Hlodzik, and T Romotoski

Infared study of the transformation of olefins, alcohols, and

ethers on zeolites.

Zeolites. 2· 179-184. (1982)

93. C Breen and A.T. Deane

The adsorption of 1,4-dioxan, tetrahydropyran, and tetrahydrofuran

from binary solution with methanol on Al^{3+}- and Cr^{3+}-montmorillonite.

Clay Min. 22· 199-205· (1987)